

## Supplementary Materials for

### **Transcriptome-wide isoform-level dysregulation in ASD, schizophrenia, and bipolar disorder**

Michael J. Gandal\*, Pan Zhang, Evi Hadjimichael, Rebecca L. Walker, Chao Chen, Shuang Liu, Hyejung Won, Harm van Bakel, Merina Varghese, Yongjun Wang, Annie W. Shieh, Jillian Haney, Sepideh Parhami, Judson Belmont, Minsoo Kim, Patricia Moran Losada, Zenab Khan, Justyna Mleczko, Yan Xia, Rujia Dai, Daifeng Wang, Yucheng T. Yang, Min Xu, Kenneth Fish, Patrick R. Hof, Jonathan Warrell, Dominic Fitzgerald, Kevin White, Andrew E. Jaffe, PsychENCODE Consortium, Mette A. Peters, Mark Gerstein, Chunyu Liu\*, Lilia M. Iakoucheva\*, Dalila Pinto\*, Daniel H. Geschwind\*

\*Corresponding author. Email: mgandal@mednet.ucla.edu (M.J.G.); liuch@upstate.edu (C.L.); lilyak@ucsd.edu (L.M.I.); dalila.pinto@mssm.edu (D.P.); dhg@mednet.ucla.edu (D.H.G.)

Published 14 December 2018, *Science* **362**, eaat8127 (2018)  
DOI: 10.1126/science.aat8127

#### This PDF file includes:

Materials and Methods  
Figs. S1 to S17  
Captions for Tables S1 to S9  
PsychENCODE Consortium Authors and Affiliations  
References

#### Other Supplementary Material for this manuscript includes the following: (available at [www.sciencemag.org/content/362/6420/eaat8127/suppl/DC1](http://www.sciencemag.org/content/362/6420/eaat8127/suppl/DC1))

Tables S1 to S9 (.xlsx)

## Materials and Methods

### Data Generation

The data generated for this manuscript represent Freeze 1 and 2 of the PsychENCODE consortium dataset. Post-mortem human brain samples were collected as part of eight studies, detailed below and in **Fig S1**. RNA-Seq and genotype array data was generated by each site and then processed together through a unified pipeline by a central data analysis core. For this capstone analysis, we restricted analysis to frontal and temporal cortex brain samples from postnatal timepoints. We provide a description of each individual study below, derived from the PsychENCODE website. All data are available at <http://www.doi.org/10.7303/syn12080241> (90).

#### Study 1 - BrainGVEX

For the BrainGVEX study, RNA-Seq data was generated from 427 post-mortem prefrontal cortex samples from subjects with schizophrenia (n=95), bipolar disorder (n=73), and non-psychiatric controls (n=259). RNA samples were collected from the Stanley Medical Research Institute (SMRI) as part of the “Array Collection”, “Consortium Collection”, “New Collection” and “Extra Collection”. Array collection and consortium collection samples were from the superior frontal gyrus (Brodmann’s area (BA) 9) whereas those from extra and new collections were from the mid frontal gyrus (BA46). Another 184 controls were obtained as fresh-frozen brain tissue from the Banner Sun Health Research Institute (BSHRI). All BSHRI samples were from the frontal cortex. RNA was extracted from BSHRI samples by first homogenizing 20-50 mg of tissue in QIAzol (Qiagen) using the Lysin Matrix D and FastPrep-24 system (MPBiomedicals). Total RNA were then isolated using the miRNeasy Kit (Qiagen) according to manufacturer’s instructions. RNA integrity was assessed with Agilent Technologies RNA 600 nano kit. Samples with RNA Integrity Number (RIN) lower than 5.5 were excluded from the study. RNA sequencing libraries were prepared using TruSeq Stranded Total RNA sample prep kit with RiboZero Gold HMR (Illumina). Libraries were multiplexed (3 per lane) for paired-end 100 bp sequencing on Illumina HiSeq2000 with read depth >70 million reads on average. Genotyping was performed using two different platforms. 144 samples (SMRI Consortium and Array Collections) were genotyped using the Affymetrix GeneChip Mapping 5.0K Array. Genotypes were called with the BRLMM-p algorithm (Affymetrix) on all arrays simultaneously (107). The remaining samples (SMRI New and Extra Collection, and BSHRI samples) were genotyped on the Human PsychChip platform, which is a custom version of the Illumina Infinium CoreExome-24 v1.1 BeadChip (#WG-331-1111). However, PsychChip data were not yet available for this study.

#### Study 2 - BrainSpan

For the BrainSpan study (146), RNA-Seq data was generated from 606 brain samples from 41 unique individuals. RNA was extracted using RNeasy Plus Mini Kit (Qiagen) for mRNA. Either approximately 30 mg of pulverized tissue (12 PCW – 40 Y specimens) or entire amount of dissected brain piece (8 – 9 PCW, smaller than 30 mg) was processed. Tissue was pulverized with liquid nitrogen in a chilled mortar and pestle and transferred to a chilled safe-lock microcentrifuge tube (Eppendorf). Per tissue mass, equal mass of chilled stainless steel beads (Next Advance, cat# SSB14B) along with two

volumes of lysis buffer were added. Tissue was homogenized for 1 min in Bullet Blender (Next Advance # SSB14B) at speed 6 and incubated at 37°C for 5 min. Lysis buffer up to 0.6 ml was again added, tissue homogenized for 1 min and incubated at 37°C for 1 min. Extraction was further carried out according to manufacturer's protocol. Genomic DNA was removed by a proprietary column provided in RNeasy Plus Mini Kit (Qiagen) or by DNase treatment using TURBO DNA-free Kit (Ambion/ Life technologies). 260:A280 ratio and RNA Integrity Number (RIN) were determined for each sample with NanoDrop (Thermo Fisher Scientific) and Agilent 2100 Bioanalyzer system, respectively. The mRNA-sequencing (mRNA-Seq) sample preparation Kit (Illumina) was used to prepare cDNA libraries per manufacturer instructions with some modifications. Briefly, polyA RNA was purified from 1 to 5 µg of total RNA using Oligo (dT) beads. Quaint-IT RiboGreen RNA Assay Kit (Invitrogen) was used to quantitate purified mRNA with the NanoDrop 3300. Following mRNA quantitation, 2.5 µl spike-in master mixes, containing five different types of RNA molecules at varying amounts ( $2.5 \times 10^{-7}$  to  $2.5 \times 10^{-14}$  mol), were added per 100 ng of mRNA. Spike-in RNAs were synthesized by the External RNA Control Consortium (ERCC) by in vitro transcription of de novo DNA sequences or DNA derived from *B. subtilis* or the deep-sea vent microbe *M. jannaschii* and were a generous gift of Dr. Mark Salit at The National Institute of Standards and Technology (NIST). Each sample was tagged by adding two spike-in RNAs unique to the region from which the sample was taken. Further, three common spike-in RNAs with gradient concentrations were added to each sample, to enable the assessment of sequencing quality. Spike-in sequences are available at [http://archive.gersteinlab.org/proj/brainseq/spike\\_in/spike\\_in.fa](http://archive.gersteinlab.org/proj/brainseq/spike_in/spike_in.fa). The mixture of mRNA and spike-in RNAs was subjected to fragmentation, reverse transcription, end repair, 3' end adenylation, and adapter ligation to generate libraries of short cDNA molecules, followed by PCR amplification. The PCR enriched product was assessed for its size distribution and concentration using Bioanalyzer DNA 1000 Kit. Genotype data were not used in this study.

### Study 3 - CommonMind

Full details of the CommonMind study have been published (18), although the data here were processed separately according to the uniform RNA-Seq pipeline described below. Samples were acquired through brain banks at three institutions: The Mount Sinai NIH Brain Bank and Tissue Repository, University of Pennsylvania Brain Bank of Psychiatric illnesses and Alzheimer's Disease Core Center, and the University of Pittsburgh NIH NeuroBioBank Brain and Tissue Repository. Details about brain banks, inclusion/exclusion criteria, and sample collection and processing have been previously described (<https://www.synapse.org/#!Synapse:syn2759792/wiki/71104>). RNA-Seq data from 613 total human post-mortem dorsolateral prefrontal cortex (DLPFC) brain samples were obtained from 603 subjects with schizophrenia (n=263), bipolar disorder (n=47), affective disorder (8), and neurotypical controls (n=285), where 10 neurotypical controls were sequenced as technical replicates. Subjects with affective disorder were not used in this study. Total RNA was extracted from 50 mg of homogenized dorsolateral prefrontal cortex tissue using RNeasy kit. Samples with RIN < 5.5 (n=51) were excluded. The remaining samples had a mean RIN of 7.7. RNA-Seq library preparation was performed using ribosomal RNA depletion, with the RiboZero Magnetic Gold Kit. Samples were

barcoded, multiplexed (n=10/lane), and sequenced across two lanes as 100 bp paired end sequencing on the Illumina HiSeq 2500 with an average of 85 million reads. Data are provided for those samples that passed all of the following QC filters: samples were required to have had a minimum of 50 million total reads and less than 5% rRNA alignment. For genotyping, DNA was isolated from approximately 10 mg dry homogenized tissue coming from the same dissected samples as the RNA isolation using the Qiagen DNeasy Blood and Tissue Kit according to manufacturer's protocol. Genotyping was performed using the Illumina Infinium HumanOmniExpressExome platform (Catalog #: WG-351-2301). All data were checked for discordance between nominal and genetically-inferred sex using Plink software to calculate the mean homozygosity rate across X-chromosome markers and to evaluate the presence or absence of Y-chromosome markers. In addition, pairwise comparison of samples across all genotypes was done to identify potentially duplicate samples (genotypes > 99% concordant) or related individuals using Plink.

#### Study 4 - Yale-ASD

For the Yale-ASD study, RNA-Seq data was generated from 45 brain samples from 37 unique individuals, including 9 with ASD and 28 controls. Total RNA was extracted using mirVana kit (Ambion) with some modifications to the manufacturer's protocol. Approximately 60 mg of tissue was pulverized with liquid nitrogen in a pre-chilled mortar and pestle and transferred to a chilled safe-lock microcentrifuge tube (Eppendorf). Per tissue mass, equal mass of chilled stainless steel beads (Next Advance, catalog # SSB14B) along with one volume of lysis/binding buffer were added. Tissue was homogenized for 1 min in Bullet Blender (Next Advance) and incubated at 37°C for 1 min. Another nine volumes of the lysis/binding buffer were added, homogenized for 1 min, and incubated at 37°C for 2 min. One-tenth volume of miRNA Homogenate Additive was added and extraction was carried out according to the manufacturer's protocol. RNA was treated with DNase using TURBO DNA-free Kit (Ambion/ Life Technologies) and RNA integrity was measured using Agilent 2200 TapeStation System. Barcoded libraries for RNA-Seq were prepared with 5 ng of RNA using TruSeq Stranded Total RNA with Ribo-Zero Gold kit (Illumina) per manufacturer's protocol. Paired-end sequencing (100bp x 2) was performed on HiSeq 2000 sequencers (Illumina) at Yale Center for Genome Analysis. Genotype data was not yet available as part of Freeze 1 or 2 of the PsychENCODE dataset.

#### Study 5 - UCLA-ASD

For the UCLA-ASD study, RNA-Seq data was generated from 253 brain samples from 97 unique individuals, across prefrontal cortex (BA9/46), temporal cortex (BA41/42/22), and cerebellum. Full details of the UCLA-ASD study have been published (19). Brain samples were obtained from the Harvard Brain Bank as part of the Autism Tissue Project (ATP). Frozen brain regions were dissected on dry ice in a dehydrated dissection chamber to reduce degradation effects from sample thawing or humidity. Approximately 50-100 mg of tissue across the cortical region of interest was isolated from each sample using the miRNeasy kit with no modifications (Qiagen). For each RNA sample, RNA quality was quantified using the RNA Integrity Number (RIN) on an Agilent Bioanalyzer. Strand-specific, rRNA-depleted RNA-Seq libraries were prepared

using TruSeq Stranded Total RNA sample prep kit with RiboZero Gold (Illumina) kits. Libraries were randomly pooled to multiplex 24 samples per lane using Illumina TruSeq barcodes. Each lane was sequenced five times on an Illumina HiSeq 2500 instrument using high output mode with standard chemistry and protocols for 50 bp paired-end reads to achieve a target depth of 70 million reads. Genotyping data was generated at the UCLA Neurogenomics Core (UNGC) on the Illumina Omni 2.5 8v1 platform (Human Exome). Illumina Genome Studio files were clustered using Illumina's standard HapMap cluster file. SNP genotypes were exported from the Illumina GenomeStudio Software as forward strand in PLINK format. SNP marker names were updated with a conversion file from Illumina which converts local marker name to rsID (plink --update-map --update-name). All quality filtering was performed using PLINK v1.07. SNPs missing more than 99.99% data were excluded (--geno 0.9999). Individuals missing > 5% data, SNPs missing > 5% data, and SNPs with HW p<0.0000001 were also excluded. The order of filtering was performed according to PLINK default procedures (plink --mind 0.05 --geno 0.05 --hwe 0.0000001).

#### Study 6 - CMC\_HBCC

Brain specimens for the CMC\_HBCC study were obtained from the NIMH Human Brain Collection Core (HBCC; <https://www.nimh.nih.gov/labs-at-nimh/research-areas/research-support-services/hbcc/human-brain-collection-core-hbcc.shtml>) under protocols approved by the CNS IRB (NCT00001260), with the permission of the next-of-kin through the Offices of the Chief Medical Examiners in the District of Columbia, Northern Virginia, and Central Virginia. All specimens were characterized neuropathologically, clinically and toxicologically. A clinical diagnosis was obtained through family interviews and review of medical records by two psychiatrists based on DSM-IV criteria. Non-psychiatric controls were defined as having no history of a psychiatric condition or substance use disorder. Brain samples were dissected at the NIMH Human Brain Collection Core and shipped to Icahn School of Medicine at Mount Sinai (ISMMS) for sample preparation and RNA-sequencing. Samples for the study were dissected from either the left or right hemisphere of fresh frozen coronal slabs cut at autopsy from the dorsolateral prefrontal cortex. Total RNA from 468 HBCC samples was isolated from approximately 100 mg homogenized tissue from each sample by TRIzol/chloroform extraction and purification with the Qiagen RNeasy kit (Cat#74106) according to manufacturer's protocol. Samples were processed in randomized batches of 12. The order of extraction was assigned randomly with respect to diagnosis and all other sample characteristics. The mean total RNA yield was 24.2 ug. The RNA Integrity Number (RIN) was determined by fractionating RNA samples on the 4200 Agilent TapeStation System. Sixty nine samples with RIN <5.5 were excluded from the study. An additional 12 samples were removed post sequencing due to evidence of sample swap or contamination, resulting in a final dataset of 387 samples (70 BD, 97 SCZ, 220 neurotypical controls) with a mean RIN of 7.5 and a mean ratio of 260/280 of 2.0. RNA sequencing raw and quantified expression data is provided for these 387 samples from 387 unique individuals. Data was generated, QCed, processed and quantified as follows: All samples submitted to the New York Genome Center for RNA-Seq were prepared for sequencing in randomized batches of 94. The sequencing libraries were prepared using the KAPA Stranded RNA-Seq Kit with RiboErase (KAPA Biosystems). rRNA was

depleted from 1ug of RNA using the KAPA RiboErase protocol that is integrated into the KAPA Stranded RNA-Seq Kit. The insert size and DNA concentration of the sequencing library was determined on Fragment Analyzer Automated CE System (Advanced Analytical) and Quant-iT PicoGreen (Thermo Fisher Scientific) respectively. A pool of 10 barcoded libraries were layered on a random selection of two of the eight lanes of the Illumina flow cell at appropriate concentration and bridge amplified to ~ 250 million raw clusters. One-hundred base pair paired end reads were obtained on a HiSeq 2500. Genotyping was performed using Illumina\_1M, Illumina\_h650, and Illumina\_Omni5 platforms.

#### Studies 7+8 - BipSeq & LIBD\_szControl

Post-mortem tissue homogenates of dorsolateral prefrontal cortex (DLPFC) approximating BA46/9 in postnatal samples and the corresponding region of PFC in fetal samples were obtained from all subjects. Total RNA was extracted from ~100 mg of tissue using the RNeasy kit (Qiagen) according to the manufacturer's protocol. The poly-A containing RNA molecules were purified from 1 µg DNase treated total RNA and sequencing libraries were constructed using the Illumina TruSeq® RNA Sample Preparation v2 kit. Sequencing indices/barcodes were inserted into Illumina adapters allowing samples to be multiplexed across lanes in each flow cell. These products were then purified and enriched with PCR to create the final cDNA library for high throughput sequencing using an Illumina HiSeq 2000 with paired end 2x100bp reads. Further details are available in (108). SNP genotyping with HumanHap650Y\_V3, Human 1M-Duo\_V3, and Omni5 BeadChips (Illumina, San Diego, CA) was carried out according to the manufacturer's instructions with DNA extracted from cerebellar tissue. Genotype data were processed and normalized with the crlmm R/Bioconductor package separately by platform.

#### RNA-sequencing Data Processing Pipeline

All sample FASTQ files were run through a unified RNA-Seq processing pipeline (**Fig S1**) run at the University of Chicago on an OpenStack cloud system and modeled after the long-rna-seq-pipeline used by the ENCODE Consortium. Fastqs were trimmed for adapter sequence and low base call quality (Phred score < 30 at ends) using cutadapt (v1.12). Trimmed reads were then aligned to the GRCH37.p13 (hg19) reference genome via STAR (2.4.2a) using comprehensive gene annotations from Gencode (v19). BAM files were produced in both genomic and transcriptome coordinates and sorted using samtools (v1.3). Gene and isoform-level quantifications were calculated using RSEM (v1.2.29). Quality control metrics were calculated using RNA-SeQC (v1.1.8), featureCounts (v1.5.1), PicardTools (v1.128), and Samtools (v1.3.1). Pipeline source code can be found on Synapse at doi.org/10.7303/syn12026837.1 (109). RNA-Seq data was processed in two batches: Freeze 1 consisted of re-processed RNA-Seq data from the following studies: BrainGVEX, BrainSpan, CMC, UCLA-ASD, Yale-ASD, iPSC; Freeze 2 consisted of BipSeq, LIBD\_szControl, CMC\_HBCC, EpiGABA. Data from EpiGABA and iPSC studies was not used in this Capstone project.

#### Genotyping and QTL Pipeline

Genotype calls were generated at each data production site separately, as described above, and centralized for imputation. Genotype imputation and QTL analyses were

performed as described in a companion manuscript (17) and on the PsychENCODE website using a uniform genotype QC and imputation pipeline for all studies. To generate high-quality observed genotypes (removing low quality and rare variants), initial QC was performed using Plink to remove SNPs with zero alternate alleles, MAF <1%, genotyping call rate < 0.95, Hardy-Weinberg p-value < 1x10<sup>-6</sup>, individuals with genotyping call rate < 0.95, and to correct strand flips. Parallel haplotype pre-phasing and imputation were done using Eagle2, Minimac3 with the HRC reference panel for imputation. Calculation of gene-level expression QTLs (eQTL) and isoform-level expression QTLs (isoQTL) was done using QTLtools, as described in a companion manuscript (17). Imputation of C4A structural variation for each genotyped sample of European ancestry was performed using Beagle5 with a custom HapMap3 CEU reference panel as described (3). Inferred copy number of C4 structural elements (C4A, C4B, C4L, and C4S) based on the imputed C4 alleles was then associated with normalized C4A expression using a linear model.

#### RNA-Seq Quality Control and Normalization

Expected counts were compiled from gene and isoform-level RSEM quantifications and imported into R for downstream analyses. Genes were filtered to include those with TPM > 0.1 in at least 25% of samples. We removed all transcripts derived from mitochondrial DNA and Y-chromosome pseudoautosomal regions (“ENSR”) as well as transcripts with immunoglobulin (IG or TR) biotypes or those shorter than 250 bp. Downstream analyses were performed on the resulting 25,774 transcribed genes based on GENCODE V19 annotations. We restricted our analysis to frontal and temporal cortex brain samples obtained from subjects at postnatal time points (**Fig S2**). We removed samples with an ambiguous diagnosis or a diagnostic label other than ASD, SCZ, BD, or CTL (n=11). We removed samples with unspecified or ambiguous age (n=2), or sex (n=2) as well as samples with less than 10 million total reads. Each individual study was then assessed for outlier samples (**Fig S2C**), defined as those with standardized sample network connectivity Z scores < -2, as published, which were removed (91). We further removed 8 samples whose documented sex was discordant from that predicted by gene expression, based on hierarchical clustering of samples using expression of XIST and the first principal component of genes on the Y chromosome.

#### Covariate Selection

We compiled a set of 187 RNA-Seq quality control metrics as the aggregate sample-level outputs from RNA-SeQC, cutadapt, featureCounts, PicardTools (CollectAlignmentSummaryMetrics, CollectInsertSizeMetrics, CollectRnaSeqMetrics, MarkDuplicates), and STAR (**Fig S2**). As many of these metrics were highly overlapping, we summarized these measures by the top 29 principal components which collectively explained 99% of the total variance. To determine which covariates to include in the final differential expression model, we performed multivariate adaptive regression as implemented in the *earth* package in R. This builds a model in two phases using a forward pass to capture maximal amount of variance explained by an underlying set of covariates, followed by a backward (pruning) pass to remove potential redundant terms. The superset of potential covariates available for all samples included: diagnosis, age, study/batch, sex, PMI, RIN, libraryPrep, sequencing platform, strand specificity,

brain bank, brain region, ethnicity, along with all 29 seqPCs. For continuous variables, we also included squared terms. These covariates with input into the *earth* model along with gene expression data (limma voom normalized, centered, and scaled). The model was run using linear predictors and otherwise default parameters. As the model fits a maximum of 1000 features (genes) simultaneously, we performed 1000 permutations randomly subsetting 1000 genes at a time. From this, we chose as a set of known covariates those present in at least half of the resulting pruned models, which consisted of: diagnosis, age, age<sup>2</sup>, study/batch, sex, PMI, RIN, RIN<sup>2</sup>, brain bank, brain region, seqPCs (1-3, 5-8, 10-14, 16, 18-25, 27-29) and seqPC3<sup>2</sup>.

The above set contained known covariates (or those derived from known sequencing quality metrics) that contributed uniquely to variance in gene expression. However, these do not capture potential underlying hidden factors or confounders that may also influence gene expression. To ensure that DGE signal is not being driven by such hidden confounding factors, we performed surrogate variable analysis (SVA) on gene expression measurements (43). To determine the optimal number of SVs to include in our final model, we randomly split our dataset into equal halves and calculated differential expression for each gene and disorder using a fixed number of SVs (**Fig S3A**). We then compared the replicability of differential expression ( $\log_2\text{FC}$ ) effect sizes between the two split halves of the dataset, quantified using spearman's correlation. This analysis was repeated 1000 times each for a fixed number of SVs increasing from 0 to 25. We found that including 4 SVs in addition to the final set of known covariates above maximized this split-dataset replicability (**Fig S3**). As such, our final model used for all differential gene expression, isoform expression, and splicing analyses consisted of: diagnosis, age, age<sup>2</sup>, study/batch, sex, PMI, RIN, RIN<sup>2</sup>, brain bank, brain region, seqPCs (1-3, 5-8, 10-14, 16, 18-25, 27-29), seqPC3<sup>2</sup>, and SVs (1-4).

#### Differential Gene and Transcript Expression/Usage

Count level quantifications were corrected for library size using TMM normalization in *edgeR* and were transformed as  $\log_2(\text{CPM}+0.5)$ . DGE was then calculated using a linear mixed-effects model using the *nlme* package in R. The covariates specified in the previous section were included as fixed effects in the model. In addition, we included a random effect term for each unique subject to account for subject overlap across sequencing studies. Resulting P-values were FDR-corrected using the Benjamini-Hochberg method, to control for multiple comparisons. Differential transcript expression (DTE) was calculated similarly as for DGE except that the transcript-level quantifications from RSEM were used as inputs for the linear mixed-effects model. Finally, differential transcript usage (DTU) was calculated similarly as for DGE except that isoform percentage data reported by RSEM was used as inputs for the linear mixed-effects model.

To ensure the robustness of DGE results, we compared  $\log_2\text{FC}$  effect size measurements for genes identified as significantly differentially expressed in several previous studies profiling gene expression using cortical brain samples from ASD, SCZ, and BD (**Fig S4A-D**). Finally, to ensure that differential gene expression in disease was not being driven by subtle differences in RNA quality or degradation, we compared differential expression T-statistics with those experimentally derived from brain tissue samples allowed to degrade for fixed intervals of time (**Fig 4E**) (22). We did not observe

substantial concordance between these RNA degradation metrics and psychiatric disease DGE summary statistics.

#### Enrichment Analysis of Gene Sets

Enrichment for Gene Ontology (GO; biological process, molecular function and cellular component) and KEGG pathways was performed using the *gProfileR* R v0.6.4 package (110). Only pathways containing less than 1000 genes were assessed. Background was restricted to brain expressed genes. An ordered query was used, ranking genes by log<sub>2</sub>FC for DE analyses or by kME for co-expression module enrichment analyses. P-values were FDR corrected to account for multiple comparisons.

Enrichment analyses were also performed using several established, hypothesis-driven gene sets including: high confidence ASD risk loci (81); CHD8 targets (103); FMRP targets (33); mutationally constrained genes (104); syndromic and highly ranked (1 and 2) genes from the SFARI GENE database; ‘vulnerable’ ASD genes (105); genes with probability of loss-of-function intolerance (pLI) > 0.99 as reported by the Exome Aggregation Consortium (111). Statistical enrichment analyses were performed using logistic regression, correcting for both gene length and GC content. All results were FDR-corrected for multiple comparisons.

#### Cell Type Enrichment Analyses

Cell type enrichment analyses were performed using uniformly processed human brain single-cell RNA-Seq datasets, compiled by a companion manuscript (17) which combined multiple published datasets (98, 112-113) with newly generated data from PsychENCODE. Clustering was performed separately for single-cell datasets using TPM and UMI quantifications. See ref (17) for further details. Enrichment was performed for cell type specific marker genes using Fisher’s exact test, followed by FDR-correction for multiple testing.

For neural-immune modules (**Fig 7**), we additionally assessed several mouse experimentally derived cell type specific expression datasets. These included: a translating ribosome affinity purification (TRAP) dataset profiling 24 genetically identified populations of CNS cell types in mouse using microarray (114); a large-scale single-cell RNA-Seq dataset of mouse somatosensory cortex and hippocampus (101); a MARS-seq dataset of FACS-sorted CD45+ cells from mouse brain tissue, representing the major CNS immune cell populations (100); and a single cell RNA-Seq dataset of cells derived from meninges and choroid plexus in mouse (99).

#### Differential Local Splicing (DS) analysis

Local splicing analysis used LeafCutter (29), which detects splicing variation using the sequencing reads that span an intron (or spliced reads) to quantify intron usage across samples, without relying on existing reference annotations and without estimation of isoform abundance or exon inclusion levels. The same BAM alignment files to the hg19 genome assembly produced by STAR (version 2.4.2a) (115) for the DGE/DTE analyses were used as input for leafcutter intron clustering. The BAM files included the XS strand tags to all canonically spliced alignments based on their intron motifs (parameters: alignSJoverhangMin =8, outSAMstrandField =intronMotif). We used LeafCutter to first call clusters of variable spliced introns across all our samples and then to identify

differential splicing between each disorder (ASD, SCZ, and BD) and the control (CTL) group by jointly modeling intron clusters using the Dirichlet-Multinomial generalized linear model (GLM) (29). We controlled for the same technical, biological covariates and hidden confounds as described above in the DGE/ DTE analyses, except that we did not incorporate a random term for individuals (random effects are not supported by the Dirichlet-Multinomial GLM). Accordingly, we also removed tissue sample replicates that were sequenced in more than one study, randomly retaining only one sample in our analysis. The dataset for LeafCutter analysis numbered 944 controls, 79 ASD, 531 SCZ and 217 BD samples (1,771 total).

We used LeafCutter to call intron clusters as follows: overlapping introns, defined as spliced reads, were clustered and filtered to keep intron clusters supported by at least 50 split reads across all 1,771 samples, retaining introns of up to 100 kb and accounting for at least 1% of the total number of reads in the entire cluster. This yielded 37,215 clusters encompassing 120,921 introns in 17,342 genes that were used for further analysis. This intron count file was then used in the differential splicing (DS) analysis.

DS intron clusters were identified in pairwise analyses comparing each psychiatric disorder (ASD, BD, SCZ) to the common set of 944 control samples. After discarding introns that were not supported by at least one read in 5 or more samples, clusters were analyzed for DS if at least 3 samples in each comparison group (*i.e.* cases or controls) had an overall coverage of 20 or more reads. *P*-values were corrected for multiple testing using the Benjamini-Hochberg (BH) method and used to select clusters with significant splicing differences (FDR  $q < 0.1$ ).

Percent-spliced-in (PSI) values were corrected for covariates using the *quantify\_PSI* function provided in the LeafCutter *psi* branch (<https://github.com/davidaknowles/leafcutter/tree/psi>). Violin plots of intron PSI values were prepared using ggplot2. Principal component analysis (PCA) plots were evaluated before and after covariate-correction (**Fig S6**). Schematic visualization of significant intron clusters was done using the *leafviz* R shiny package [<https://davidaknowles.github.io/leafcutter/articles/Visualization.html>]. All DS events were further annotated using *leafviz* and custom R code, manually inspected, and classified into single- or multi-exon skipping events (changes in cassette splicing), alternative 5' and 3' exon usage, and alternative 5' (donor) or 3' (acceptor) splice site usage. Intron clusters that did not match any of these categories were classified as complex events involving multiple changes. DS intron clusters were mapped onto transcripts using *gViz* (v3.7) (111) and *ensemblDb* (v3.7) (<https://github.com/jotsetung/ensemblDb>) bioconductor R packages. SMART (117) and PFAM (118) protein domains were mapped onto transcript structures using the *proteinToGenome* function of *ensemblDb*.

#### DeltaPSI ( $\Delta$ PSI) Correlation Across Disorders

To determine significance for the correlation of  $\Delta$ PSI across disorders for significant intron clusters identified by LeafCutter, we permuted the case/control status within each disorder 3,000 times and repeated the LeafCutter analysis with the same GLM described above. In each permutation we assessed the  $\Delta$ PSI correlation between disorders using Spearman's correlation ( $\rho$ ) to yield a null distribution of  $\rho$  values that was used to assess the significance of the observed correlations.

### Cross-disorder DS Overlaps

For cross-disorder DS overlaps we selected all genes associated with significant intron clusters identified by LeafCutter at FDR <10%. Venn diagrams area-proportional to the number of genes with significant DS clusters in each disorder were then created using the *eulerr* R package. Hypergeometric p-values for pairwise overlaps between disorders were calculated using the *phyper* function in R and setting the size of the ‘universe’ to all genes with intron clusters meeting the LeafCutter clustering criteria.

### Functional Enrichment of DS Genes

Gene set enrichment for Gene Ontology (GO) biological process, molecular function and cellular component aspects was performed using the *gProfileR* v0.6.4 package in R (110) with moderate hierarchical filtering and using an ordered query, after ranking genes in increasing order of the LeafCutter p-value (*i.e.* most significant at the top). In case a gene had multiple significant intron clusters, the most significant cluster was used for the ranking. The custom background set for each disorder consisted of all 10,677 genes with intron clusters that were evaluated in pairwise LeafCutter analyses between each disorder and control groups, as described above. Visualization of enriched GO terms used custom *ggplot2* functions.

Gene-set enrichment for RBFOX1 targets (32), FMRP targets (33), and a curated list of genes coding for RNA binding proteins (RBPs) (34), used the same custom background of genes with LeafCutter intron clusters as in the GO enrichment analysis, and was assessed using Fisher’s exact test and correcting for multiple testing by FDR. The curated list of RBP genes included those with high confidence for RNA binding (119–121) and those annotated as RNA-binding in Ensembl including known and potentially auxiliary splice factors (34).

The comparison of LeafCutter DS events with Parikshak *et al.* 2016 (19) MATS events was based on genomic coordinates overlap using BEDtools, irrespective of the event type assigned by each algorithm.

### Microexon Enrichment

Transcripts that carry at least one exon of 3-27 nucleotides in length (*i.e.* microexon) (30) were extracted from the GENCODE V19 database. Statistical enrichment analyses were performed using logistic regression, correcting for both gene and transcript length on linear and log<sub>10</sub> scales. As an additional control, transcripts that carry exon(s) of average length (143±5% nucleotides) were also extracted and their overlap with switch transcripts was also tested with logistic regression. All results were FDR-corrected for multiple comparisons by the Benjamini-Hochberg method.

### Construction of Disease-specific Isoform-level Co-expressed PPI Networks

Pairwise spearman correlation coefficients (SCC) between transcript of interest and all other transcripts were calculated using either ASD samples or SCZ samples. To obtain age-balanced datasets, only samples from donors of age 17-67 years old were used. A cutoff of SCC > 0.5 was used to filter for the coexpressed partners of the transcript of interest in either ASD samples or SCZ samples. PPI data was compiled from well-characterized PPI databases, including Bioplex (122), HPRD (123), Inweb (124), HINT

(125), Biogrid (126), GeneMANIA (127), STRING (128) and CORUM (129). Only physical interactions and co-complex associations were kept. Coexpressed partners which are also supported by PPI were used to construct the coexpressed PPI network.

### ncRNA Annotation

To identify ncRNAs that may be relevant to neuropsychiatric disorders, we compiled a list of non-protein-coding genes exhibiting differential gene (DGE) or transcript expression (DTE) at  $FDR < 0.05$  in at least one disorder (**Table S2**). As ncRNA designation can change based on genomic annotation, we filtered out genes that were designated as protein coding in the most recent version of Gencode v27, yielding a total of 944 unique ncRNAs, many of which were differentially expressed across more than one disorder or at both gene and transcript-level features. Differentially expressed ncRNAs were annotated according to sequence and expression characteristics. Human tissue-specific expression was assessed using data from GTEx v6. Median RPKM values per tissue were obtained and averaged into broad categories (**Fig 1F**). To identify ncRNAs broadly expressed across human tissues, we ran an ANOVA on  $\log_2(RPKM + 1)$  values across tissues, and selected those with uncorrected  $P > 0.05$ . Brain-specific expression was defined as  $RPKM_{\text{brain}} / \sum(RPKM_{\text{all tissues}}) > 0.8$ . CNS cell type specificity was assessed in a similar fashion using single-nucleus RNA-Seq from the Lake et al. dataset (98). Expression counts were CPM normalized and then averaged together across defined cell clusters. We ran an ANOVA on  $\log_2(CPM + 1)$  values across cell clusters, and report those ncRNAs with  $P > 0.05$  as “broadly expressed” with regard to cell type. Cell type specificity was quantified by  $CPM_{\text{max cluster}} / \sum(CPM_{\text{all cell clusters}}) > 0.8$ .

Evolutionary conservation was assessed using phastCons and phyloP scores (92, 93). Both methods assign a score to each base in the human genome, quantifying its degree of conservation across selected species. Whereas phastCons base scores are smoothed according to scores of neighboring bases, phyloP evaluates each base independently. We downloaded phastCons and phyloP per-base scores for hg19 from UCSC, computed from 17-way (primate), 30-way (mammalian), and 100-way (vertebrate) Multiz alignments, to calculate a mean base score for each ncRNA across 1) the gene, and 2) its exonic regions only. The per-exon scores were averaged over all exons belonging to a gene to produce a more robust metric for gene conservation.

Context-dependent tolerance (CDTS) scores were used to quantify patterns of human selective constraint (27). CDTS scores are computed for each 10bp window in high-confidence regions of the genome, which we intersected with exonic coordinates for ncRNAs using Bedtools (130). To produce a per-gene score, we first computed the mean across all 10bp windows intersecting a single exon, then averaged the mean exon scores across all exons for a gene.

### Signed Gene and Isoform Co-Expression Network Analysis

To place results from individual genes within their systems-level network architecture, we performed weighted gene correlation network analysis (WGCNA) separately for gene- and isoform-level quantifications (50). All covariates except for diagnostic group were first regressed from our expression dataset. Network analysis was performed with the WGCNA package using signed networks. A soft-threshold power of

<sup>7</sup> was used for all studies to achieve approximate scale-free topology ( $R^2 > 0.8$ ). Networks were constructed using the blockwiseModules function. The network dendrogram was created using average linkage hierarchical clustering of the topological overlap dissimilarity matrix (1-TOM). Modules were defined as branches of the dendrogram using the hybrid dynamic tree-cutting method. Modules were summarized by their first principal component (ME, module eigengene) and modules with eigengene correlations of  $> 0.9$  were merged together. A robust version of WGCNA (rWGCNA) was run to reduce the influence of potential outlier samples on network architecture (94). Module robustness was ensured by randomly resampling (2/3 of the total) from the initial set of samples 100 times followed by consensus network analysis, a meta-analytic approach, to define modules using a consensus quantile threshold of 0.2. Modules were defined using biweight midcorrelation (bicor), with a minimum module size of 50, deepsplit of 4, merge threshold of 0.1, and negative pamStage. Module (eigengene)-disease associations were evaluated using a linear mixed-effects model, using a random effect of subject, to account for subject overlap across datasets. Significance values were FDR-corrected to account for multiple comparisons. Results from module-eigengene association tests are shown in **Fig 5**. Genes within each module were prioritized based on their module membership (kME), defined as correlation to the module eigengene. The top 'hub' genes for several of the modules are shown in **Figs 5-7** and through an interactive portal on our companion website (Resource.PsychENCODE.org).

The robustness of all network modules was tested as described previously (49). In brief, each module's density (defined as the average intramodular topological overlap) was compared to the density of modules of equivalent size selected randomly from the same network ( $n = 5,000$  permutations). Density p-values were determined for each initial module by calculating the percentage of trials in which the density of the "random" modules exceeded the density of the initial module. All modules have density p-values less than 0.05.

### csuWGCNA

We also used a modified version of WGCNA named *Combination of Signed and Unsigned WGCNA* (csuWGCNA), which captures strong and moderate negative correlations in the co-expression network (73). Current versions of WGCNA allow unsigned, signed and signed hybrid options for network types, but have disadvantages when trying to capture moderate negatively correlated features such as lncRNA-mRNA regulatory relationships. Signed and signed hybrid networks down-weight negatively correlated pairs in network. Unsigned networks highlight strong positive and negative correlations, but has worse performance on identifying functionally-related gene pathways than its signed counterparts (131). To address these limitations, we modified two functions for picking soft thresholding power and calculating the network adjacency. The core modification of csuWGCNA is in its definition of adjacency,  $a_{ij} = ((1 + |\text{cor}(x_i, x_j)|)/2)^\beta$ , which integrates the advantages of signed networks ( $a_{ij} = |(1 + \text{cor}(x_i, x_j))/2|^\beta$ ) and unsigned networks ( $a_{ij} = |\text{cor}(x_i, x_j)|^\beta$ ). Using this adjacency function, csuWGCNA then constructs a topological overlap matrix (TOM) and follows the procedure described above for clustering, tree cutting, and network module detection. Using this method, csuWGCNA can detect modules containing genes with negative correlations, which may be more useful when lncRNAs and miRNAs are included in the network (**Fig S14**).

### Assessment of Psychiatric Medications

To assess the potential impact of medications on differential expression and co-expression results, we analyzed several published datasets of animal models exposed to multiple classes of psychiatric medications. These included: 1) a published RNA-Seq dataset of the DLPFC from non-human primates exposed for six months to haloperidol, clozapine, or placebo (18); 2) a published microarray dataset (GSE66276) of cortex from mice exposed to the SSRI fluoxetine for 21 days (132); 3) a microarray dataset (GSE66276) of rats exposed lithium, lamotrigine or placebo for 21 days. All datasets were reprocessed and analyzed as described below.

The antipsychotic dataset consisted of ~6 year old rhesus macaques treated with medications or placebo orally for six months, including high doses of haloperidol (4 mg/kg/d; n=7), low doses of haloperidol (0.14 mg/kg/d; n=10), clozapine (5.2 mg/kg/d; n=9), or vehicle (n=8). DLPFC tissue was extracted and RNA-Seq was run using rRNA-depleted libraries. Genes were kept that had expression greater than 0.1 cpm (counts per million) in at least half of samples. Limma voom normalization using TMM normalization factors was used for subsequent differential gene expression analysis, including the covariates: age, sex, sequencing batch factors, RNA quality statistics (RIN and RNA concentration) and sequencing statistics. In accordance with results from (18), none of the groups (clozapine, haloperidol\_low\_dose, and haloperidol\_high\_dose) had any genes significantly differentially expressed from placebo after FDR-correcting for multiple comparisons. We therefore used an unadjusted p-value threshold of 0.01 for downstream analyses, resulting in 133, 120, and 188 genes for clozapine, haloperidol\_low\_dose, and haloperidol\_high\_dose, respectively. Genes were grouped based on direction of effect (up or downregulated) and mapped to human orthologues using Ensembl. Overlap with PsychENCODE disease gene sets (DE and DS genes, gene and isoform-level co-expression modules) was assessed using Fisher's exact test followed by FDR correction. Although some gene sets showed nominal overlap with antipsychotic genes, no enrichments were significant after correction for multiple comparisons (**Fig S11**).

In the SSRI dataset (132), thirty mouse strains were treated for 21 days with fluoxetine (18 mg/kg per day) or vehicle, cortical RNA was extracted and profiled with an Affymetrix expression microarray (GeneChip Mouse Genome 430 2.0 array). Raw microarray data was normalized using the RMA function from the 'affy' package in R. Batch correction was performed using ComBat, and differential expression was detected using the lmFit and eBayes functions from the 'limma' R package (covariates for the linear model: fluoxetine treatment, strain, and RNA degradation score). In our analysis, only two genes were found to be significantly differentially expressed (downregulated) in the fluoxetine group after correction for multiple comparisons (FDR p-value < 0.05): SST, a hormone regulating factor, and FDFT1, an enzyme involved in cholesterol biosynthesis. For downstream enrichment analyses, we used the relaxed threshold of p < 0.01 (uncorrected), corresponding to 558 genes.

In the third dataset (GSE66276), rats (n=5 per group) were administered lithium in chow (0.2%) or lamotrigine via subcutaneous injection (30 mg/kg) and compared to a vehicle chow group or vehicle injection group. All regimens were administered once daily for 21 days and tissues were collected from frontal cortex, striatum, and

hippocampus for analysis via an Affymetrix expression microarray (Affymetrix Rat Genome 230 2.0 Array). Differential expression analysis was performed as described above. For lamotrigine, no genes were differentially expressed following FDR-correction, so for downstream enrichment analyses we used the relaxed threshold of  $p < 0.01$  corresponding to 121 genes. For lithium, 2338 genes at FDR-corrected  $p < 0.05$  were used for downstream enrichment analyses.

### Assessment of Non-linear Age Effects

To assess the influence of age on the magnitude of differential expression, and to account for potentially non-linear effects of age, we performed a local regression analysis using the ‘locfit’ package in R. For each gene expression measure, a local regression function was fit to model the effect of age on expression in control samples, as follows:

```
fit = locfit(Expr ~ Age, data=df[df$Group=="CTL", ]).
```

For each non-control sample, expression was then converted to a Z-score using the interpolated mean expression in controls at the same age. We then assessed the correlation between z-transformed expression and age within each disease group (ASD, SCZ, BD) separately, to identify those genes whose magnitude of differential expression was associated with age. Several examples are shown in **Fig S10**.

### GWAS Datasets

We performed a number of GWAS enrichment analyses as described in the following sections. In each analysis, we used summary statistics from the largest publicly available GWAS in SCZ (59), ASD (38), and BD (97). Additional secondary analyses were performed using a variety of relevant traits, including major depressive disorder (MDD; ref (133)), neuroticism (134), educational attainment (135), diabetes (136), as well as previous GWA studies of SCZ (137), ASD (138), and BD (139).

### GWAS Enrichment in DE Genes and Modules

We used stratified LD score regression (s-LDSR) (39) to investigate whether differentially expressed or spliced genes, and/or co-expression modules, are enriched for disease-associated genetic variation using the summary statistics described above. SNPs were assigned to these custom gene categories if they fell within  $\pm 10$  kb of a gene in the set. These categories were added to a ‘full baseline model’ that includes 53 functional categories capturing a broad set of genomic annotations, as published (39). Enrichment was calculated as the proportion of SNP heritability accounted for by each module divided by the proportion of total SNPs within the module. Significance was assessed using a block jackknife procedure, followed by FDR correction of P values.

### Polygenic Risk Score Calculation

Polygenic risk scores (PRS) were calculated using the same GWAS summary statistics as above, for SCZ (59), BD (97) and ASD datasets (38). Samples were restricted to those of European ancestry based on clustering with samples from HapMap3 (140). Genotypes were additionally filtered as follows, using plink: `plink --bfile PECDC_EUR --geno 0 --maf 0.05 --hardy --hwe 1e-40 --make-bed -out PECDC_EUR_PRSfilter`. To calculate PRS, we used LDpred (95) with the 1000 Genomes phase 3 European subset as a reference panel. The first five genotype principal components (gPC1-5, as calculated with plink) were included in the PRS calculation, to

account for ancestry and technical effects. We then compared PRS for each diagnostic group with the strict set of non-psychiatric controls, contrasting baseline and full models. PRS significance was measured with a likelihood ratio test and Nagelkerke's pseudo-R<sup>2</sup>.

```
mod.baseline=glm(dx~study+sex+age+gPC1+gPC2+gPC3+gPC4+gPC5,family=binomial)
mod.full=glm(dx~PRS+study+sex+age+gPC1+gPC2+gPC3+gPC4+gPC5,family=binomial)
adjustedR2=NagelkerkeR2(mod.full)$R2-NagelkerkeR2(mod.baseline)$R2
prs.significance=lrtest(mod.baseline, mod.full)
```

The default LDpred GWAS p-value thresholds were used (.001, .003, .01, .03, .1, .3, 1, and Inf). Maximal Nagelkerke pseudo-R<sup>2</sup> values were achieved for prediction of psychiatric diagnosis using thresholds of 0.001 for ASD, 0.01 for BD, and 1 for SCZ. Association between PRS and measures of gene, isoform, or module (eigengene) expression was performed as described above, except using linear regression analogs. Figure 3 shows those genes/isoforms exhibiting genome-wide significant association with PRS defined with the GWAS p-value thresholds listed above which maximally separated cases from controls in our cohort. For completeness, full results at all p-value thresholds are compiled in **Table S4**.

#### Transcriptome-wide Association Study (TWAS)

To identify genes whose *cis*-regulated expression is associated with disease, we performed a transcriptome wide association study (TWAS) to identify putative molecular (e.g., *cis*-eQTL) phenotypes in brain underlying disease GWAS associations (46). TWAS was implemented using the fusion package ([https://github.com/gusevlab/fusion\\_twas](https://github.com/gusevlab/fusion_twas); (46)) with custom SNP-expression weights generated from brain using our dataset of 1321 unique individuals with imputed genotypes. Using the AI-REML algorithm implemented in GCTA (96) by the fusion package, we first identified the subset (n=14,750) of total expressed genes found to have significant *cis* SNP-heritability in our dataset (*cis*-  $h^2_g$  P<0.05 within 1 Mb window around the gene body). SNP-expression weights were calculated in a 1Mb region around all heritable genes using expression measurements adjusted for diagnosis, study, age, age<sup>2</sup>, RIN, RIN<sup>2</sup>, sex, tissue, PMI, 20 ancestry PCs, and 100 hidden covariates (141). Accuracy of five expression prediction models were tested (best *cis*-eQTL, best linear unbiased predictor, Bayesian linear mixed model, Elastic-net regression, LASSO regression) using the most accurate model for final weight calculations as implemented in fusion. TWAS disease-association statistics were computed using these custom weights, LD structure calculated from our PsychENCODE samples' genotypes, and disease GWAS summary statistics described above. For each disease, TWAS association statistics were Bonferroni-corrected for multiple comparisons. At loci (+/- 100 kb) with multiple significant associations, joint and conditional association analyses were further performed as implemented in the FUSION.post\_process.R script. Full results are compiled in **Table S4**.

#### Summary-data based Mendelian Randomization (SMR)

As a corollary to TWAS, we ran summary based mendelian randomization (SMR) and the associated HEIDI test (48) to identify potential pleiotropic associations among eQTL and GWAS signals. To match the data used in TWAS, we recomputed *cis* eQTLs using expression measurements adjusted for diagnosis, study, age, age<sup>2</sup>, RIN, RIN<sup>2</sup>, sex, tissue, PMI, 20 ancestry PCs, and 100 hidden covariates (141). The set based SMR test

was run (--smr-multi) using SNPs in the *cis*-window with  $P_{eql} < 10^{-5}$  (--peql-smr 1e-5). Of note, we observed highly significant concordance between TWAS Z-scores and SMR beta values across all loci for each disease GWAS (all R's  $> 0.75$ ,  $P < 10^{-16}$ ). For replication of genome-wide significant TWAS associations, we required that genes exhibit significant SMR association ( $P_{SMR} < 0.05$ ), pass the HEIDI test ( $P_{HEIDI} > 0.05$ ), with concordant direction of effect.

### Integration of TWAS, PRS, and SMR Results

As described above, GWAS candidate gene prioritization was performed using three separate methods – TWAS, SMR, and correlation with PRS, each with slightly different assumptions and interpretations. Notably, the “background” set of genes assessed was different for each method, as TWAS was restricted to genes with evidence of significant *cis*-heritability ( $n=14,750$ ), SMR was assessed for each gene with nominal  $P_{eQTL} < 10^{-5}$ , and PRS correlations were assessed for all genes and isoforms considered expressed in our dataset. To integrate resulting candidate gene associations, and identify those with concordant associations across multiple methods, we required the following: (1) genome-wide significant association (e.g., Bonferroni corrected  $P < 0.05$ ) from at least one method; (2) significant replication by a second method at  $P < 0.05$ ; (3) consistent direction of effect. For TWAS, we further required that genome-wide significant associations also exhibit joint/conditional significance, for loci with multiple hits. For significant SMR associations, genes were also required to pass the HEIDI test ( $P_{HEIDI} > 0.05$ ). Together, these analyses identified 5, 11, and 64 candidate genes supported by multiple methods in ASD, BD, and SCZ, respectively (**Table S4**).

### Rare Variant Enrichment Analyses

Gene and isoform co-expression modules were also assessed for enrichment of rare variants identified in disease, compiled from several datasets. These included: 71 risk loci harboring rare *de novo* variants associated with ASD through the transmission and *de novo* association test (TADA) (81); Syndromic and highly ranked (1 and 2) genes from SFARI Gene database; genes harboring recurrent *de novo* copy-number variants associated with ASD or SCZ, as defined in (13); genes harboring an excess of rare exonic variants in ASD, SCZ, intellectual disability (ID), developmental delay (DD), and epilepsy as assessment through an extended version of TADA (extTADA) (142); genes harboring disruptive and damaging ultra-rare variants (dURVs) in SCZ (55); a list of high confidence epilepsy risk genes, compiled in (143). For binary gene sets, enrichment among gene and isoform modules was calculated using logistic regression, correcting for linear- and log-transformed gene and transcript lengths as well as GC content. For dURVs, a two step procedure was used, first creating a logistic regression model for dURV genes identified in controls and a second model for those affected in cases and controls. A likelihood ratio test was used to calculate significance. Finally, for the extTADA datasets, the posterior-probability (PP) was used in the logistic regression model in place of a binary annotation. P-values were FDR-corrected for multiple comparisons. Results are shown in **Fig S13** and compiled in **Table S5**.

### Experimental Validation

Initial optimization of the PCR conditions for all splicing and isoform primers used cDNA samples derived from total brain or cortex RNA (Clontech), and were performed on a Mastercycler Nexus Gradient Thermal Cycler (Eppendorf) and amplicons resolved on precast 96-well 2% agarose E-Gels (Invitrogen) stained with SYBR safe.

#### Splicing validation

For differential splicing (DS) analysis, selected exon-skipping events were validated by semiquantitative RT-PCR in ASD, BD, SCZ, and control samples. Total RNA (1-2 µg) was treated with 1 unit of Baseline-ZERO DNase (Lucigen), cleaned up with 1.8x AMPure XP (Beckman Coulter), and reverse-transcribed using SuperScript III reverse transcriptase and random hexamer primers (Invitrogen). After clean-up with 1.8x AMPure XP, DS events were PCR amplified from 20 ng of cDNA for 30 cycles in 25 µL volume containing exon-specific primers at a concentration 0.5 µM each, and ChoiceTaq Blue MasterMix (Denville) according to manufacturer instructions. Exon-specific PCR primers (**Table S8**) were designed in the flanking exons of each skipping event using Primer3 (144) and BLAST (145). PCR products were cleaned up with 1.8x AMPure XP (Beckman Coulter) and analyzed on DNA 1000 chips on an Agilent 2100 Bioanalyzer system. Peaks corresponding to the amplicon including or excluding the skipped exon were quantified using the Bioanalyzer Expert software, and percent spliced in (PSI) ratios were calculated by dividing the molarity of the lower band (exon skipped) by the sum of the molarity of the lower and upper band (exon included). The ΔPSI between cases and control for each event was calculated as the difference between the average PSI in cases and average PSI in controls. Sample details and primers are reported in **Table S8**.

#### Isoform Validation

For DTE analysis, selected isoforms were validated by semiquantitative RT-PCR using a similar approach as for DS. Each isoform was PCR amplified from 20 or 40 ng of cDNA for 30 or 35 cycles in a 25 µL volume containing isoform-specific primers at a concentration 0.5 µM each and ChoiceTaq Blue MasterMix with DNA polymerase (Denville), or 0.4 µM each and LongAmp Hot Start Taq DNA polymerase (New England Biolabs) (**Table S8**), according to manufacturer instructions. Isoform-specific PCR primers (**Table S8**) were designed using Primer3 (144) and BLAST (145), and based on GENCODE v19 annotations. PCR products were resolved on 1.5 or 2% agarose gels, counterstained with GelStar Nucleic Acid Gel Stain (Lonza) for visualization, and *GAPDH* and *ACTB* were used as loading controls. Gels were quantified using ImageLab (BioRad). The intensity of each isoform was first normalized to the average expression levels of *GAPDH* and *ACTB* in each sample. The intensity ratio between cases and controls for each isoform was then calculated by dividing the average intensity of cases by the average intensity of controls. The log<sub>2</sub> intensity ratios were then compared to the log<sub>2</sub> ratio differences from the DTE analysis. Sample details and primers are reported in **Table S8**.

#### Fluorescent in situ hybridization (FISH)

Fresh-frozen tissue blocks from the Brodmann's area 9 of the prefrontal cortex of five neurologically normal control donors were obtained from the Mount Sinai Neuropathology Research Core and Brain Bank and stored at -80°C. Clinical information

on the subjects is summarized in **Table S9A**. The blocks were embedded in O.C.T. compound, frozen at -20°C, 10 µm-thick sections were cut using a cryostat (Leica), and the sections were collected onto Superfrost Plus slides. The slides were stored in an airtight box at -80°C until FISH was conducted.

The *in situ* hybridization probes for detecting human *GAD1*, *LINC00643*, and *LINC01166* as well as the positive and negative control probes were designed by Advanced Cell Diagnostics (ACD; see **Table S9B** for RNAscope probe information). For the assay, we used RNAscope Multiplex Fluorescent Reagent Kit v2 (ACD), that provided the hydrogen peroxide, protease IV, amplification reagents (Amp1-3), HRP reagents, and wash buffer for probe hybridization. DAPI, TSA buffer (ACD) and TSA Plus fluorophores (PerkinElmer) were used for detection of the signal. We used a modified version of the manufacturer's protocol for sample preparation, probe hybridization, and signal detection. Briefly, the fresh frozen sections on slides were retrieved from -80°C and immediately fixed by immersion in freshly prepared cold 4% paraformaldehyde for 2 h. After fixation, the sections were rinsed briefly with phosphate buffered saline (PBS) and then dehydrated in an ethanol series (5 min each in 50%, 70%, and two changes of 100% ethanol) at room temperature (RT). The sections were air-dried for 5 min and a hydrophobic barrier was created around the section using an Immedge pen (Vector Laboratories). After the barrier had completely dried, the sections were treated with hydrogen peroxide for 10 min at RT, washed twice with PBS, treated with protease IV for 15 min at RT, and washed twice with PBS. The LINC-C2 or LINC-C3 probes for detecting lncRNAs were diluted at 1:50 in the *GAD1*-C1 probe. The sections were then hybridized with the probes at 40°C for 2 h in the HybEZ Hybridization System (ACD), washed twice with wash buffer, and stored overnight at RT in 5x SSC buffer. The next day, the slides were rinsed twice with wash buffer, followed by the three amplification steps (AMP 1, AMP 2, and AMP 3 at 40°C for 30, 30, and 15 min respectively, with two washes of 2 min each with wash buffer after each amplification step). The signal was developed by treating the sections in sequence with the HRP reagent corresponding to each channel (e.g. HRP-C1) at 40°C for 15 min, followed by the TSA Plus fluorophore assigned to the probe channel (fluorescein for *GAD1*-C1 probe and cyanine 5 or Cy5 for LINC-C3 probes, prepared at a dilution of 1:750) at 40°C for 30 min, and HRP blocker at 40°C for 15 min, again with two wash steps after each of the incubation steps. As autofluorescence due to lipofuscin was detected in both the green and the red channels whereas the far red channel was relatively free of background, the highly expressed *GAD1*-C1 probe was assigned to the green fluorescein channel, the red cyanine 3 channel was left empty and the lncRNAs were probed on separate sections in the far red Cy5 channel. The sections were treated with TrueBlack Lipofuscin Autofluorescence Quencher (Biotium) for 30 s, rinsed twice with PBS, counterstained with DAPI for 30 s, mounted using ProLong Gold mounting medium (Thermo Fisher Scientific) and slides were stored at 4 °C until ready for imaging. Two experiments were performed with two to three biological replicates each, and using positive and negative control probes to test for RNA quality and background signal respectively.

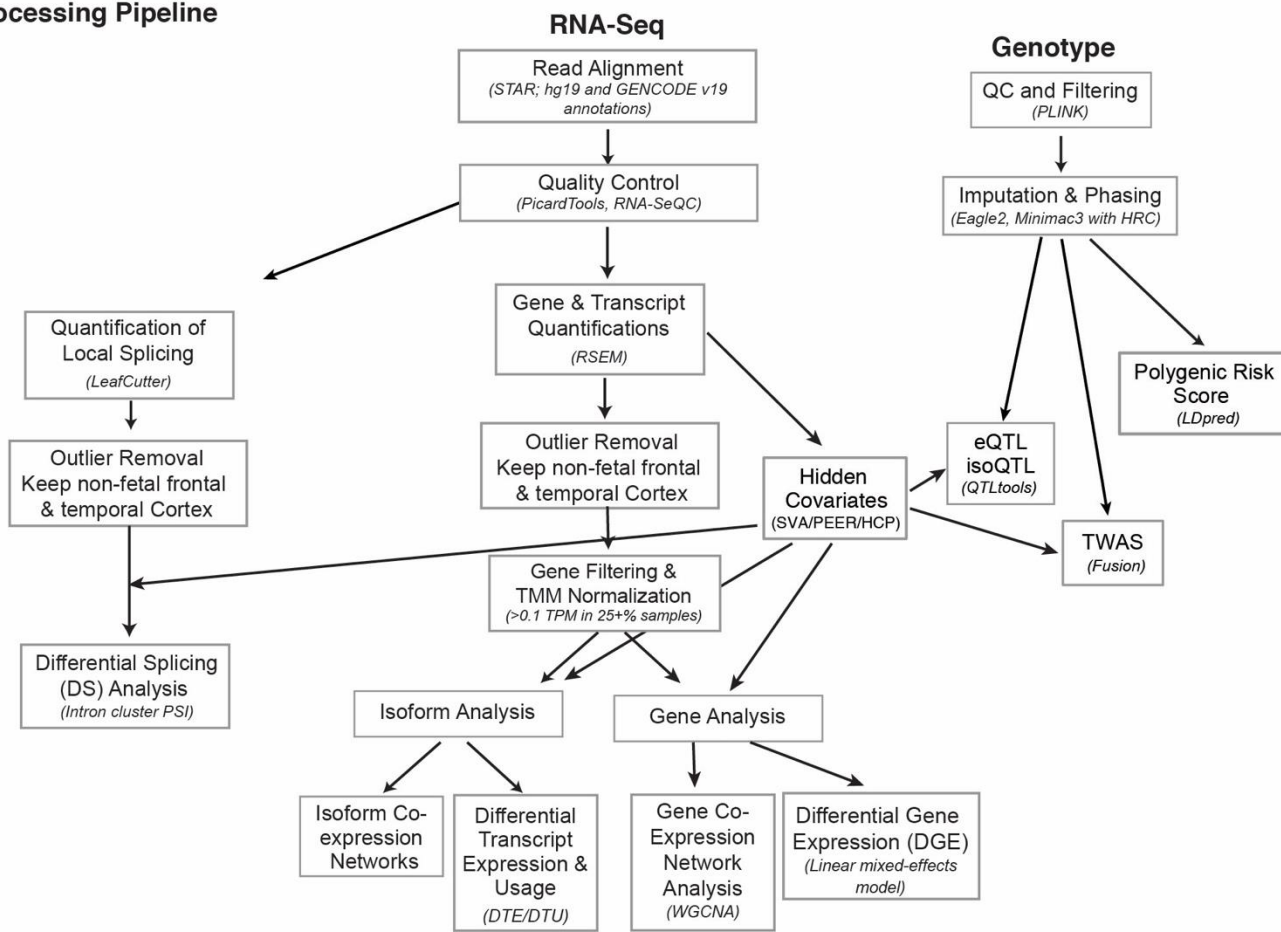
Layer III of area 9 was identified using a 5x/0.16 N.A. objective and the sections were imaged using a 63x/1.4 N.A. or 100x/1.4 N.A. oil DIC Plan Apochromat objectives on an AxioImager.M2 microscope (Carl Zeiss), equipped with a motorized stage (MBF Biosciences) and an Orca-R<sup>2</sup> digital camera (Hamamatsu), and operated using

Neurolucida software (version 11.11.3 64-bit, MBF Biosciences). Camera exposure times were set for each of the four channels (red for lipofuscin, blue for DAPI, green for fluorescein, and magenta for Cy5) and were kept similar among the cases imaged in each experiment in order to enable comparison. The images at 100x magnification were presented as maximum intensity projections of Z-stacks imaged at 0.5  $\mu\text{m}$  intervals. Adobe Photoshop was used for adjusting brightness/contrast and sharpness of the images.

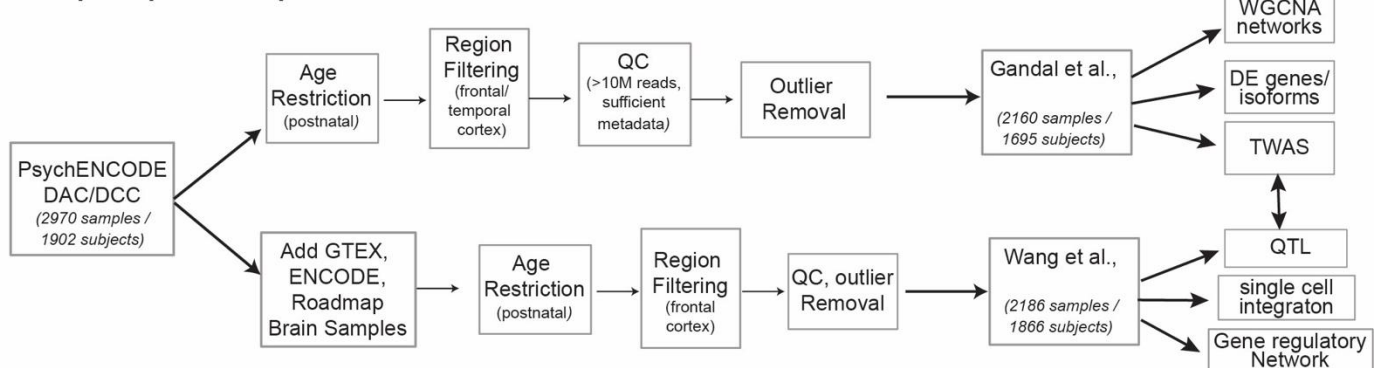
## A Individual Studies

Dataset	Groups	Samples in Dataset	Samples in final analysis	Tissue	Library	Stranded	RNAseq protocol	Platform	Genotyping Platform	Published / Reference
BrainGVEX	SCZ BD CTL	430	409	DLPFC	rRNA - dep	stranded (reverse)	100bp Paired End	HiSeq 2000 / 2500 / 4000	Affy 5.0 and Illumina PsychChip	153 samples included as replication in PMID 29439242
BrainSpan	CTL	606	163	many	polyA	unstranded	76bp Single End	GAIIX	N/A	Companion Manuscript
Common Mind	SCZ BD CTL	613	572	BA9/46	rRNA - dep	unstranded	100bp Paired End	HiSeq2000	Infinium Human Omni Express Exome	PMID 27668389
UCLA -ASD	ASD CTL	253	151	BA9/46, BA41, CBL	rRNA - dep	unstranded	50bp Paired End	HiSeq2000	Infinium Omni 2.5 Exome, Infinium Omni 2.5	PMID 27919067
Yale -ASD	ASD CTL	45	12	DLPFC, TC, V1, CBL	rRNA - dep	stranded (reverse)	100bp Paired End	HiSeq2500	N/A	Unpublished
BipSeq	BD	69	65	BA9/46	polyA	unstranded	100bp Paired End	HiSeq2000	Illumina_1M, Illumina_h650	Unpublished
LIBD szControl	SCZ CTL	495	422	DLPFC	polyA	unstranded	100bp Paired End	HiSeq2000	Illumina 1M, Illumina_h650, Illumina_Omni5	PMID 30050107
CMC_HBCC	SCZ BD CTL	387	366	DLPFC	rRNA - dep	stranded	100bp Paired End	HiSeq2500	Illumina 1M, Illumina_h650, Illumina_Omni5	Unpublished

## B Processing Pipeline

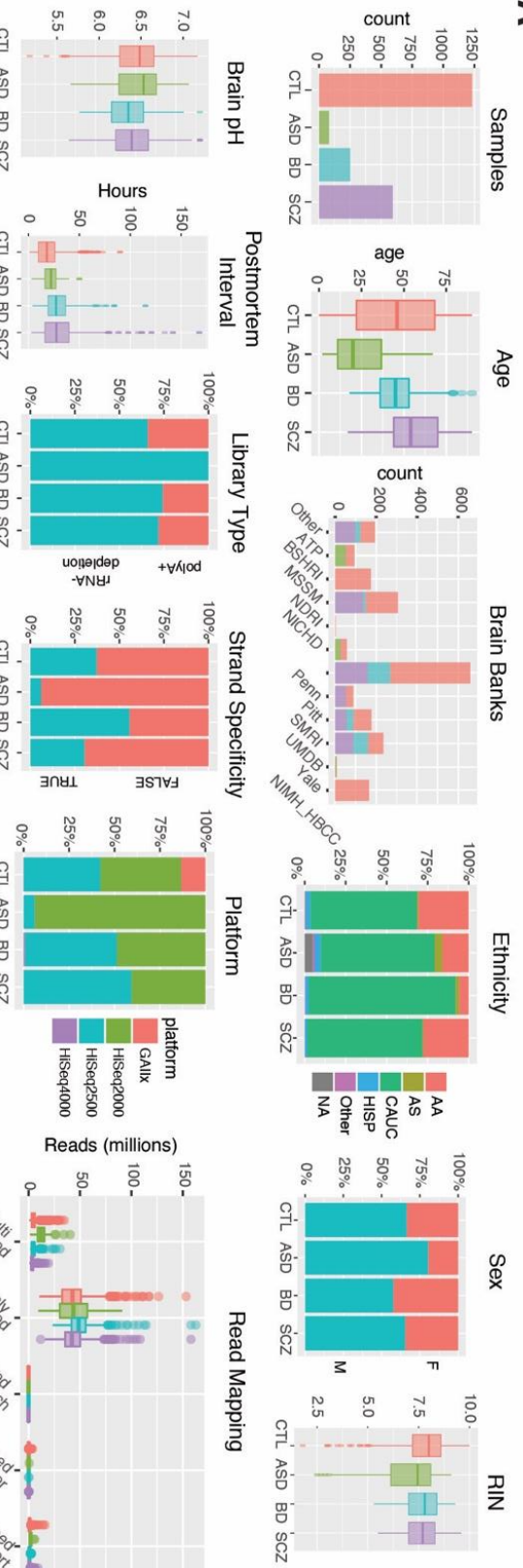


## C RNA-Seq Sample Overlap

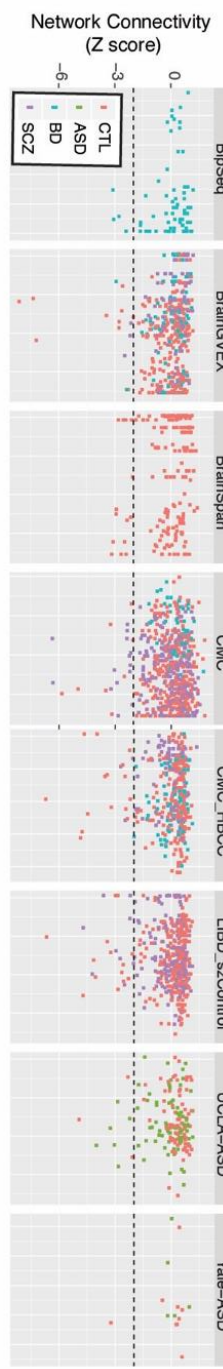
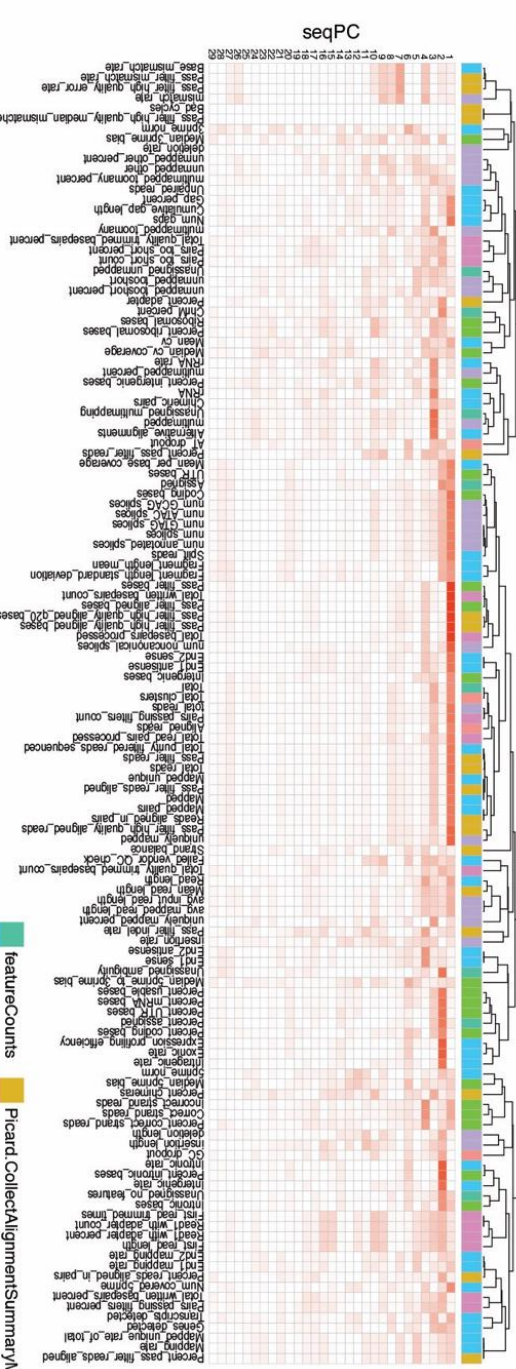


**Fig. S1. Dataset composition, analysis and integration pipeline**

A) Description of individual studies contributing to this PsychENCODE analysis. B) Analysis pipeline through which all samples were uniformly processed. C) Comparison of samples overlapping between this manuscript and a companion paper (17).

**A****B**

## Expression PC loadings

**C****D**

Spearman Rho  
Expression PC

0.2 0.4 0.6 0.8

featureCounts  
RNA.SeQC  
CutterStar

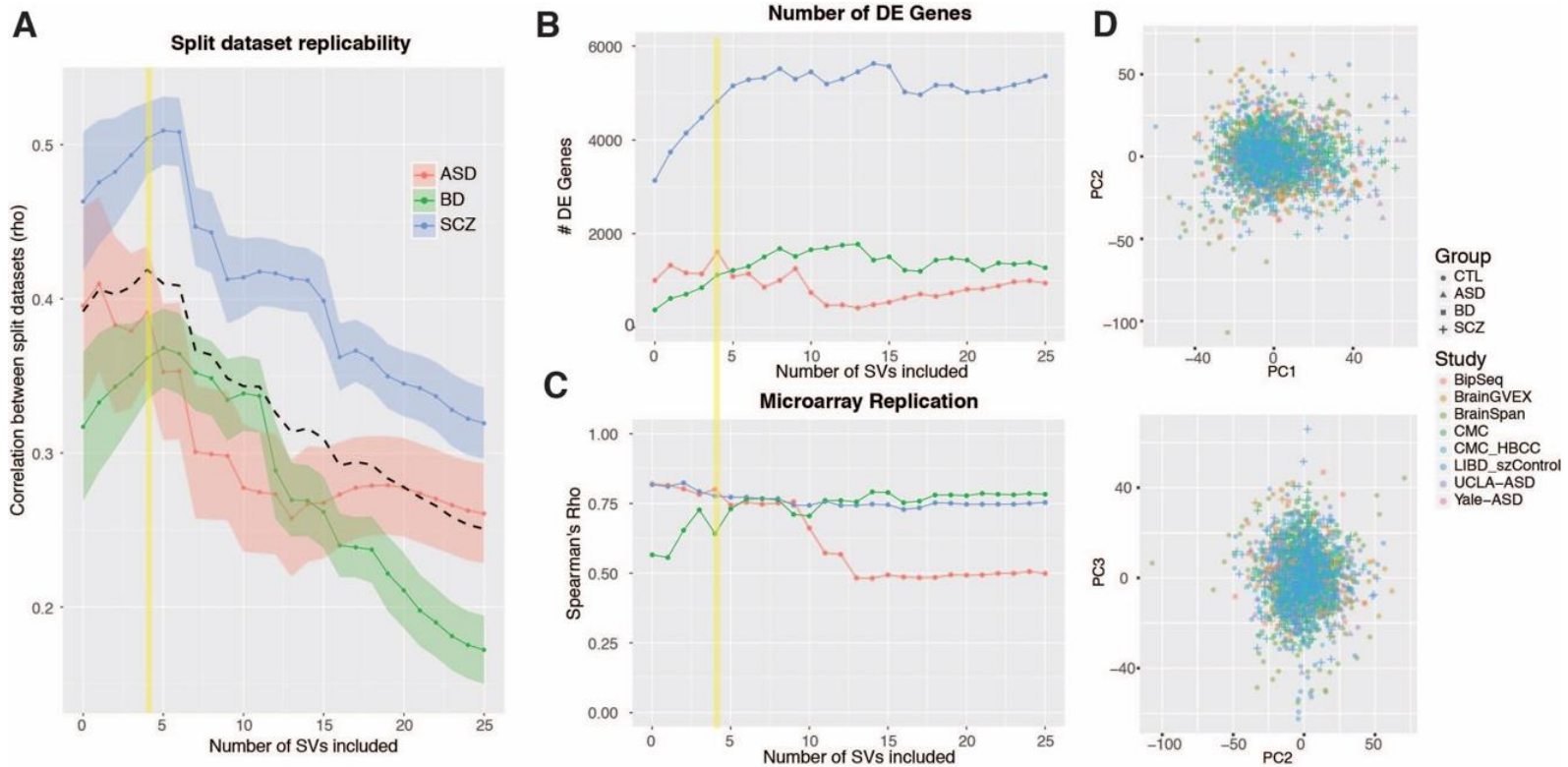
Picard CollectAlignmentSummaryMetrics

Picard CollectGbBlastMetrics

Picard CollectRnaSeqMetrics

**Fig. S2. Dataset demographics and quality control**

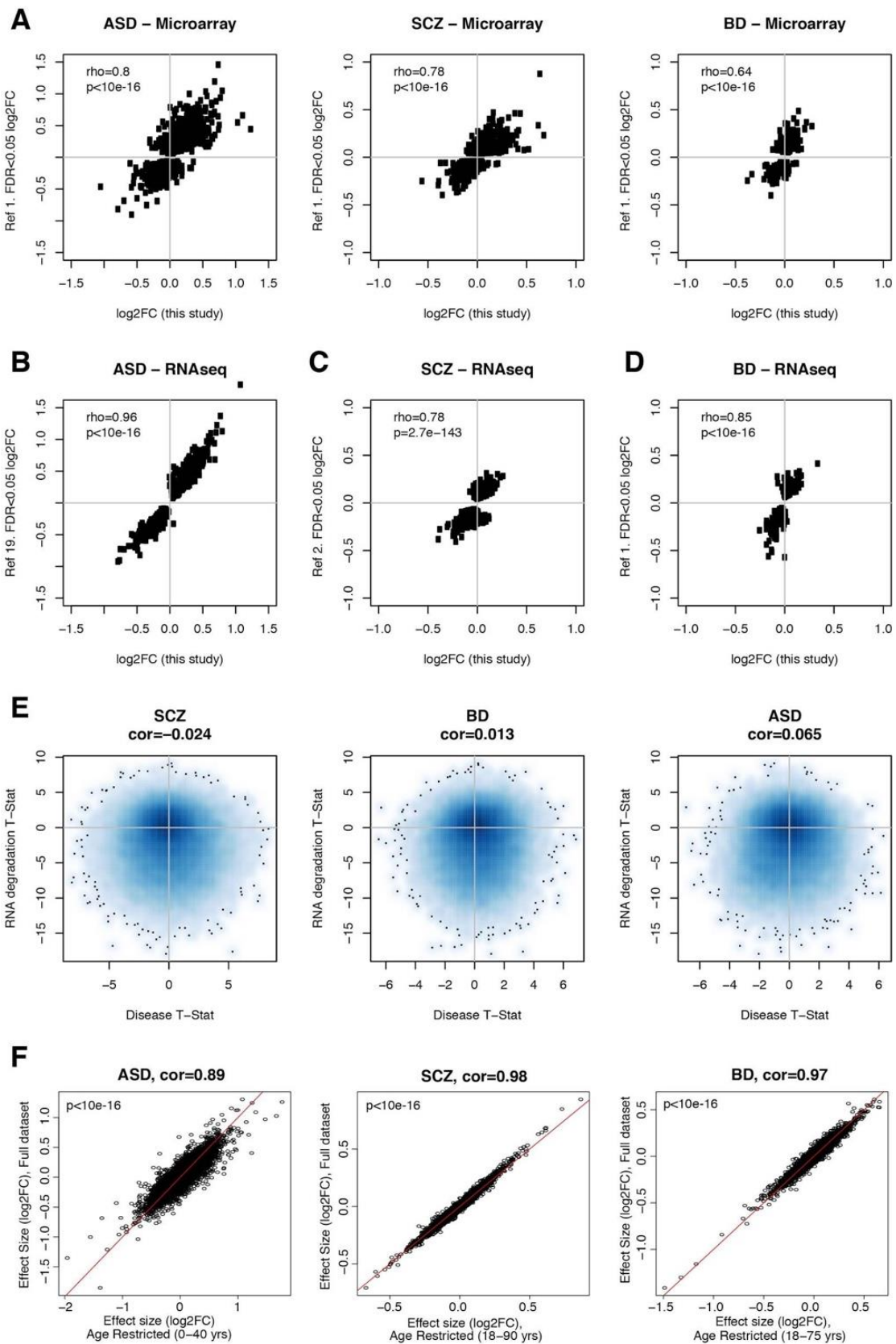
A) Sample information, subject demographics, and sequencing characteristics are shown for each group. This study only used frontal and temporal cortex samples from subjects at postnatal time points. B) Spearman's  $\rho$  values are shown for correlations between dataset covariates with the top 20 expression PCs. C) Sample outlier removal was performed individually for each study before combining data, based on Z-scores of standardized network connectivity (**Methods**). D) Sequencing surrogate variables ('seqPCs') were calculated as the top 29 principal components of the matrix of sequencing QC metrics. Loadings are shown between seqPCs and individual metrics, colored by the source of the QC metrics.



**Fig. S3. Selection of Covariates**

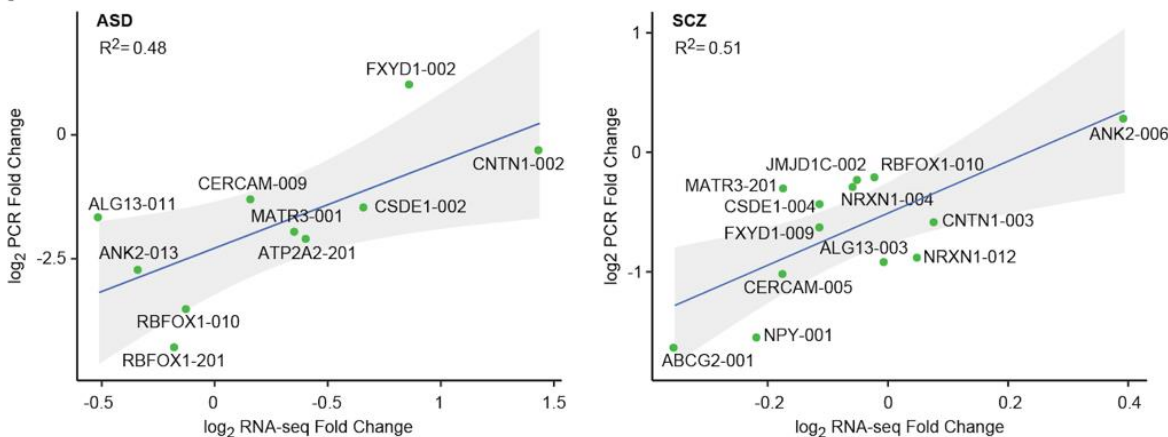
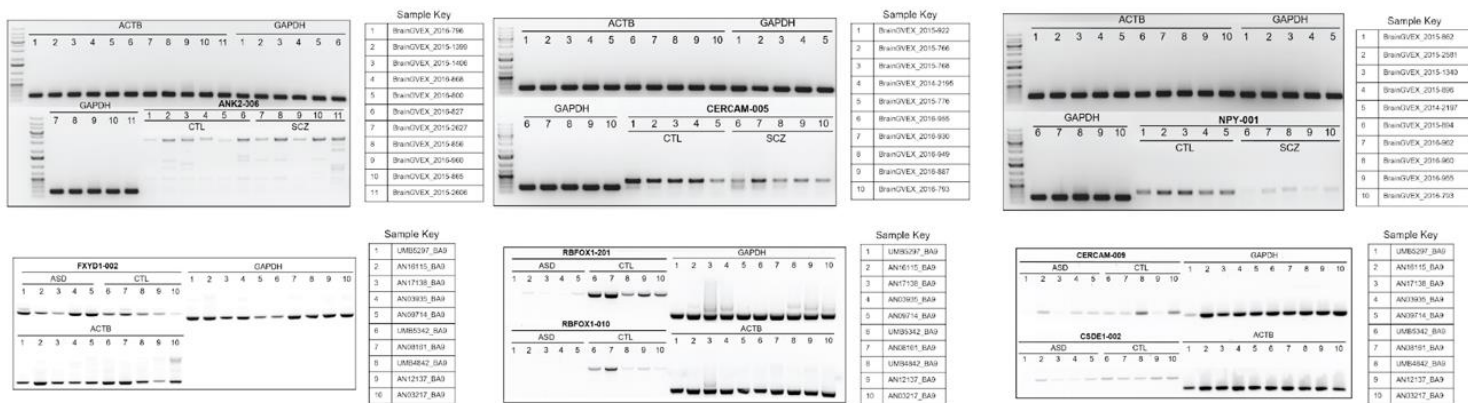
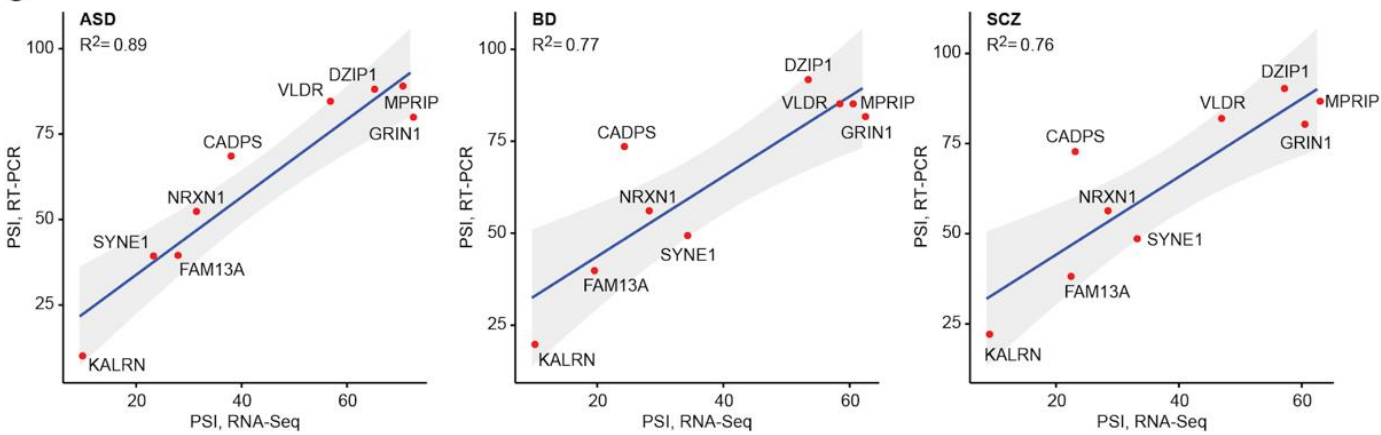
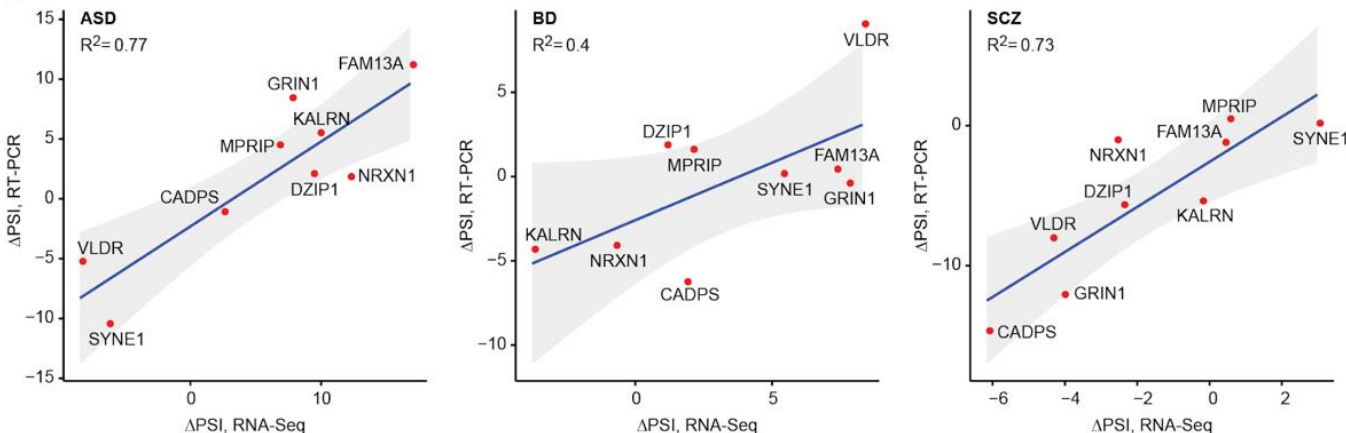
To capture the full range of factors influencing gene expression in our dataset, the final differential expression model included known covariates, aggregate sequencing metrics (seqPCs), and surrogate variables (SVs) calculated using SVA to correct for unmeasured sources of variation. A) To determine the appropriate number of SVs to use, we randomly split our dataset into two halves and calculated differential gene expression for each disorder using a fixed number of SVs ranging from 0 to 25. We compared DGE for each disorder between the split datasets using spearman's correlation of  $\log_2FC$  effect sizes for all brain-expressed genes ( $N=25,774$  genes). We then repeated this analysis 1000 times and compared results across the range of SVs included. Addition of 4 SVs yielded the greatest cross-dataset replicability. B) Here, we plot the number of genes considered differentially expressed as a function of the number of SVs included in the differential expression model. C) DE results from this study are compared with published microarray datasets for each disorder (*I*) as a function of the number of SVs included. Spearman's correlation is shown for DGE  $\log_2FC$  effect sizes for genes previously identified as DE (FDR<0.05) in the microarray dataset, as described in **Fig S4**. D) Multidimensional

scaling plots are shown for the top 3 PC's of the covariate-corrected dataset, colored by study/batch and diagnosis.



**Fig. S4. Validation of DGE Results**

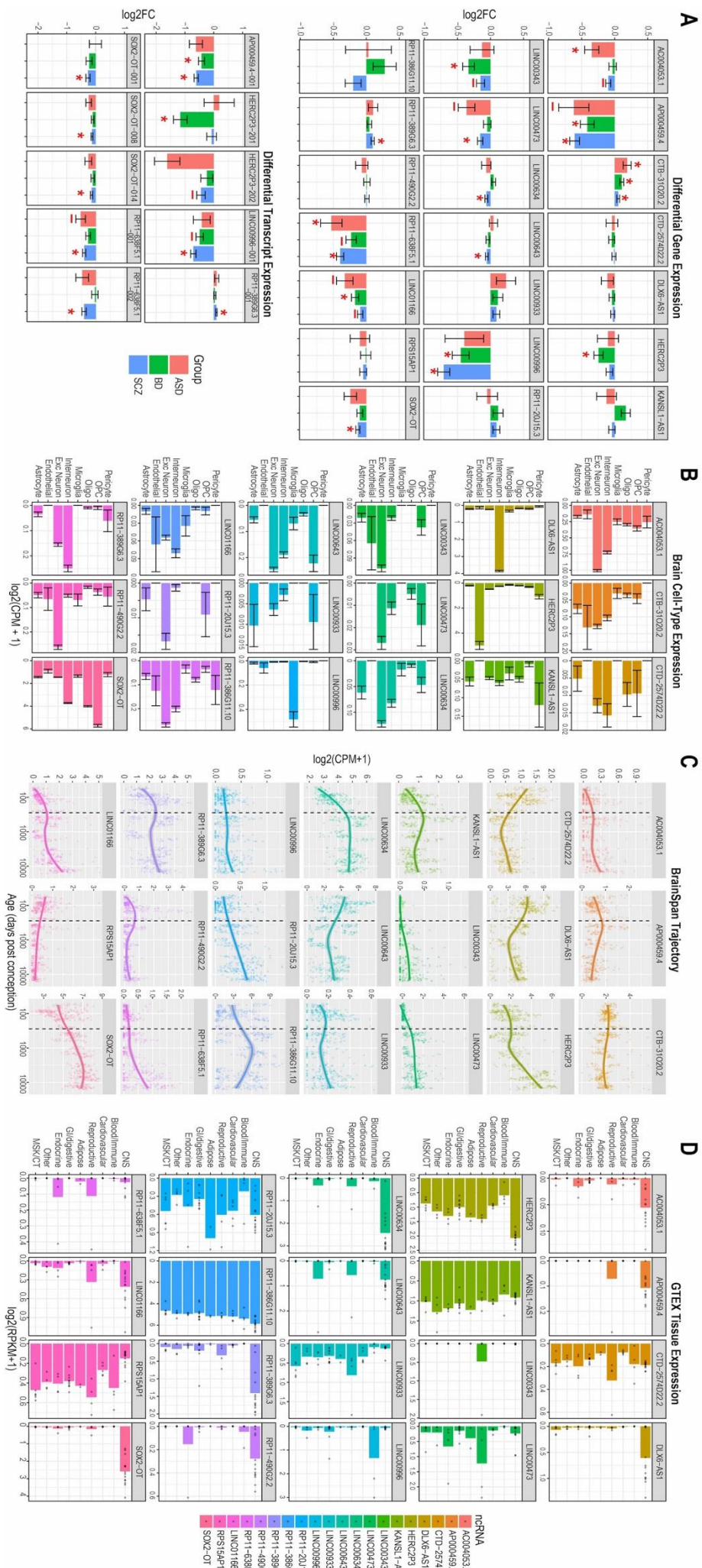
Differential gene expression results from this study were compared with several published microarray and RNA-Seq datasets. A) log<sub>2</sub>FC effect sizes are plotted in comparison to a microarray meta-analysis of ASD, SCZ, and BD for genes identified as DGE (FDR<0.05) (13). We see substantial concordance of gene-level effect sizes across studies and platforms. Similar concordance is observed in comparison to results from RNA-Seq studies in B) ASD (19), C) SCZ (18), and D) BD (13). There is some overlap in samples across studies, due to the limited availability of post-mortem brain tissue from subjects with psychiatric disease. E) To ensure that differential gene expression in disease was not being driven by differences in RNA quality or degradation, we compared differential expression T-statistics with those experimentally derived from brain tissue samples allowed to degrade for fixed intervals of time (22). We did not observe substantial concordance between these RNA degradation metrics and psychiatric disease DGE summary statistics. F) Age balancing of case-control comparisons (0-40 years for ASD/CTL; 18-90 years for SCZ/CTL; 18-75 years for BD/CTL) does not substantially alter disease DGE signal.

**A****B****C****D**



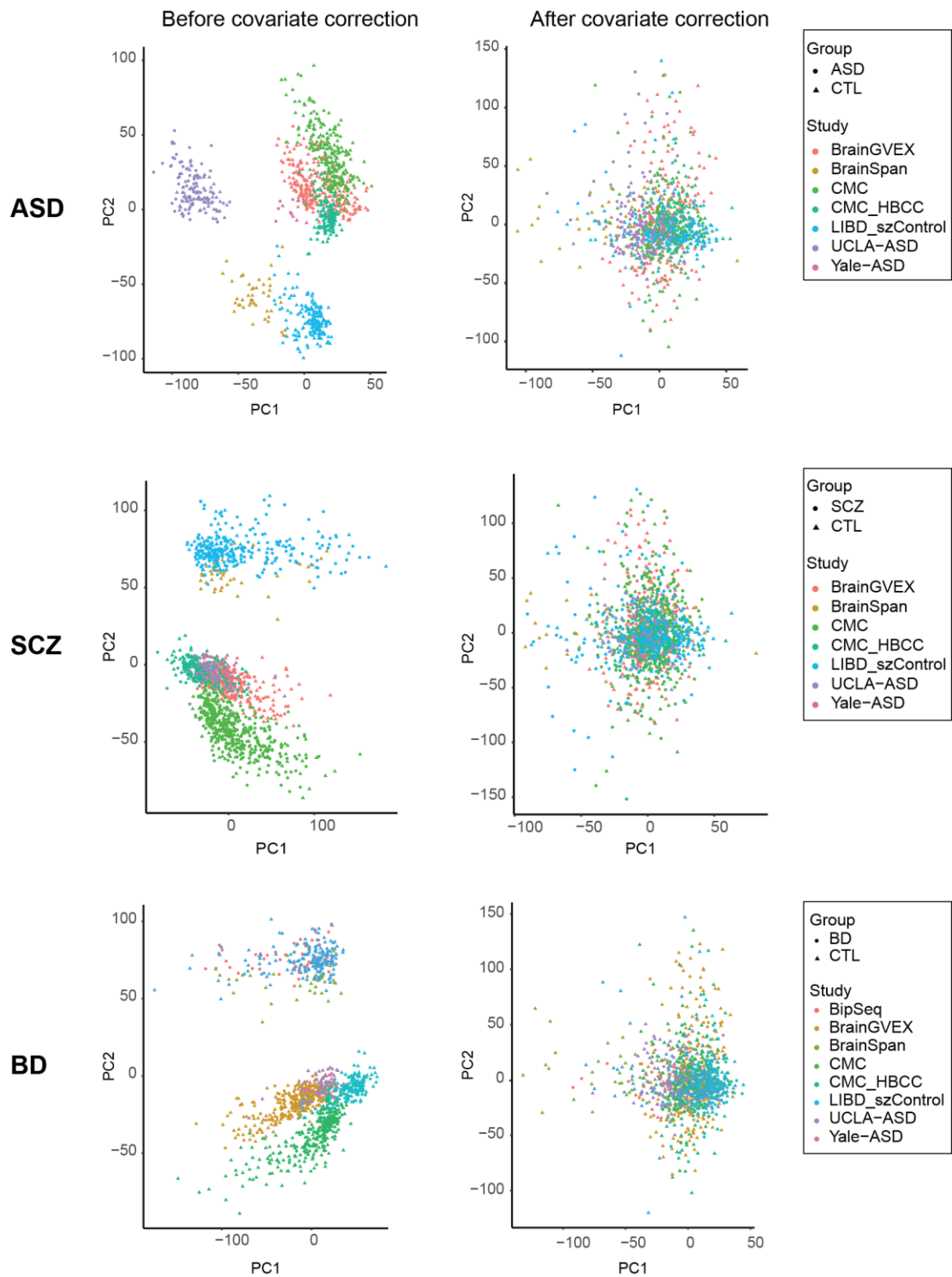
**Fig. S5. Validation of differential transcript expression and differential splicing**

A) Comparison of fold changes obtained from RSEM-based isoform quantification of RNA-Seq data to semiquantitative PCR results for 10 isoforms tested in ASD and control samples (left) and 13 isoforms tested in SCZ and control samples (right). Fold changes were calculated between cases and control samples. B) Representative 1.5 to 2% agarose gel images obtained for isoform validation. C) Scatter plots comparing the average percent spliced-in (PSI) of exon-skipping events called by LeafCutter from RNA-Seq data to semi-quantitative PCR. A total of 9 genes were tested in 5 cases and 5 controls in ASD, BD and SCZ. An additional 5 cases and 5 controls were tested for *FAM13A* and *SYNE1* in BD and SCZ to resolve outliers. D) Same as C, but now comparing the change in average PSI ( $\Delta$ PSI) between cases and controls in each disorder. E) Representative Agilent 2100 Bioanalyzer gel images (DNA 1000 chips) obtained for splicing validation. A-E) Gene or isoform names are indicated at each point. Regression lines with 95% confidence intervals are shown in blue and grey, respectively and the corresponding  $R^2$  values are shown at the top-left in each plot.



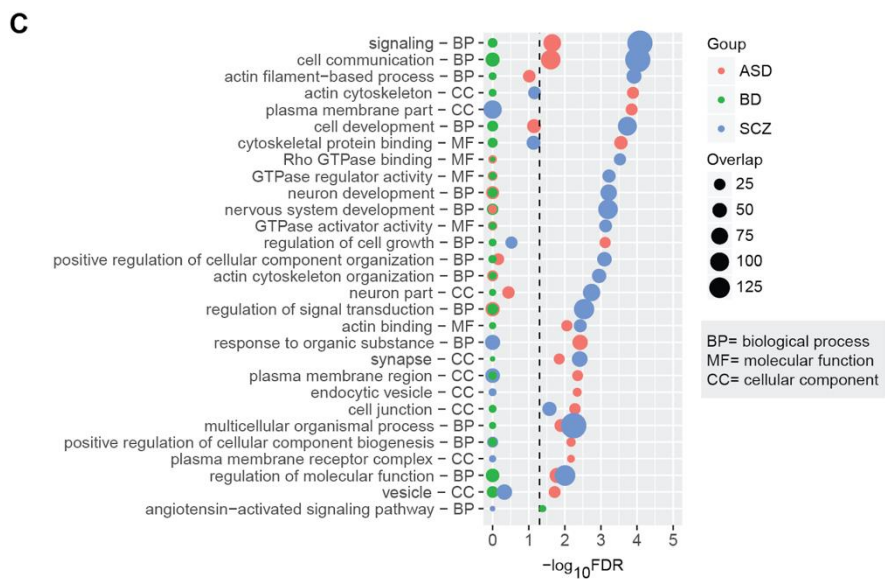
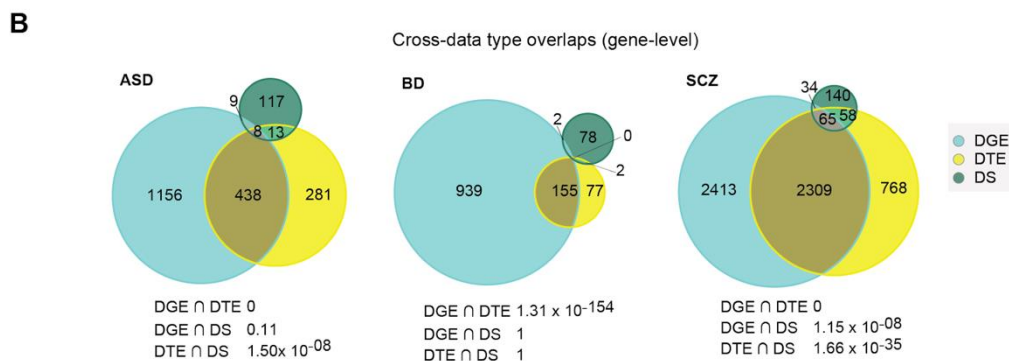
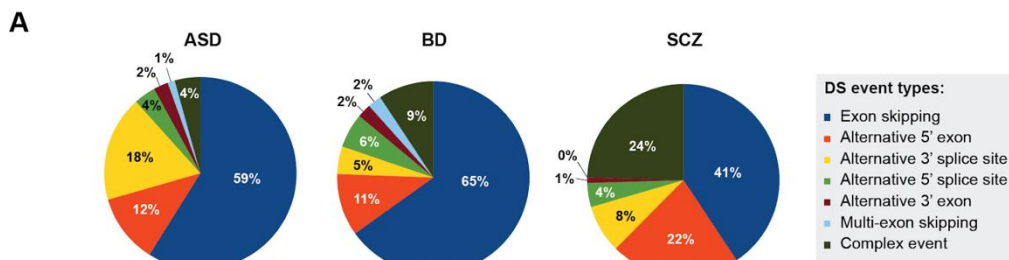
**Fig. S6. Annotation of individual ncRNAs**

We highlight several ncRNAs differentially expressed in psychiatric disease or identified as hubs of relevant co-expression modules. A) Differential gene expression (DGE; top) and differential transcript expression (DTE; bottom) in SCZ, BD, and ASD. \*FDR<0.05, -- FDR<0.1. B) Human brain cell type expression patterns are shown for each ncRNA using data from ref (98). Plots show mean expression for cells identified in specific clusters. C) Developmental expression trajectory is shown for each ncRNA using data from BrainSpan (146). Plots show expression versus age (days post-conception) on a  $\log_{10}$  scale, with the dotted line denoting birth. D) Human tissue-specific expression levels are shown for each ncRNA using data from GTEX (82).



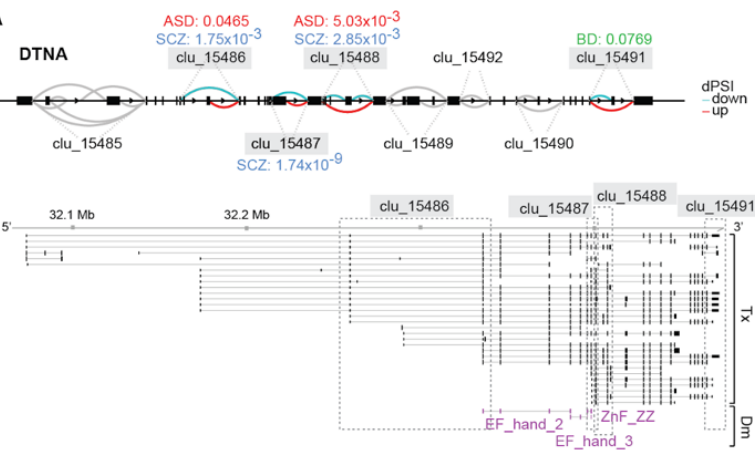
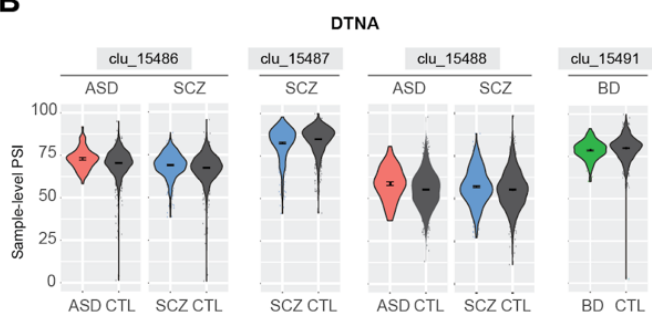
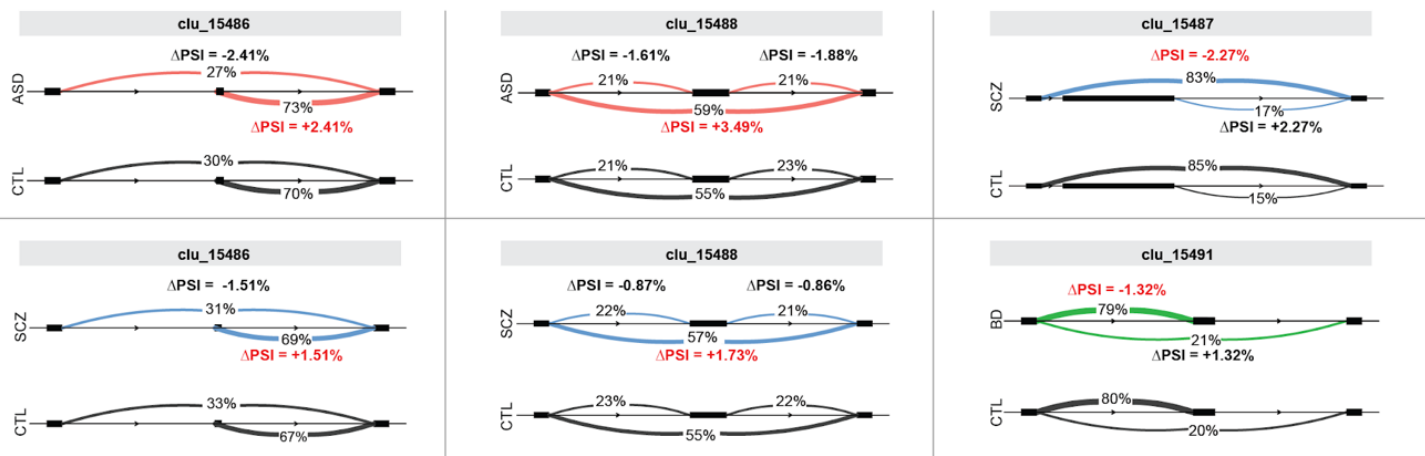
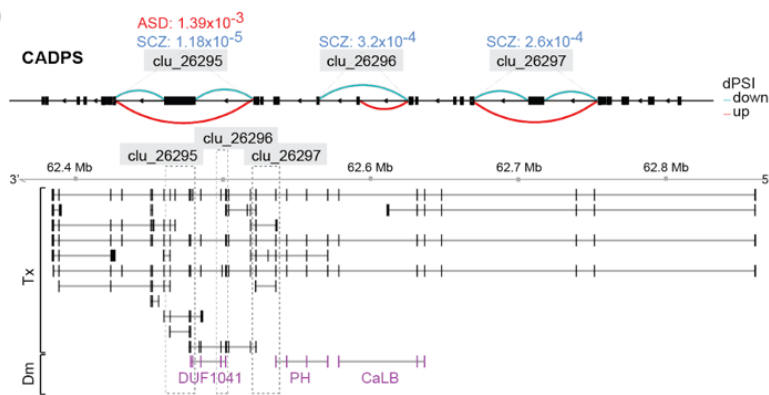
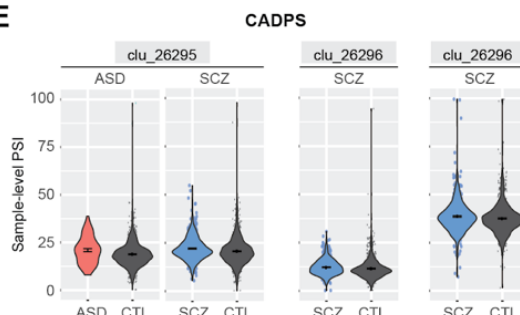
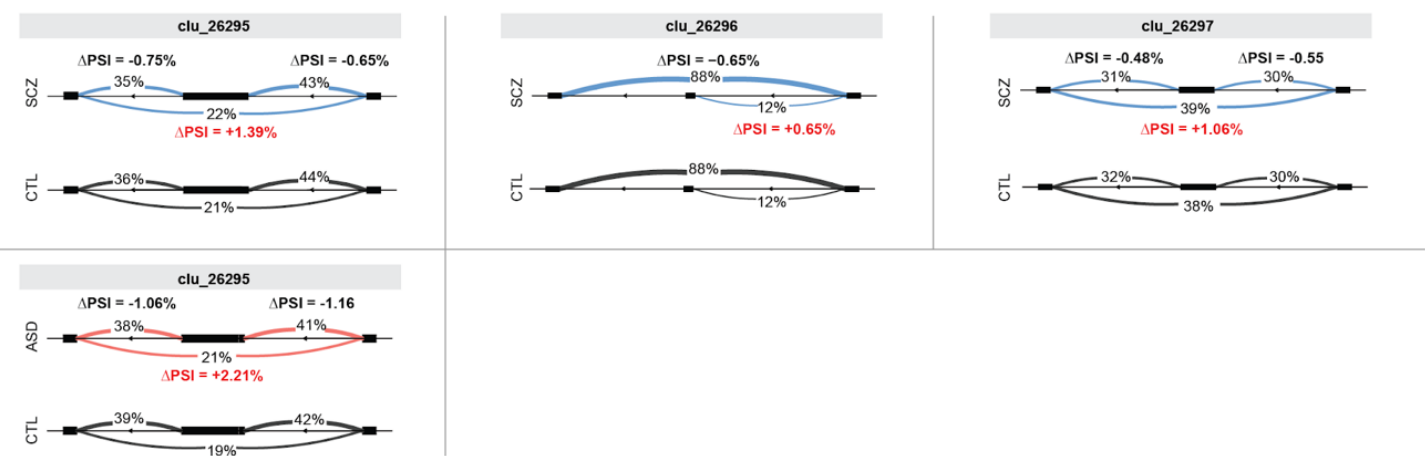
**Fig. S7. Covariate correction of DS**

Top two principal components (PCs) of percent spliced-in (PSI) values are shown before (left) and after (right) covariate correction for the ASD, BD and SCZ datasets. Points are colored according to study origin and shape denotes disorder (circle) or control (CTL) status. See inset legends for further details.



**Fig. S8. Annotation of DS events, Cross data DGE-DTE-DS overlaps**

A) Pie charts with breakdown of DS event types identified in each disorder. B) Venn diagrams showing overlaps between genes with significant DGE, DTE or DS changes for each disorder. P values for hypergeometric tests of pairwise overlaps between data types are shown at the bottom of the Venn diagrams for each disorder. C) Top 20 gene ontology (GO) enrichments for DS genes in each disorder.

**A****B****C****D****E****F**

**Fig. S9. Additional differential local splicing examples**

A) Top: Significant differentially spliced (DS) intron clusters in *DTNA* for ASD, SCZ and BD. Increased or decreased intron usage in cases compared to controls (CTL) are shown in red and blue, respectively. Bottom: Overview of known isoforms (GENCODE v19) and protein domains for *DTNA*. Locations of significant DS clusters are indicated by dotted lines. Protein domains (purple) are annotated as EF\_hand\_2 - EF hand domain 2; EF\_hand\_3 - EF hand domain 3; ZnF\_ZZ - Zinc-binding domain, present in Dystrophin, CREB-binding protein. B) Violin-plots with the distribution of covariate-adjusted percent spliced in (PSI) *per* sample for the intron with the maximum change in PSI for each cluster and disorder. C) Visualization of introns in each significant cluster for each disorder, with their change in PSI (PSI). Covariate-adjusted average PSI levels in disorder *vs* CTL are indicated for each intron. D) Same as A), but for *CADPS*. Protein domains (purple) are annotated as PH - Pleckstrin homology domain; CaLB - C2 domain (Calcium/lipid-binding domain, CaLB) superfamily; DUF1041 - Domain of unknown function. E) Same as B), but for *CADPS*. F) Same as C), but for *CADPS*.

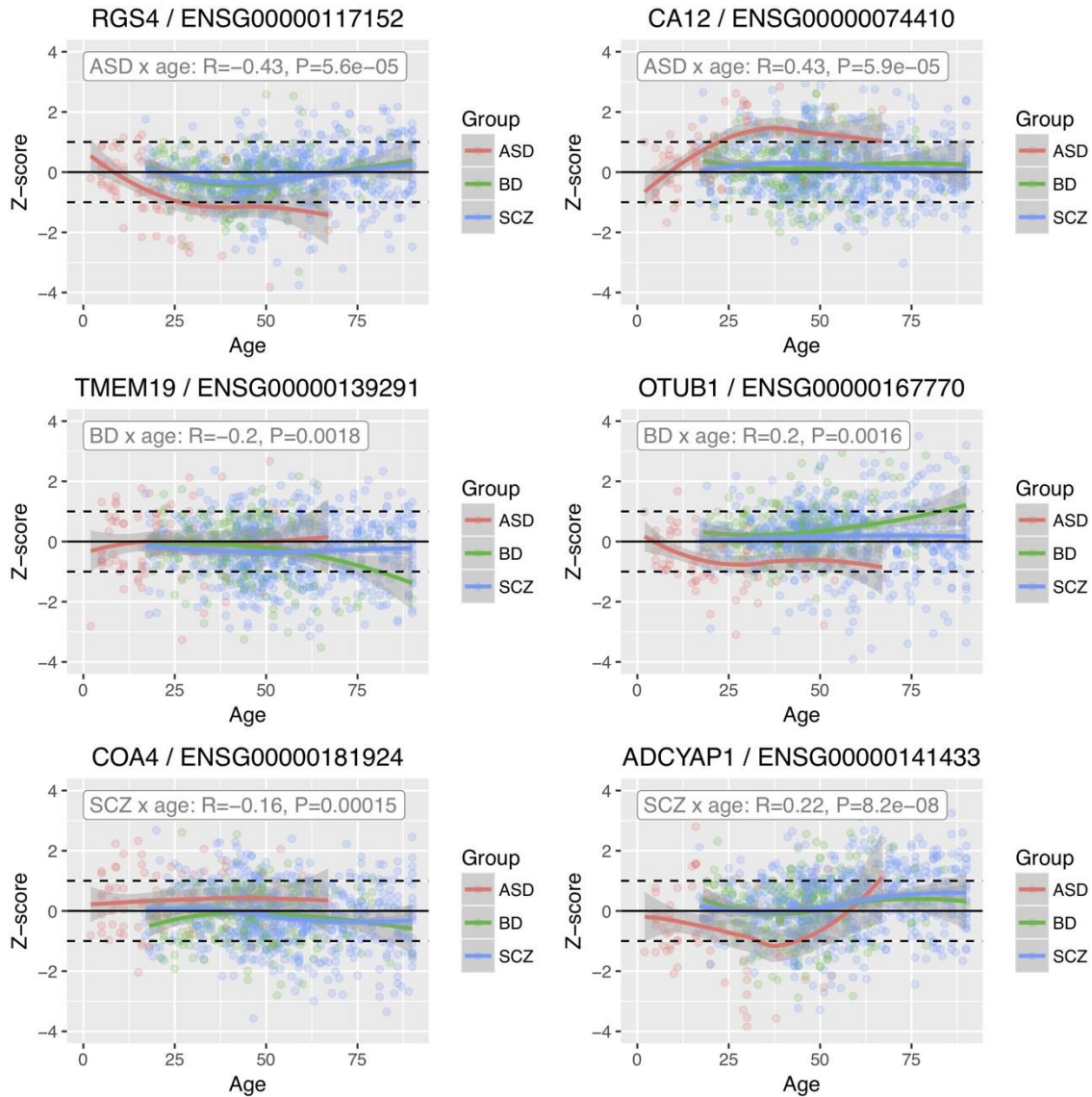
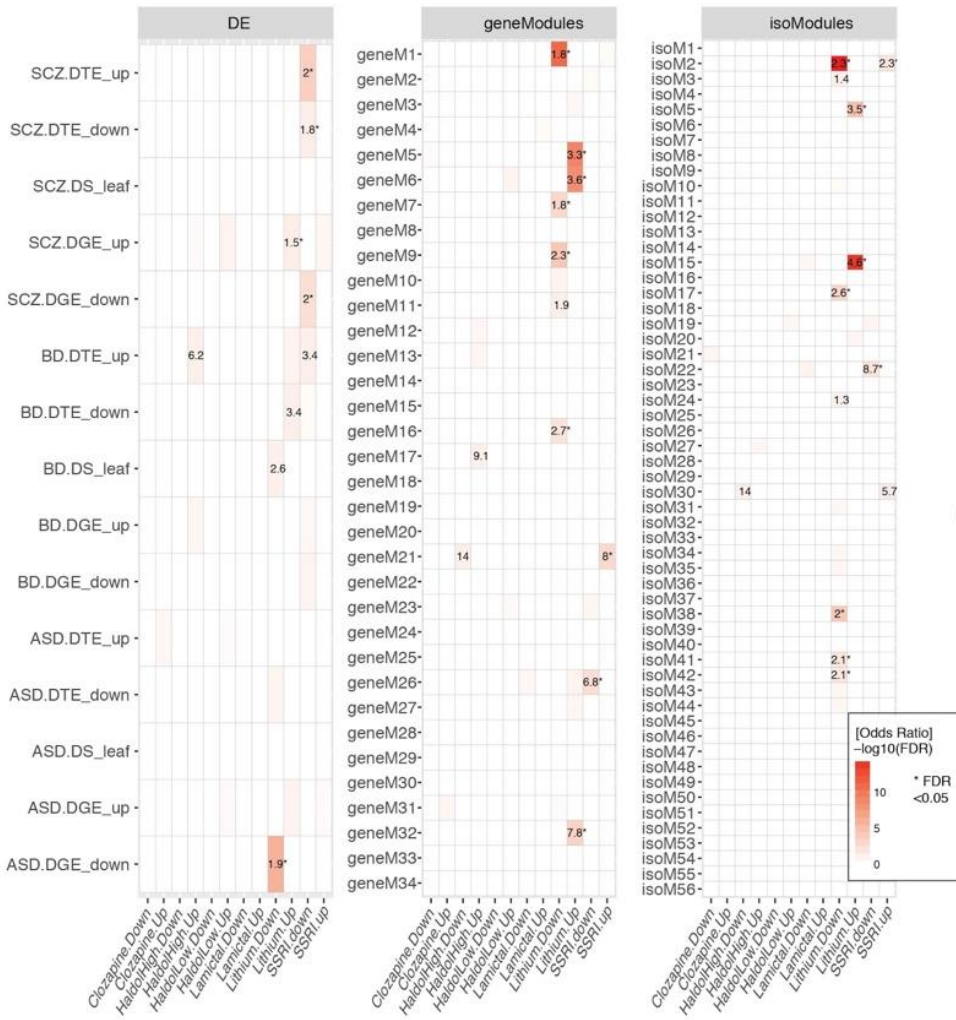


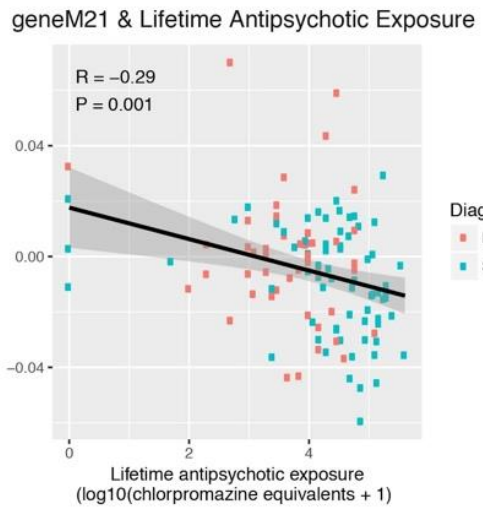
**Fig. S10. Age effects on differential gene expression**

Examples are shown for genes whose magnitude of differential expression in a given disorder is significantly associated with age. For each gene, a local regression function was fit to model the effect of age on expression in control samples, and expression in cases was then converted to a Z-score relative to the interpolated mean in controls. We then assessed the correlation between Z-transformed expression and age within each disease group (ASD, SCZ, BD) separately. We find that 143 of the 4821 DGE genes in SCZ show a nominal increase in effect size magnitude as a function of age, consistent with a reactive interpretation. In ASD, 85 of 1611 DE genes showed this same pattern and in BD there were 29 of the 1119 DE genes.

A



B



C

geneM21 &amp; Postmortem Toxicology

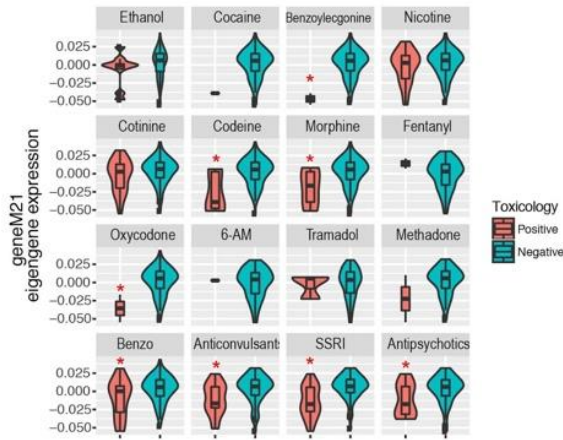


### Fig. S11. Assessment of psychiatric medication effects

A) We investigated whether antipsychotic medications could explain differential gene expression and module associations identified in SCZ, BD, and ASD. We used three experimental datasets: (1) an RNA-Seq dataset from DLPFC of nonhuman primates exposed for 6 months to clozapine, haloperidol (low dose), or haloperidol (high dose) compared to placebo; (2) a microarray dataset from mouse brain following chronic exposure to the SSRI fluoxetine; (3) a microarray dataset from rat cortex following chronic exposure to the mood stabilizers lithium or lamotrigine compared with vehicle (21). Overlap of DE genes and modules with genes up or downregulated by medications (at nominal significance thresholds, except for lithium) was assessed by Fisher's exact test. Plot shows odds-ratios of enrichment for  $P<0.05$  significant associations, with \* denoting  $FDR<0.05$  associations. With the exception of lithium, medications show minimal overlap with disease-associated transcriptomic changes. The one exception was for the activity dependent module pair, geneM21/isoM30, which did seem to be associated with SSRIs and high dose haloperidol. B) To investigate this relationship further, we compared geneM21 eigengene expression with medication history in those subjects where this information was available. There was a significant negative

correlation between geneM21 expression and lifetime antipsychotic exposure (chlorpromazine equivalents, log scale). C) A subset of samples also had results from post-mortem toxicology testing. We found broadly decreased levels of geneM21 eigengene expression in those subjects who tested positive for a host of psychiatric medications, including antipsychotics (\*FDR<0.05).

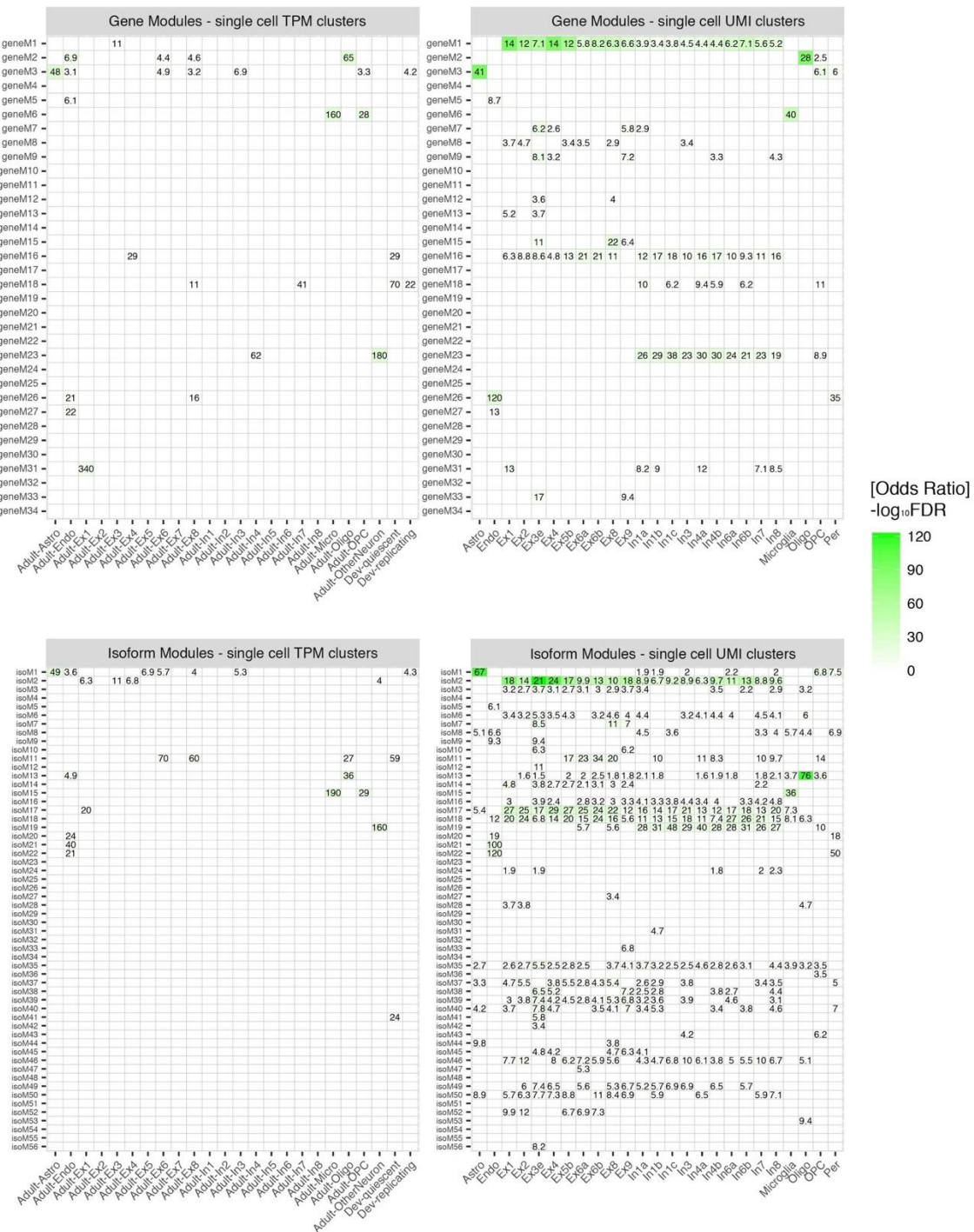


**Fig. S12. Co-expression network cell type enrichments**

Plots show enrichment of gene and isoform-level co-expression modules for established markers of CNS cell types from human brain single-cell RNA-Seq clusters, as compiled in the companion manuscript (18). Clusters were defined separately for TPM- and UMI-

based scRNA-Seq quantifications. Text denotes odds ratios of enrichment for significant associations ( $FDR < 0.05$ ). The UMI dataset is from adult human brain, whereas the TPM dataset includes two fetal cell types. (Ex# - excitatory neuron cluster; In# - interneuron cluster; Per- pericyte; OPC-oligodendrocyte progenitor cell; Oligo - oligodendrocyte; Micro - microglia; End - endothelial; Ast - astrocyte).

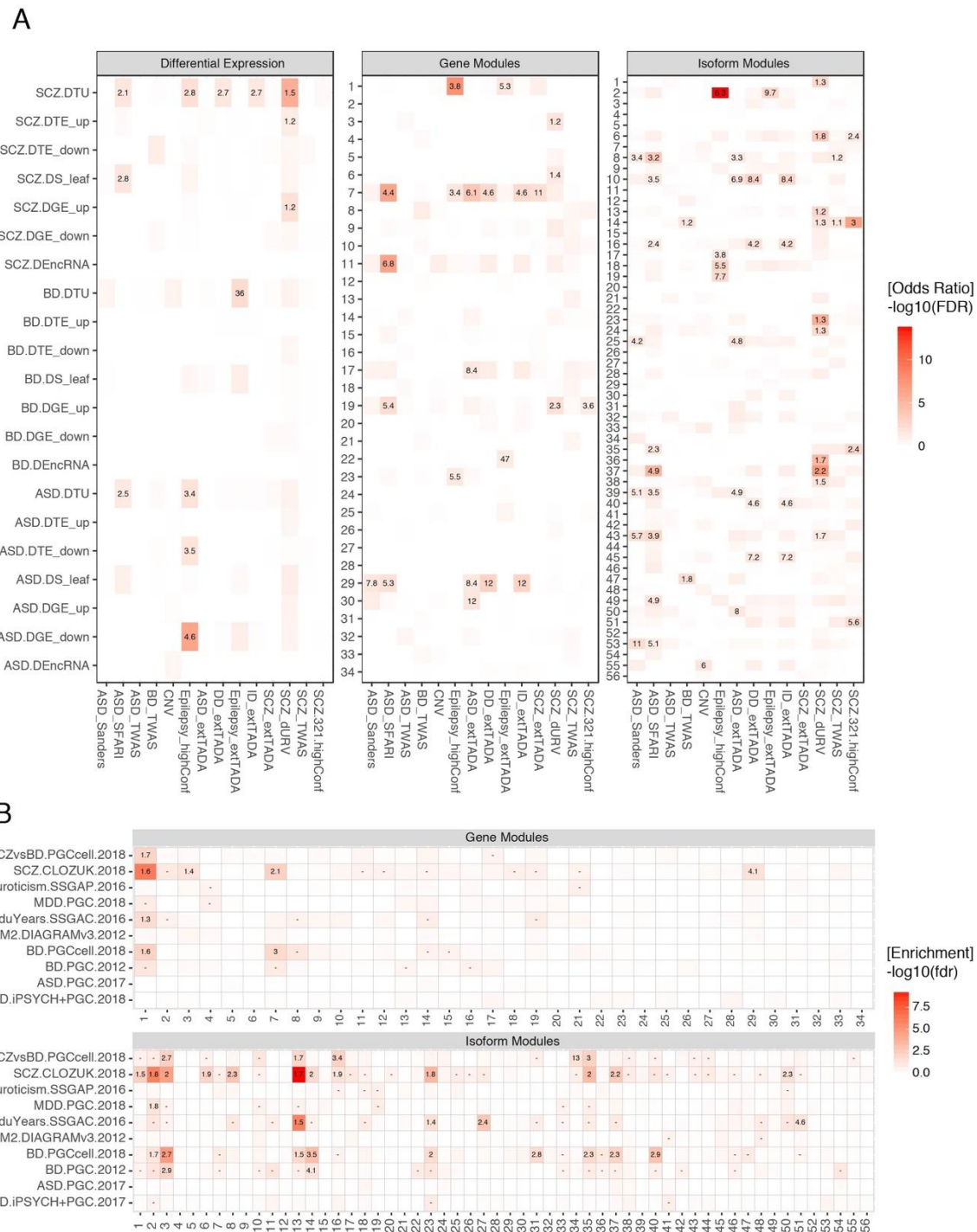


### **Fig. S13. Genetic enrichment analyses**

A) Enrichment for several sets of disease risk genes was assessed among DE features, gene, and isoform-co-expression modules, including those harboring rare *de novo* variants identified in each disorder, as well as in related neurodevelopmental and psychiatric traits. TWAS signal for each disorder was also included as was the list of 321 “high confidence” SCZ risk genes identified in a companion manuscript (17). Enrichment was calculated using logistic regression, controlling for gene and transcript length as well

as GC content (21). Risk gene sets include: 71 risk loci harboring rare *de novo* variants associated with ASD through the transmission and *de novo* association test (TADA; “ASD\_Sanders”) (81); Syndromic and highly ranked (1 and 2) genes from SFARI Gene database (“ASD\_SFARI”); genes harboring recurrent *de novo* copy-number variants associated with ASD or SCZ, as defined in (13) (“CNV”); genes harboring an excess of rare exonic variants in ASD, SCZ, intellectual disability (ID), developmental delay (DD), and epilepsy as assessment through an extended version of TADA (“extTADA”) (142); genes harboring disruptive and damaging ultra-rare variants in SCZ (55) (“SCZ\_dURVs”); a list of high confidence epilepsy risk genes, compiled from (143). B) Enrichment of GWAS signal among gene and isoform co-expression modules, using stratified LD score regression (s-LDSR) with summary statistics from several psychiatric, cognitive, and behavioral traits (21). Cells are labeled with GWAS enrichment, for those with FDR < 0.05. Cells labeled with “-” are nominally (P<0.05) significant but do not pass FDR-correction.



**Fig. S14. Module-trait associations after SCZ downsampling**

To determine whether differences in module associations observed across disorders was due to the larger sample size of the SCZ dataset, we repeated our module-trait association analyses using a randomly subsampled SCZ dataset to match the sample size of ASD and BD datasets. We repeated this 100 times and reran our module-level associations using these matched sample sizes. Plots show module-trait association  $\beta$  values with standard errors. \* $P<0.05$ .

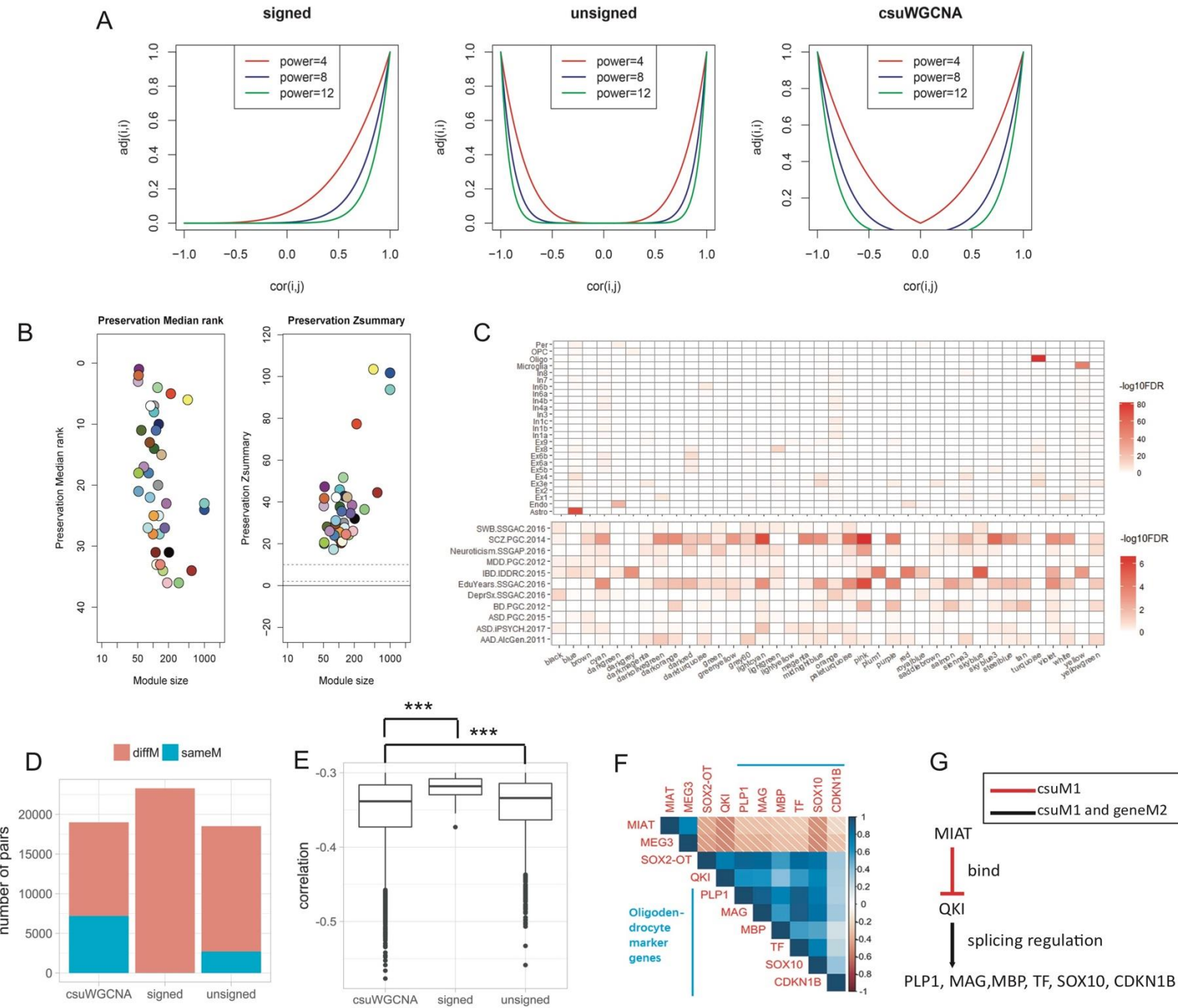


**Fig. S15. csuWGCNA identifies putative lncRNA negative regulatory relationships**

A) Network adjacency (y-axis) versus correlation (x-axis) in the signed network, unsigned network, and csuWGCNA network. The color of the line denotes the soft threshold power setting. Note that correlation=-1 leads to adjacency=0 in the signed network and adjacency=1 in the unsigned and csuWGCNA network. B) All modules detected by csuWGCNA were well preserved in the signed networks (Z score summary>10 indicates high preservation). C) The enrichment of cell type and GWAS signal in csuWGCNA modules. D) csuWGCNA captures more negative lncRNA-gene pairs ( $\text{cor} < -0.3$ ) in the same module than signed and unsigned WGCNA (csuWGCNA=7186, signed=20, unsigned=2701). E) csuWGCNA captures stronger negative relationships than signed and unsigned network types (Welch two sample t-test,  $p < 10^{-6}$  and  $p < 10^{-11}$ , respectively). F) The lncRNAs *MIAT* and *MEG3* are negatively

correlated with most of the hubs in oligodendrocyte modules (shown in **Fig 5C**), including *SOX2-OT* and oligodendrocyte marker genes (*PLP1*, *MAG*, *MBP*, *TF*, *SOX10*, and *CDKN1B*). The blue color indicates negative correlations and the red indicates positive correlations. G) Putative target relationships for the lncRNA *MIAT*. The red line indicates a negative relationship only detected in csuM1, and the black line indicates positive relationships detected in both csuM1 and geneM2.

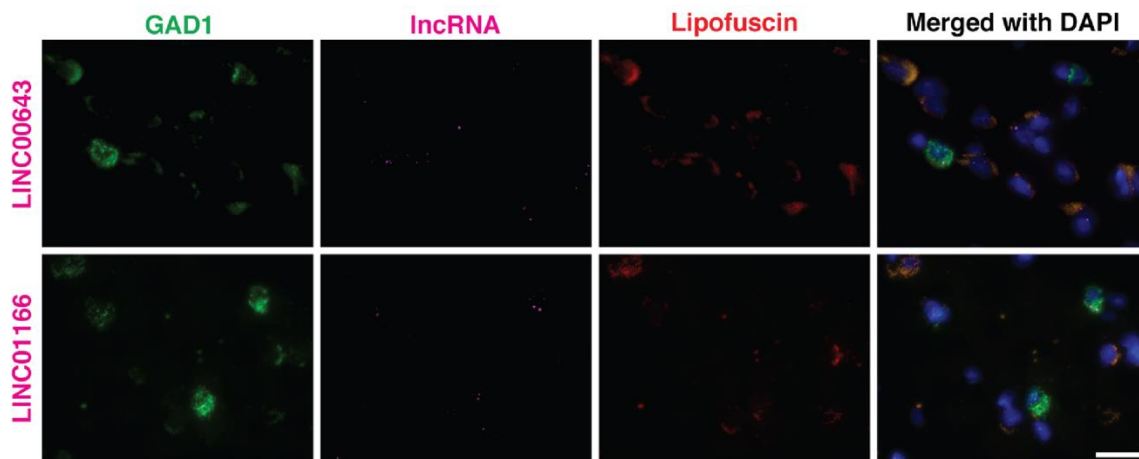


**Fig. S16. *LINC00643* and *LINC01166* expression in human prefrontal cortex**

Sections from human prefrontal cortex (area 9) were labeled with *GAD1* probe (green) and lncRNA (magenta) probes for *LINC00643* (upper panel) or for *LINC01166* (lower panel). All sections were counterstained with DAPI (blue) to reveal cell nuclei. Lipofuscin autofluorescence is visible in both the green and red channels and appears yellow/orange in the merged image. The lncRNAs are present both in GABAergic interneurons and cells without *GAD1* signal. Scale bar, 25  $\mu$ m.

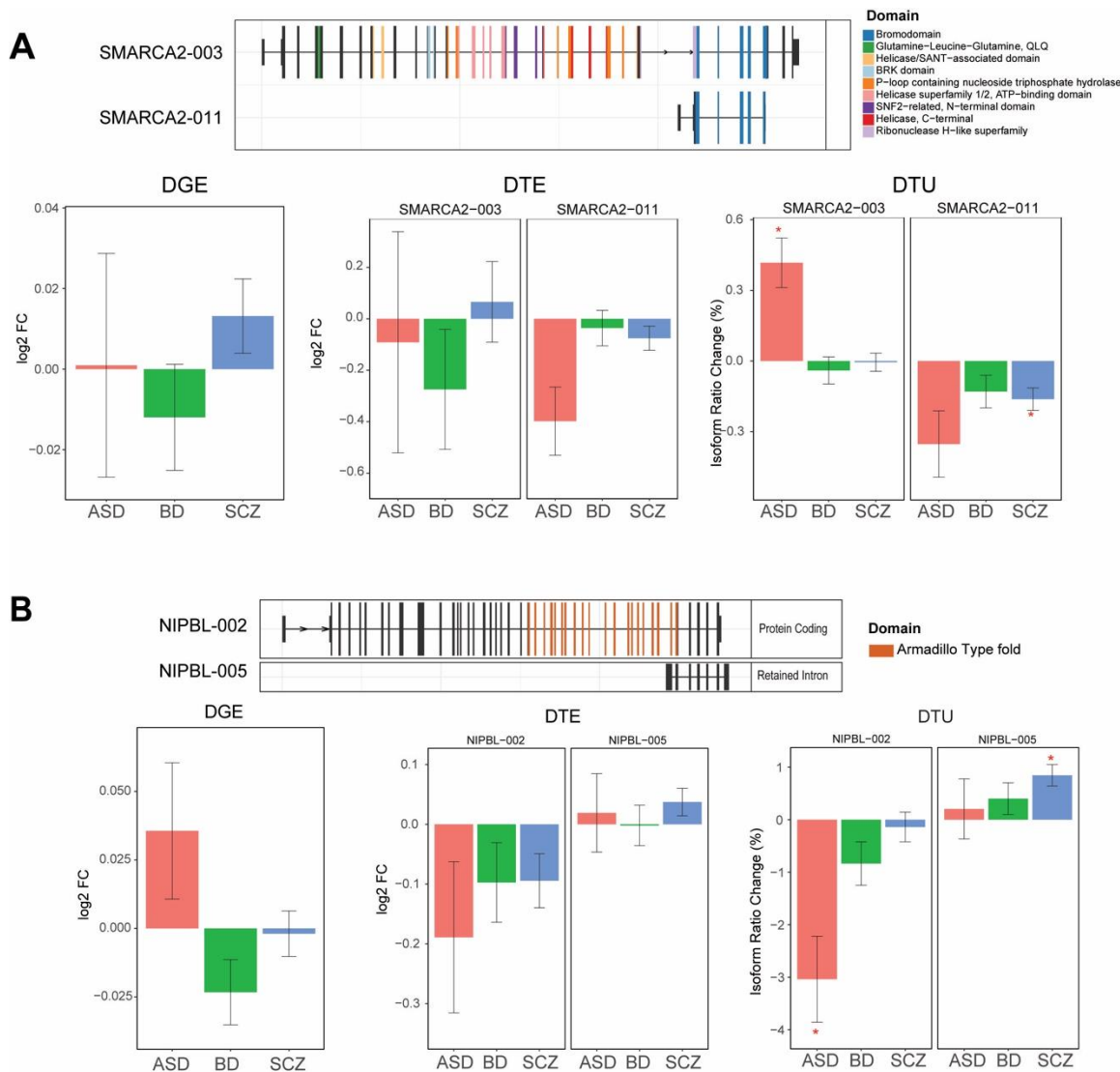


**Fig. S17. Additional switch isoforms**

A) The isoform ratio of two *SMARCA2* isoforms, *SMARCA2-003* and *SMARCA2-011*, are up and downregulated in ASD and SCZ, respectively. B) The isoform ratio of two *NIPBL* isoforms, *NIPBL-002* and *NIPBL-005*, are down and upregulated in ASD and SCZ, respectively. \*FDR < 0.05

**Table S1**

Differential gene and isoform expression summary statistics and DE enrichment analyses

**Table S2**

Annotation of neuropsychiatric ncRNAs ('NPncRNAs')

**Table S3**

Differential splicing summary statistics, annotation and disease overlaps

**Table S4**

TWAS and SMR summary statistics, PRS associations with gene and isoform expression

**Table S5**

Gene and isoform co-expression module annotation

**Table S6**

csuWGNA network annotation and putative lncRNA-mRNA targets

**Table S7**

Switch isoform and microexon characterization

**Table S8**

Splicing and isoform validation primers and samples

**Table S9**

RNAscope - Tissue samples and RNA FISH probes

## PsychENCODE Consortium Authors and Affiliations

‡ Allison E Ashley-Koch, Duke University; Gregory E Crawford, Duke University; Melanie E Garrett, Duke University; Lingyun Song, Duke University; Alexias Safi, Duke University; Graham D Johnson, Duke University; Gregory A Wray, Duke University; Timothy E Reddy, Duke University; Fernando S Goes, Johns Hopkins University; Peter Zandi, Johns Hopkins University; Julien Bryois, Karolinska Institutet; Andrew E Jaffe, Lieber Institute for Brain Development; Amanda J Price, Lieber Institute for Brain Development; Nikolay A Ivanov, Lieber Institute for Brain Development; Leonardo Collado-Torres, Lieber Institute for Brain Development; Thomas M Hyde, Lieber Institute for Brain Development; Emily E Burke, Lieber Institute for Brain Development; Joel E Kleiman, Lieber Institute for Brain Development; Ran Tao, Lieber Institute for Brain Development; Joo Heon Shin, Lieber Institute for Brain Development; Schahram Akbarian, Icahn School of Medicine at Mount Sinai; Kiran Girdhar, Icahn School of Medicine at Mount Sinai; Yan Jiang, Icahn School of Medicine at Mount Sinai; Marija Kundakovic, Icahn School of Medicine at Mount Sinai; Leanne Brown, Icahn School of Medicine at Mount Sinai; Bibi S Kassim, Icahn School of Medicine at Mount Sinai; Royce B Park, Icahn School of Medicine at Mount Sinai; Jennifer R Wiseman, Icahn School of Medicine at Mount Sinai; Elizabeth Zharovsky, Icahn School of Medicine at Mount Sinai; Rivka Jacobov, Icahn School of Medicine at Mount Sinai; Olivia Devillers, Icahn School of Medicine at Mount Sinai; Elie Flatow, Icahn School of Medicine at Mount Sinai; Gabriel E Hoffman, Icahn School of Medicine at Mount Sinai; Barbara K Lipska, Human Brain Collection Core, National Institutes of Health, Bethesda, MD; David A Lewis, University of Pittsburgh; Vahram Haroutunian, Icahn School of Medicine at Mount Sinai and James J Peters VA Medical Center; Chang-Gyu Hahn, University of Pennsylvania; Alexander W Charney, Mount Sinai; Stella Dracheva, Mount Sinai; Alexey Kozlenkov, Mount Sinai; Dalila Pinto, Icahn School of Medicine at Mount Sinai; Judson Belmont, Icahn School of Medicine at Mount Sinai; Diane DelValle, Icahn School of Medicine at Mount Sinai; Nancy Francoeur, Icahn School of Medicine at Mount Sinai; Evi Hadjimichael, Icahn School of Medicine at Mount Sinai; Harm van Bakel, Icahn School of Medicine at Mount Sinai; Panos Roussos, Mount Sinai; John F Fullard, Mount Sinai; Jaroslav Bendl, Mount Sinai; Mads E Hauberg, Mount Sinai; Lara M Mangravite, Sage Bionetworks; Mette A Peters, Sage Bionetworks; Yooree Chae, Sage Bionetworks; Junmin Peng, St. Jude Children's Hospital; Mingming Niu, St. Jude Children's Hospital; Xusheng Wang, St. Jude Children's Hospital; Maree J Webster, Stanley Medical Research Institute; Thomas G Beach, Banner Sun Health Research Institute; Chao Chen, Central South University; Yi Jiang, Central South University; Rujia Dai, Central South University; Annie W Shieh, SUNY Upstate Medical University; Chunyu Liu, SUNY Upstate Medical University; Kay S. Grennan, SUNY Upstate Medical University; Yan Xia, SUNY Upstate Medical University/Central South University; Ramu Vadukapuram, SUNY Upstate Medical University; Yongjun Wang, Central South University; Dominic Fitzgerald, The University of Chicago; Lijun Cheng, The University of Chicago; Miguel Brown, The University of Chicago; Mimi Brown, The University of Chicago; Tonya Brunetti, The University of Chicago; Thomas Goodman, The University of Chicago; Majd Alsayed, The University of Chicago; Michael J Gandal, University of California, Los Angeles; Daniel H Geschwind, University of California, Los Angeles; Hyejung Won, University of California, Los

Angeles; Damon Polioudakis, University of California, Los Angeles; Brie Wamsley, University of California, Los Angeles; Jiani Yin, University of California, Los Angeles; Tarik Hadzic, University of California, Los Angeles; Luis De La Torre Ubieta, UCLA; Vivek Swarup, University of California, Los Angeles; Stephan J Sanders, University of California, San Francisco; Matthew W State, University of California, San Francisco; Donna M Werling, University of California, San Francisco; Joon-Yong An, University of California, San Francisco; Brooke Sheppard, University of California, San Francisco; A Jeremy Willsey, University of California, San Francisco; Kevin P White, The University of Chicago; Mohana Ray, The University of Chicago; Gina Giase, SUNY Upstate Medical University; Amira Kefi, University of Illinois at Chicago; Eugenio Mattei, University of Massachusetts Medical School; Michael Purcaro, University of Massachusetts Medical School; Zhiping Weng, University of Massachusetts Medical School; Jill Moore, University of Massachusetts Medical School; Henry Pratt, University of Massachusetts Medical School; Jack Huey, University of Massachusetts Medical School; Tyler Borrman, University of Massachusetts Medical School; Patrick F Sullivan, University of North Carolina - Chapel Hill; Paola Giusti-Rodriguez, University of North Carolina - Chapel Hill; Yunjung Kim, University of North Carolina - Chapel Hill; Patrick Sullivan, University of North Carolina - Chapel Hill; Jin Szatkiewicz, University of North Carolina - Chapel Hill; Suhn Kyong Rhie, University of Southern California; Christopher Armoskus, University of Southern California; Adrian Camarena, University of Southern California; Peggy J Farnham, University of Southern California; Valeria N Spitsyna, University of Southern California; Heather Witt, University of Southern California; Shannon Schreiner, University of Southern California; Oleg V Evgrafov, SUNY Downstate Medical Center; James A Knowles, SUNY Downstate Medical Center; Mark Gerstein, Yale University; Shuang Liu, Yale University; Daifeng Wang, Yale University; Fabio C. P. Navarro, Yale University; Jonathan Warrell, Yale University; Declan Clarke, Yale University; Prashant S. Emani, Yale University; Mengting Gu, Yale University; Xu Shi, Yale University; Min Xu, Yale University; Yucheng T. Yang, Yale University; Robert R. Kitchen, Yale University; Gamze Gürsoy, Yale University; Jing Zhang, Yale University; Becky C Carlyle, Yale University; Angus C Nairn, Yale University; Mingfeng Li, Yale University; Sirisha Pochareddy, Yale University; Nenad Sestan, Yale University; Mario Skarica, Yale University; Zhen Li, Yale University; Andre M.M. Sousa, Yale University; Gabriel Santpere, Yale University; Jinmyung Choi, Yale University; Ying Zhu, Yale University; Tianliuyun Gao, Yale University; Daniel J Miller, Yale University; Adriana Cherskov, Yale University; Mo Yang, Yale University; Anahita Amiri, Yale University; Gianfilippo Coppola, Yale University; Jessica Mariani, Yale University; Soraya Scuderi, Yale University; Anna Szekely, Yale University; Flora M Vaccarino, Yale University; Feinan Wu, Yale University; Sherman Weissman, Yale University; Tanmoy Roychowdhury, Mayo Clinic Rochester; Alexej Abyzov, Mayo Clinic Rochester

## References and Notes

1. H. A. Whiteford, A. J. Ferrari, L. Degenhardt, V. Feigin, T. Vos, The global burden of mental, neurological and substance use disorders: An analysis from the Global Burden of Disease Study 2010. *PLOS ONE* **10**, e0116820 (2015). [doi:10.1371/journal.pone.0116820](https://doi.org/10.1371/journal.pone.0116820) [Medline](#)
2. M. J. Gandal, V. Leppa, H. Won, N. N. Parkash, D. H. Geschwind, The road to precision psychiatry: Translating genetics into disease mechanisms. *Nat. Neurosci.* **19**, 1397–1407 (2016). [doi:10.1038/nn.4409](https://doi.org/10.1038/nn.4409) [Medline](#)
3. A. Sekar, A. R. Bialas, H. de Rivera, A. Davis, T. R. Hammond, N. Kamitaki, K. Tooley, J. Presumey, M. Baum, V. Van Doren, G. Genovese, S. A. Rose, R. E. Handsaker, M. J. Daly, M. C. Carroll, B. Stevens, S. A. McCarroll; Schizophrenia Working Group of the Psychiatric Genomics Consortium, Schizophrenia risk from complex variation of complement component 4. *Nature* **530**, 177–183 (2016). [doi:10.1038/nature16549](https://doi.org/10.1038/nature16549) [Medline](#)
4. L. de la Torre-Ubieta, H. Won, J. L. Stein, D. H. Geschwind, Advancing the understanding of autism disease mechanisms through genetics. *Nat. Med.* **22**, 345–361 (2016). [doi:10.1038/nm.4071](https://doi.org/10.1038/nm.4071) [Medline](#)
5. M. T. Maurano, R. Humbert, E. Rynes, R. E. Thurman, E. Haugen, H. Wang, A. P. Reynolds, R. Sandstrom, H. Qu, J. Brody, A. Shafer, F. Neri, K. Lee, T. Kutyavin, S. Stehling-Sun, A. K. Johnson, T. K. Canfield, E. Giste, M. Diegel, D. Bates, R. S. Hansen, S. Neph, P. J. Sabo, S. Heimfeld, A. Raubitschek, S. Ziegler, C. Cotsapas, N. Sotoodehnia, I. Glass, S. R. Sunyaev, R. Kaul, J. A. Stamatoyannopoulos, Systematic localization of common disease-associated variation in regulatory DNA. *Science* **337**, 1190–1195 (2012). [doi:10.1126/science.1222794](https://doi.org/10.1126/science.1222794) [Medline](#)
6. L. D. Ward, M. Kellis, Interpreting noncoding genetic variation in complex traits and human disease. *Nat. Biotechnol.* **30**, 1095–1106 (2012). [doi:10.1038/nbt.2422](https://doi.org/10.1038/nbt.2422) [Medline](#)
7. A. Visel, E. M. Rubin, L. A. Pennacchio, Genomic views of distant-acting enhancers. *Nature* **461**, 199–205 (2009). [doi:10.1038/nature08451](https://doi.org/10.1038/nature08451) [Medline](#)
8. K. G. Ardlie, D. S. Deluca, A. V. Segre, T. J. Sullivan, T. R. Young, E. T. Gelfand, C. A. Trowbridge, J. B. Maller, T. Tukiainen, M. Lek, L. D. Ward, P. Kheradpour, B. Iriarte, Y. Meng, C. D. Palmer, T. Esko, W. Winckler, J. N. Hirschhorn, M. Kellis, D. G. MacArthur, G. Getz, A. A. Shabalin, G. Li, Y.-H. Zhou, A. B. Nobel, I. Rusyn, F. A. Wright, T. Lappalainen, P. G. Ferreira, H. Ongen, M. A. Rivas, A. Battle, S. Mostafavi, J. Monlong, M. Sammeth, M. Mele, F. Reverter, J. M. Goldmann, D. Koller, R. Guigo, M. I. McCarthy, E. T. Dermitzakis, E. R. Gamazon, H. K. Im, A. Konkashbaev, D. L. Nicolae, N. J. Cox, T. Flutre, X. Wen, M. Stephens, J. K. Pritchard, Z. Tu, B. Zhang, T. Huang, Q. Long, L. Lin, J. Yang, J. Zhu, J. Liu, A. Brown, B. Mestichelli, D. Tidwell, E. Lo, M. Salvatore, S. Shad, J. A. Thomas, J. T. Lonsdale, M. T. Moser, B. M. Gillard, E. Karasik, K. Ramsey, C. Choi, B. A. Foster, J. Syron, J. Fleming, H. Magazine, R. Hasz, G. D. Walters, J. P. Bridge, M. Miklos, S. Sullivan, L. K. Barker, H. M. Traino, M. Mosavel, L. A. Siminoff, D. R. Valley, D. C. Rohrer, S. D. Jewell, P. A. Branton, L. H. Sabin, M. Barcus, L. Qi, J. McLean, P. Hariharan, K. S. Um, S. Wu, D. Tabor, C. Shive, A. M. Smith, S. A. Buia, A. H. Undale, K. L. Robinson, N. Roche, K. M. Valentino, A.

- Britton, R. Burges, D. Bradbury, K. W. Hambright, J. Seleski, G. E. Korzeniewski, K. Erickson, Y. Marcus, J. Tejada, M. Taherian, C. Lu, M. Basile, D. C. Mash, S. Volpi, J. P. Struewing, G. F. Temple, J. Boyer, D. Colantuoni, R. Little, S. Koester, L. J. Carithers, H. M. Moore, P. Guan, C. Compton, S. J. Sawyer, J. P. Demchok, J. B. Vaught, C. A. Rabiner, N. C. Lockhart, K. G. Ardlie, G. Getz, F. A. Wright, M. Kellis, S. Volpi, E. T. Dermitzakis; GTEx Consortium, Human genomics. The Genotype-Tissue Expression (GTEx) pilot analysis: Multitissue gene regulation in humans. *Science* **348**, 648–660 (2015). [doi:10.1126/science.1262110](https://doi.org/10.1126/science.1262110) [Medline](#)
9. S. K. Reilly, J. Yin, A. E. Ayoub, D. Emera, J. Leng, J. Cotney, R. Sarro, P. Rakic, J. P. Noonan, Evolutionary genomics. Evolutionary changes in promoter and enhancer activity during human corticogenesis. *Science* **347**, 1155–1159 (2015). [doi:10.1126/science.1260943](https://doi.org/10.1126/science.1260943) [Medline](#)
10. The ENCODE Project Consortium, Identification and analysis of functional elements in 1% of the human genome by the ENCODE pilot project. *Nature* **447**, 799–816 (2007). [doi:10.1038/nature05874](https://doi.org/10.1038/nature05874) [Medline](#)
11. A. Kundaje, W. Meuleman, J. Ernst, M. Bilenky, A. Yen, A. Heravi-Moussavi, P. Kheradpour, Z. Zhang, J. Wang, M. J. Ziller, V. Amin, J. W. Whitaker, M. D. Schultz, L. D. Ward, A. Sarkar, G. Quon, R. S. Sandstrom, M. L. Eaton, Y.-C. Wu, A. R. Pfennig, X. Wang, M. Claussnitzer, Y. Liu, C. Coarfa, R. A. Harris, N. Shores, C. B. Epstein, E. Gjoneska, D. Leung, W. Xie, R. D. Hawkins, R. Lister, C. Hong, P. Gascard, A. J. Mungall, R. Moore, E. Chuah, A. Tam, T. K. Canfield, R. S. Hansen, R. Kaul, P. J. Sabo, M. S. Bansal, A. Carles, J. R. Dixon, K.-H. Farh, S. Feizi, R. Karlic, A.-R. Kim, A. Kulkarni, D. Li, R. Lowdon, G. Elliott, T. R. Mercer, S. J. Neph, V. Onuchic, P. Polak, N. Rajagopal, P. Ray, R. C. Sallari, K. T. Siebenthal, N. A. Sinnott-Armstrong, M. Stevens, R. E. Thurman, J. Wu, B. Zhang, X. Zhou, A. E. Beaudet, L. A. Boyer, P. L. De Jager, P. J. Farnham, S. J. Fisher, D. Haussler, S. J. M. Jones, W. Li, M. A. Marra, M. T. McManus, S. Sunyaev, J. A. Thomson, T. D. Tlsty, L.-H. Tsai, W. Wang, R. A. Waterland, M. Q. Zhang, L. H. Chadwick, B. E. Bernstein, J. F. Costello, J. R. Ecker, M. Hirst, A. Meissner, A. Milosavljevic, B. Ren, J. A. Stamatoyannopoulos, T. Wang, M. Kellis; Roadmap Epigenomics Consortium, Integrative analysis of 111 reference human epigenomes. *Nature* **518**, 317–330 (2015). [doi:10.1038/nature14248](https://doi.org/10.1038/nature14248) [Medline](#)
12. R. Andersson, C. Gebhard, I. Miguel-Escalada, I. Hoof, J. Bornholdt, M. Boyd, Y. Chen, X. Zhao, C. Schmidl, T. Suzuki, E. Ntini, E. Arner, E. Valen, K. Li, L. Schwarzfischer, D. Glatz, J. Raithel, B. Lilje, N. Rapin, F. O. Bagger, M. Jørgensen, P. R. Andersen, N. Bertin, O. Rackham, A. M. Burroughs, J. K. Baillie, Y. Ishizu, Y. Shimizu, E. Furuhata, S. Maeda, Y. Negishi, C. J. Mungall, T. F. Meehan, T. Lassmann, M. Itoh, H. Kawaji, N. Kondo, J. Kawai, A. Lennartsson, C. O. Daub, P. Heutink, D. A. Hume, T. H. Jensen, H. Suzuki, Y. Hayashizaki, F. Müller, A. R. R. Forrest, P. Carninci, M. Rehli, A. Sandelin, An atlas of active enhancers across human cell types and tissues. *Nature* **507**, 455–461 (2014). [doi:10.1038/nature12787](https://doi.org/10.1038/nature12787) [Medline](#)
13. M. J. Gandal, J. R. Haney, N. N. Parikshak, V. Leppa, G. Ramaswami, C. Hartl, A. J. Schork, V. Appadurai, A. Buil, T. M. Werge, C. Liu, K. P. White, S. Horvath, D. H. Geschwind; CommonMind Consortium; PsychENCODE Consortium; iPSYCH-BROAD Working Group, Shared molecular neuropathology across major psychiatric disorders

parallels polygenic overlap. *Science* **359**, 693–697 (2018). [doi:10.1126/science.aad6469](https://doi.org/10.1126/science.aad6469) [Medline](#)

14. N. N. Parikshak, M. J. Gandal, D. H. Geschwind, Systems biology and gene networks in neurodevelopmental and neurodegenerative disorders. *Nat. Rev. Genet.* **16**, 441–458 (2015). [doi:10.1038/nrg3934](https://doi.org/10.1038/nrg3934) [Medline](#)
15. I. Voineagu, X. Wang, P. Johnston, J. K. Lowe, Y. Tian, S. Horvath, J. Mill, R. M. Cantor, B. J. Blencowe, D. H. Geschwind, Transcriptomic analysis of autistic brain reveals convergent molecular pathology. *Nature* **474**, 380–384 (2011). [doi:10.1038/nature10110](https://doi.org/10.1038/nature10110) [Medline](#)
16. S. Akbarian, C. Liu, J. A. Knowles, F. M. Vaccarino, P. J. Farnham, G. E. Crawford, A. E. Jaffe, D. Pinto, S. Dracheva, D. H. Geschwind, J. Mill, A. C. Nairn, A. Abyzov, S. Pochareddy, S. Prabhakar, S. Weissman, P. F. Sullivan, M. W. State, Z. Weng, M. A. Peters, K. P. White, M. B. Gerstein, A. Amiri, C. Armoskus, A. E. Ashley-Koch, T. Bae, A. Beckel-Mitchener, B. P. Berman, G. A. Coetzee, G. Coppola, N. Francoeur, M. Fromer, R. Gao, K. Grennan, J. Herstein, D. H. Kavanagh, N. A. Ivanov, Y. Jiang, R. R. Kitchen, A. Kozlenkov, M. Kundakovic, M. Li, Z. Li, S. Liu, L. M. Mangravite, E. Mattei, E. Markenscoff-Papadimitriou, F. C. P. Navarro, N. North, L. Omberg, D. Panchision, N. Parikshak, J. Poschmann, A. J. Price, M. Purcaro, T. E. Reddy, P. Roussos, S. Schreiner, S. Scuderi, R. Sebra, M. Shibata, A. W. Shieh, M. Skarica, W. Sun, V. Swarup, A. Thomas, J. Tsuji, H. van Bakel, D. Wang, Y. Wang, K. Wang, D. M. Werling, A. J. Willsey, H. Witt, H. Won, C. C. Y. Wong, G. A. Wray, E. Y. Wu, X. Xu, L. Yao, G. Senthil, T. Lehner, P. Sklar, N. Sestan; PsychENCODE Consortium, The PsychENCODE project. *Nat. Neurosci.* **18**, 1707–1712 (2015). [doi:10.1038/nn.4156](https://doi.org/10.1038/nn.4156) [Medline](#)
17. Daifeng Wang, Shuang Liu, Jonathan Warrell, Hyejung Won, Xu Shi, Fabio C. P. Navarro, Declan Clarke, Mengting Gu, Prashant Emani, Yucheng T. Yang, Min Xu, Michael J. Gandal, Shaoke Lou, Jing Zhang, Jonathan J. Park, Chengfei Yan, Suhn Kyong Rhie, Kasidet Manakongtreeep, Holly Zhou, Aparna Nathan, Mette Peters, Eugenio Mattei, Dominic Fitzgerald, Tonya Brunetti, Jill Moore, Yan Jiang, Kiran Girdhar, Gabriel E. Hoffman, Selim Kalayci, Zeynep H. Gümuş, Gregory E. Crawford, PsychENCODE Consortium, Panos Roussos, Schahram Akbarian, Andrew E. Jaffe, Kevin P. White, Zhiping Weng, Nenad Sestan, Daniel H. Geschwind, James A. Knowles, Mark B. Gerstein, Comprehensive functional genomic resource and integrative model for the human brain. *Science* **362**, eaat8464 (2018).
18. M. Fromer, P. Roussos, S. K. Sieberts, J. S. Johnson, D. H. Kavanagh, T. M. Perumal, D. M. Ruderfer, E. C. Oh, A. Topol, H. R. Shah, L. L. Klei, R. Kramer, D. Pinto, Z. H. Gümuş, A. E. Cicek, K. K. Dang, A. Browne, C. Lu, L. Xie, B. Readhead, E. A. Stahl, J. Xiao, M. Parvizi, T. Hamamsy, J. F. Fullard, Y.-C. Wang, M. C. Mahajan, J. M. J. Derry, J. T. Dudley, S. E. Hemby, B. A. Logsdon, K. Talbot, T. Raj, D. A. Bennett, P. L. De Jager, J. Zhu, B. Zhang, P. F. Sullivan, A. Chess, S. M. Purcell, L. A. Shinobu, L. M. Mangravite, H. Toyoshiba, R. E. Gur, C.-G. Hahn, D. A. Lewis, V. Haroutunian, M. A. Peters, B. K. Lipska, J. D. Buxbaum, E. E. Schadt, K. Hirai, K. Roeder, K. J. Brennand, N. Katsanis, E. Domenici, B. Devlin, P. Sklar, Gene expression elucidates functional impact of

polygenic risk for schizophrenia. *Nat. Neurosci.* **19**, 1442–1453 (2016).  
[doi:10.1038/nn.4399](https://doi.org/10.1038/nn.4399) [Medline](#)

19. N. N. Parikshak, V. Swarup, T. G. Belgard, M. Irimia, G. Ramaswami, M. J. Gandal, C. Hartl, V. Leppa, L. T. Ubieta, J. Huang, J. K. Lowe, B. J. Blencowe, S. Horvath, D. H. Geschwind, Genome-wide changes in lncRNA, splicing, and regional gene expression patterns in autism. *Nature* **540**, 423–427 (2016). [doi:10.1038/nature20612](https://doi.org/10.1038/nature20612) [Medline](#)
20. H. J. Kang, Y. I. Kawasawa, F. Cheng, Y. Zhu, X. Xu, M. Li, A. M. M. Sousa, M. Pletikos, K. A. Meyer, G. Sedmak, T. Guennel, Y. Shin, M. B. Johnson, Z. Krsnik, S. Mayer, S. Fertuzinhos, S. Umlauf, S. N. Lisgo, A. Vortmeyer, D. R. Weinberger, S. Mane, T. M. Hyde, A. Huttner, M. Reimers, J. E. Kleinman, N. Šestan, Spatio-temporal transcriptome of the human brain. *Nature* **478**, 483–489 (2011). [doi:10.1038/nature10523](https://doi.org/10.1038/nature10523) [Medline](#)
21. See supplementary materials and methods.
22. A. E. Jaffe, R. Tao, A. L. Norris, M. Kealhofer, A. Nellore, J. H. Shin, D. Kim, Y. Jia, T. M. Hyde, J. E. Kleinman, R. E. Straub, J. T. Leek, D. R. Weinberger, qSVA framework for RNA quality correction in differential expression analysis. *Proc. Natl. Acad. Sci. U.S.A.* **114**, 7130–7135 (2017). [doi:10.1073/pnas.1617384114](https://doi.org/10.1073/pnas.1617384114) [Medline](#)
23. B. Li, C. N. Dewey, RSEM: Accurate transcript quantification from RNA-Seq data with or without a reference genome. *BMC Bioinformatics* **12**, 323 (2011). [doi:10.1186/1471-2105-12-323](https://doi.org/10.1186/1471-2105-12-323) [Medline](#)
24. A. E. Jaffe, R. E. Straub, J. H. Shin, R. Tao, Y. Gao, L. Collado-Torres, T. Kam-Thong, H. S. Xi, J. Quan, Q. Chen, C. Colantuoni, W. S. Ulrich, B. J. Maher, A. Deep-Soboslay, A. J. Cross, N. J. Brandon, J. T. Leek, T. M. Hyde, J. E. Kleinman, D. R. Weinberger; BrainSeq Consortium, Developmental and genetic regulation of the human cortex transcriptome illuminate schizophrenia pathogenesis. *Nat. Neurosci.* **21**, 1117–1125 (2018). [doi:10.1038/s41593-018-0197-y](https://doi.org/10.1038/s41593-018-0197-y) [Medline](#)
25. Y. I. Li, B. van de Geijn, A. Raj, D. A. Knowles, A. A. Petti, D. Golan, Y. Gilad, J. K. Pritchard, RNA splicing is a primary link between genetic variation and disease. *Science* **352**, 600–604 (2016). [doi:10.1126/science.aad9417](https://doi.org/10.1126/science.aad9417) [Medline](#)
26. P. J. Batista, H. Y. Chang, Long noncoding RNAs: Cellular address codes in development and disease. *Cell* **152**, 1298–1307 (2013). [doi:10.1016/j.cell.2013.02.012](https://doi.org/10.1016/j.cell.2013.02.012) [Medline](#)
27. J. di Iulio, I. Bartha, E. H. M. Wong, H.-C. Yu, V. Lavrenko, D. Yang, I. Jung, M. A. Hicks, N. Shah, E. F. Kirkness, M. M. Fabani, W. H. Biggs, B. Ren, J. C. Venter, A. Telenti, The human noncoding genome defined by genetic diversity. *Nat. Genet.* **50**, 333–337 (2018). [doi:10.1038/s41588-018-0062-7](https://doi.org/10.1038/s41588-018-0062-7) [Medline](#)
28. C. K. Vuong, D. L. Black, S. Zheng, The neurogenetics of alternative splicing. *Nat. Rev. Neurosci.* **17**, 265–281 (2016). [doi:10.1038/nrn.2016.27](https://doi.org/10.1038/nrn.2016.27) [Medline](#)
29. Y. I. Li, D. A. Knowles, J. Humphrey, A. N. Barbeira, S. P. Dickinson, H. K. Im, J. K. Pritchard, Annotation-free quantification of RNA splicing using LeafCutter. *Nat. Genet.* **50**, 151–158 (2018). [doi:10.1038/s41588-017-0004-9](https://doi.org/10.1038/s41588-017-0004-9) [Medline](#)
30. M. Irimia, R. J. Weatheritt, J. D. Ellis, N. N. Parikshak, T. Gonatopoulos-Pournatzis, M. Babor, M. Quesnel-Vallières, J. Tapial, B. Raj, D. O'Hanlon, M. Barrios-Rodiles, M. J.

- E. Sternberg, S. P. Cordes, F. P. Roth, J. L. Wrana, D. H. Geschwind, B. J. Blencowe, A highly conserved program of neuronal microexons is misregulated in autistic brains. *Cell* **159**, 1511–1523 (2014). [doi:10.1016/j.cell.2014.11.035](https://doi.org/10.1016/j.cell.2014.11.035) Medline
31. N. Akula, J. Barb, X. Jiang, J. R. Wendland, K. H. Choi, S. K. Sen, L. Hou, D. T. W. Chen, G. Laje, K. Johnson, B. K. Lipska, J. E. Kleinman, H. Corrada-Bravo, S. Detera-Wadleigh, P. J. Munson, F. J. McMahon, RNA-sequencing of the brain transcriptome implicates dysregulation of neuroplasticity, circadian rhythms and GTPase binding in bipolar disorder. *Mol. Psychiatry* **19**, 1179–1185 (2014). [doi:10.1038/mp.2013.170](https://doi.org/10.1038/mp.2013.170) Medline
32. J.-A. Lee, A. Damianov, C.-H. Lin, M. Fontes, N. N. Parikshak, E. S. Anderson, D. H. Geschwind, D. L. Black, K. C. Martin, Cytoplasmic Rbfox1 Regulates the Expression of Synaptic and Autism-Related Genes. *Neuron* **89**, 113–128 (2016). [doi:10.1016/j.neuron.2015.11.025](https://doi.org/10.1016/j.neuron.2015.11.025) Medline
33. J. C. Darnell, S. J. Van Driesche, C. Zhang, K. Y. S. Hung, A. Mele, C. E. Fraser, E. F. Stone, C. Chen, J. J. Fak, S. W. Chi, D. D. Licatalosi, J. D. Richter, R. B. Darnell, FMRP stalls ribosomal translocation on mRNAs linked to synaptic function and autism. *Cell* **146**, 247–261 (2011). [doi:10.1016/j.cell.2011.06.013](https://doi.org/10.1016/j.cell.2011.06.013) Medline
34. E. Sebestyén, B. Singh, B. Miñana, A. Pagès, F. Mateo, M. A. Pujana, J. Valcárcel, E. Eyras, Large-scale analysis of genome and transcriptome alterations in multiple tumors unveils novel cancer-relevant splicing networks. *Genome Res.* **26**, 732–744 (2016). [doi:10.1101/gr.199935.115](https://doi.org/10.1101/gr.199935.115) Medline
35. J. Gauthier, T. J. Siddiqui, P. Huashan, D. Yokomaku, F. F. Hamdan, N. Champagne, M. Lapointe, D. Spiegelman, A. Noreau, R. G. Lafrenière, F. Fathalli, R. Joober, M.-O. Krebs, L. E. DeLisi, L. Mottron, E. Fombonne, J. L. Michaud, P. Drapeau, S. Carbonetto, A. M. Craig, G. A. Rouleau, Truncating mutations in NRXN2 and NRXN1 in autism spectrum disorders and schizophrenia. *Hum. Genet.* **130**, 563–573 (2011). [doi:10.1007/s00439-011-0975-z](https://doi.org/10.1007/s00439-011-0975-z) Medline
36. F. F. Hamdan, J. Gauthier, Y. Araki, D.-T. Lin, Y. Yoshizawa, K. Higashi, A.-R. Park, D. Spiegelman, S. Dobrzeniecka, A. Piton, H. Tomitori, H. Daoud, C. Massicotte, E. Henrion, O. Diallo, M. Shekarabi, C. Marineau, M. Shevell, B. Maranda, G. Mitchell, A. Nadeau, G. D’Anjou, M. Vanasse, M. Srour, R. G. Lafrenière, P. Drapeau, J. C. Lacaille, E. Kim, J.-R. Lee, K. Igarashi, R. L. Huganir, G. A. Rouleau, J. L. Michaud; S2D Group, Excess of de novo deleterious mutations in genes associated with glutamatergic systems in nonsyndromic intellectual disability. *Am. J. Hum. Genet.* **88**, 306–316 (2011). [doi:10.1016/j.ajhg.2011.02.001](https://doi.org/10.1016/j.ajhg.2011.02.001) Medline
37. B. Treutlein, O. Gokce, S. R. Quake, T. C. Südhof, Cartography of neurexin alternative splicing mapped by single-molecule long-read mRNA sequencing. *Proc. Natl. Acad. Sci. U.S.A.* **111**, E1291–E1299 (2014). [doi:10.1073/pnas.1403244111](https://doi.org/10.1073/pnas.1403244111) Medline
38. J. Grove *et al.*, Common risk variants identified in autism spectrum disorder. bioRxiv 224774 [Preprint]. 27 November 2017. <https://doi.org/10.1101/224774>.
39. H. K. Finucane, B. Bulik-Sullivan, A. Gusev, G. Trynka, Y. Reshef, P.-R. Loh, V. Anttila, H. Xu, C. Zang, K. Farh, S. Ripke, F. R. Day, S. Purcell, E. Stahl, S. Lindstrom, J. R. B. Perry, Y. Okada, S. Raychaudhuri, M. J. Daly, N. Patterson, B. M. Neale, A. L. Price;

ReproGen Consortium; Schizophrenia Working Group of the Psychiatric Genomics Consortium; RACI Consortium, Partitioning heritability by functional annotation using genome-wide association summary statistics. *Nat. Genet.* **47**, 1228–1235 (2015).  
[doi:10.1038/ng.3404](https://doi.org/10.1038/ng.3404) Medline

40. A. E. West, M. E. Greenberg, Neuronal activity-regulated gene transcription in synapse development and cognitive function. *Cold Spring Harb. Perspect. Biol.* **3**, a005744 (2011). [doi:10.1101/cshperspect.a005744](https://doi.org/10.1101/cshperspect.a005744) Medline
41. Y. Zhu, L. Wang, Y. Yin, E. Yang, Systematic analysis of gene expression patterns associated with postmortem interval in human tissues. *Sci. Rep.* **7**, 5435 (2017). [doi:10.1038/s41598-017-05882-0](https://doi.org/10.1038/s41598-017-05882-0) Medline
42. J. Z. Li, M. P. Vawter, D. M. Walsh, H. Tomita, S. J. Evans, P. V. Choudary, J. F. Lopez, A. Avelar, V. Shokoohi, T. Chung, O. Mesarwi, E. G. Jones, S. J. Watson, H. Akil, W. E. Bunney Jr., R. M. Myers, Systematic changes in gene expression in postmortem human brains associated with tissue pH and terminal medical conditions. *Hum. Mol. Genet.* **13**, 609–616 (2004). [doi:10.1093/hmg/ddh065](https://doi.org/10.1093/hmg/ddh065) Medline
43. J. T. Leek, J. D. Storey, Capturing heterogeneity in gene expression studies by surrogate variable analysis. *PLOS Genet.* **3**, e161 (2007). [doi:10.1371/journal.pgen.0030161](https://doi.org/10.1371/journal.pgen.0030161) Medline
44. GTEx Consortium, Genetic effects on gene expression across human tissues. *Nature* **550**, 204–213 (2017). [doi:10.1038/nature24277](https://doi.org/10.1038/nature24277) Medline
45. M. C. Zody, Z. Jiang, H.-C. Fung, F. Antonacci, L. W. Hillier, M. F. Cardone, T. A. Graves, J. M. Kidd, Z. Cheng, A. Abouelleil, L. Chen, J. Wallis, J. Glasscock, R. K. Wilson, A. D. Reily, J. Duckworth, M. Ventura, J. Hardy, W. C. Warren, E. E. Eichler, Evolutionary toggling of the MAPT 17q21.31 inversion region. *Nat. Genet.* **40**, 1076–1083 (2008). [doi:10.1038/ng.193](https://doi.org/10.1038/ng.193) Medline
46. A. Gusev, A. Ko, H. Shi, G. Bhatia, W. Chung, B. W. J. H. Penninx, R. Jansen, E. J. C. de Geus, D. I. Boomsma, F. A. Wright, P. F. Sullivan, E. Nikkola, M. Alvarez, M. Civelek, A. J. Lusis, T. Lehtimäki, E. Raitoharju, M. Kähönen, I. Seppälä, O. T. Raitakari, J. Kuusisto, M. Laakso, A. L. Price, P. Pajukanta, B. Pasaniuc, Integrative approaches for large-scale transcriptome-wide association studies. *Nat. Genet.* **48**, 245–252 (2016). [doi:10.1038/ng.3506](https://doi.org/10.1038/ng.3506) Medline
47. E. R. Gamazon, H. E. Wheeler, K. P. Shah, S. V. Mozaffari, K. Aquino-Michaels, R. J. Carroll, A. E. Eyler, J. C. Denny, D. L. Nicolae, N. J. Cox, H. K. Im; GTEx Consortium, A gene-based association method for mapping traits using reference transcriptome data. *Nat. Genet.* **47**, 1091–1098 (2015). [doi:10.1038/ng.3367](https://doi.org/10.1038/ng.3367) Medline
48. Z. Zhu, F. Zhang, H. Hu, A. Bakshi, M. R. Robinson, J. E. Powell, G. W. Montgomery, M. E. Goddard, N. R. Wray, P. M. Visscher, J. Yang, Integration of summary data from GWAS and eQTL studies predicts complex trait gene targets. *Nat. Genet.* **48**, 481–487 (2016). [doi:10.1038/ng.3538](https://doi.org/10.1038/ng.3538) Medline
49. M. C. Oldham, G. Konopka, K. Iwamoto, P. Langfelder, T. Kato, S. Horvath, D. H. Geschwind, Functional organization of the transcriptome in human brain. *Nat. Neurosci.* **11**, 1271–1282 (2008). [doi:10.1038/nn.2207](https://doi.org/10.1038/nn.2207) Medline

50. B. Zhang, S. Horvath, A general framework for weighted gene co-expression network analysis. *Stat. Appl. Genet. Mol. Biol.* **4**, e17 (2005). [doi:10.2202/1544-6115.1128](https://doi.org/10.2202/1544-6115.1128) [Medline](#)
51. J. A. Miller, M. C. Oldham, D. H. Geschwind, A systems level analysis of transcriptional changes in Alzheimer's disease and normal aging. *J. Neurosci.* **28**, 1410–1420 (2008). [doi:10.1523/JNEUROSCI.4098-07.2008](https://doi.org/10.1523/JNEUROSCI.4098-07.2008) [Medline](#)
52. C. Chen, L. Cheng, K. Grennan, F. Pibiri, C. Zhang, J. A. Badner, E. S. Gershon, C. Liu; Members of the Bipolar Disorder Genome Study (BiGS) Consortium, Two gene co-expression modules differentiate psychotics and controls. *Mol. Psychiatry* **18**, 1308–1314 (2013). [doi:10.1038/mp.2012.146](https://doi.org/10.1038/mp.2012.146) [Medline](#)
53. R. Daneman, L. Zhou, D. Agalliu, J. D. Cahoy, A. Kaushal, B. A. Barres, The mouse blood-brain barrier transcriptome: A new resource for understanding the development and function of brain endothelial cells. *PLOS ONE* **5**, e13741 (2010). [doi:10.1371/journal.pone.0013741](https://doi.org/10.1371/journal.pone.0013741) [Medline](#)
54. B. Obermeier, R. Daneman, R. M. Ransohoff, Development, maintenance and disruption of the blood-brain barrier. *Nat. Med.* **19**, 1584–1596 (2013). [doi:10.1038/nm.3407](https://doi.org/10.1038/nm.3407) [Medline](#)
55. G. Genovese, M. Fromer, E. A. Stahl, D. M. Ruderfer, K. Chambert, M. Landén, J. L. Moran, S. M. Purcell, P. Sklar, P. F. Sullivan, C. M. Hultman, S. A. McCarroll, Increased burden of ultra-rare protein-altering variants among 4,877 individuals with schizophrenia. *Nat. Neurosci.* **19**, 1433–1441 (2016). [doi:10.1038/nn.4402](https://doi.org/10.1038/nn.4402) [Medline](#)
56. S. E. Ellis, R. Panitch, A. B. West, D. E. Arking, Transcriptome analysis of cortical tissue reveals shared sets of downregulated genes in autism and schizophrenia. *Transl. Psychiatry* **6**, e817 (2016). [doi:10.1038/tp.2016.87](https://doi.org/10.1038/tp.2016.87) [Medline](#)
57. R. C. Ramaker, K. M. Bowling, B. N. Lasseigne, M. H. Hagenauer, A. A. Hardigan, N. S. Davis, J. Gertz, P. M. Cartagena, D. M. Walsh, M. P. Vawter, E. G. Jones, A. F. Schatzberg, J. D. Barchas, S. J. Watson, B. G. Bunney, H. Akil, W. E. Bunney, J. Z. Li, S. J. Cooper, R. M. Myers, Post-mortem molecular profiling of three psychiatric disorders. *Genome Med.* **9**, 72 (2017). [doi:10.1186/s13073-017-0458-5](https://doi.org/10.1186/s13073-017-0458-5) [Medline](#)
58. C. K. Vuong, W. Wei, J.-A. Lee, C.-H. Lin, A. Damianov, L. de la Torre-Ubieta, R. Halabi, K. O. Otis, K. C. Martin, T. J. O'Dell, D. L. Black, Rbfox1 Regulates Synaptic Transmission through the Inhibitory Neuron-Specific vSNARE Vamp1. *Neuron* **98**, 127–141.e7 (2018). [doi:10.1016/j.neuron.2018.03.008](https://doi.org/10.1016/j.neuron.2018.03.008) [Medline](#)
59. A. F. Pardiñas, P. Holmans, A. J. Pocklington, V. Escott-Price, S. Ripke, N. Carrera, S. E. Legge, S. Bishop, D. Cameron, M. L. Hamshere, J. Han, L. Hubbard, A. Lynham, K. Mantripragada, E. Rees, J. H. MacCabe, S. A. McCarroll, B. T. Baune, G. Breen, E. M. Byrne, U. Dannlowksi, T. C. Eley, C. Hayward, N. G. Martin, A. M. McIntosh, R. Plomin, D. J. Porteous, N. R. Wray, A. Caballero, D. H. Geschwind, L. M. Huckins, D. M. Ruderfer, E. Santiago, P. Sklar, E. A. Stahl, H. Won, E. Agerbo, T. D. Als, O. A. Andreassen, M. Bækvad-Hansen, P. B. Mortensen, C. B. Pedersen, A. D. Børglum, J. Bybjerg-Grauholt, S. Djurovic, N. Durmishi, M. G. Pedersen, V. Golimbet, J. Grove, D. M. Hougaard, M. Mattheisen, E. Molden, O. Mors, M. Nordentoft, M. Pejovic-Milovancevic, E. Sigurdsson, T. Silagadze, C. S. Hansen, K. Stefansson, H. Stefansson, S. Steinberg, S. Tosato, T. Werge, D. A. Collier, D. Rujescu, G. Kirov, M. J. Owen, M.

- C. O'Donovan, J. T. R. Walters; GERAD1 Consortium; CRESTAR Consortium; GERAD1 Consortium; CRESTAR Consortium; GERAD1 Consortium; CRESTAR Consortium, Common schizophrenia alleles are enriched in mutation-intolerant genes and in regions under strong background selection. *Nat. Genet.* **50**, 381–389 (2018). [doi:10.1038/s41588-018-0059-2](https://doi.org/10.1038/s41588-018-0059-2) [Medline](#)
60. L. T. Gehman, P. Stoilov, J. Maguire, A. Damianov, C.-H. Lin, L. Shiue, M. Ares Jr., I. Mody, D. L. Black, The splicing regulator Rbfox1 (A2BP1) controls neuronal excitation in the mammalian brain. *Nat. Genet.* **43**, 706–711 (2011). [doi:10.1038/ng.841](https://doi.org/10.1038/ng.841) [Medline](#)
61. B. L. Fogel, E. Wexler, A. Wahnich, T. Friedrich, C. Vijayendran, F. Gao, N. Parikshak, G. Konopka, D. H. Geschwind, RBFOX1 regulates both splicing and transcriptional networks in human neuronal development. *Hum. Mol. Genet.* **21**, 4171–4186 (2012). [doi:10.1093/hmg/ddz240](https://doi.org/10.1093/hmg/ddz240) [Medline](#)
62. A. M. Bond, M. J. W. Vangompel, E. A. Sametsky, M. F. Clark, J. C. Savage, J. F. Disterhoft, J. D. Kohtz, Balanced gene regulation by an embryonic brain ncRNA is critical for adult hippocampal GABA circuitry. *Nat. Neurosci.* **12**, 1020–1027 (2009). [doi:10.1038/nn.2371](https://doi.org/10.1038/nn.2371) [Medline](#)
63. N. G. Skene, J. Bryois, T. E. Bakken, G. Breen, J. J. Crowley, H. A. Gaspar, P. Giusti-Rodriguez, R. D. Hodge, J. A. Miller, A. B. Muñoz-Manchado, M. C. O'Donovan, M. J. Owen, A. F. Pardiñas, J. Ryge, J. T. R. Walters, S. Linnarsson, E. S. Lein, P. F. Sullivan, J. Hjerling-Leffler; Major Depressive Disorder Working Group of the Psychiatric Genomics Consortium, Genetic identification of brain cell types underlying schizophrenia. *Nat. Genet.* **50**, 825–833 (2018). [doi:10.1038/s41588-018-0129-5](https://doi.org/10.1038/s41588-018-0129-5) [Medline](#)
64. B. Labonté, O. Engmann, I. Purushothaman, C. Menard, J. Wang, C. Tan, J. R. Scarpa, G. Moy, Y. E. Loh, M. Cahill, Z. S. Lorsch, P. J. Hamilton, E. S. Calipari, G. E. Hodes, O. Issler, H. Kronman, M. Pfau, A. L. J. Obradovic, Y. Dong, R. L. Neve, S. Russo, A. Kazarskis, C. Tamminga, N. Mechawar, G. Turecki, B. Zhang, L. Shen, E. J. Nestler, Sex-specific transcriptional signatures in human depression. *Nat. Med.* **23**, 1102–1111 (2017). [doi:10.1038/nm.4386](https://doi.org/10.1038/nm.4386) [Medline](#)
65. A. de Bartolomeis, E. F. Buonaguro, G. Latte, R. Rossi, F. Marmo, F. Iasevoli, C. Tomasetti, Immediate-Early Genes Modulation by Antipsychotics: Translational Implications for a Putative Gateway to Drug-Induced Long-Term Brain Changes. *Front. Behav. Neurosci.* **11**, 240 (2017). [doi:10.3389/fnbeh.2017.00240](https://doi.org/10.3389/fnbeh.2017.00240) [Medline](#)
66. R. Birnbaum, A. E. Jaffe, Q. Chen, J. H. Shin, J. E. Kleinman, T. M. Hyde, D. R. Weinberger, BrainSeq Consortium, Investigating the neuroimmunogenic architecture of schizophrenia. *Mol. Psychiatry* **23**, 1251–1260 (2018). [doi:10.1038/mp.2017.89](https://doi.org/10.1038/mp.2017.89) [Medline](#)
67. S. G. Fillman, N. Cloonan, V. S. Catts, L. C. Miller, J. Wong, T. McCrossin, M. Cairns, C. S. Weickert, Increased inflammatory markers identified in the dorsolateral prefrontal cortex of individuals with schizophrenia. *Mol. Psychiatry* **18**, 206–214 (2013). [doi:10.1038/mp.2012.110](https://doi.org/10.1038/mp.2012.110) [Medline](#)
68. R. Pacifico, R. L. Davis, Transcriptome sequencing implicates dorsal striatum-specific gene network, immune response and energy metabolism pathways in bipolar disorder. *Mol. Psychiatry* **22**, 441–449 (2017). [doi:10.1038/mp.2016.94](https://doi.org/10.1038/mp.2016.94) [Medline](#)

69. J. S. Rao, G. J. Harry, S. I. Rapoport, H. W. Kim, Increased excitotoxicity and neuroinflammatory markers in postmortem frontal cortex from bipolar disorder patients. *Mol. Psychiatry* **15**, 384–392 (2010). [doi:10.1038/mp.2009.47](https://doi.org/10.1038/mp.2009.47) [Medline](#)
70. S. Gupta, S. E. Ellis, F. N. Ashar, A. Moes, J. S. Bader, J. Zhan, A. B. West, D. E. Arking, Transcriptome analysis reveals dysregulation of innate immune response genes and neuronal activity-dependent genes in autism. *Nat. Commun.* **5**, 5748 (2014). [doi:10.1038/ncomms6748](https://doi.org/10.1038/ncomms6748) [Medline](#)
71. I. Rusinova, S. Forster, S. Yu, A. Kannan, M. Masse, H. Cumming, R. Chapman, P. J. Hertzog, Interferome v2.0: An updated database of annotated interferon-regulated genes. *Nucleic Acids Res.* **41** (D1), D1040–D1046 (2013). [doi:10.1093/nar/gks1215](https://doi.org/10.1093/nar/gks1215) [Medline](#)
72. A. Necsulea, M. Soumillon, M. Warnefors, A. Liechti, T. Daish, U. Zeller, J. C. Baker, F. Grützner, H. Kaessmann, The evolution of lncRNA repertoires and expression patterns in tetrapods. *Nature* **505**, 635–640 (2014). [doi:10.1038/nature12943](https://doi.org/10.1038/nature12943) [Medline](#)
73. R. Dai, Y. Xia, C. Liu, C. Chen, csuWGCNA: A combination of signed and unsigned WGCNA to capture negative correlations. bioRxiv 288225 [Preprint]. 27 September 2018. <https://doi.org/10.1101/288225>.
74. P. Pruunsild, C. P. Bengtson, H. Bading, Networks of Cultured iPSC-Derived Neurons Reveal the Human Synaptic Activity-Regulated Adaptive Gene Program. *Cell Reports* **18**, 122–135 (2017). [doi:10.1016/j.celrep.2016.12.018](https://doi.org/10.1016/j.celrep.2016.12.018) [Medline](#)
75. P. P. Amaral, C. Neyt, S. J. Wilkins, M. E. Askarian-Amiri, S. M. Sunkin, A. C. Perkins, J. S. Mattick, Complex architecture and regulated expression of the Sox2ot locus during vertebrate development. *RNA* **15**, 2013–2027 (2009). [doi:10.1261/rna.1705309](https://doi.org/10.1261/rna.1705309) [Medline](#)
76. T. R. Mercer, M. E. Dinger, S. M. Sunkin, M. F. Mehler, J. S. Mattick, Specific expression of long noncoding RNAs in the mouse brain. *Proc. Natl. Acad. Sci. U.S.A.* **105**, 716–721 (2008). [doi:10.1073/pnas.0706729105](https://doi.org/10.1073/pnas.0706729105) [Medline](#)
77. K. Aberg, P. Saetre, N. Jareborg, E. Jazin, Human QKI, a potential regulator of mRNA expression of human oligodendrocyte-related genes involved in schizophrenia. *Proc. Natl. Acad. Sci. U.S.A.* **103**, 7482–7487 (2006). [doi:10.1073/pnas.0601213103](https://doi.org/10.1073/pnas.0601213103) [Medline](#)
78. G. Barry, J. A. Briggs, D. P. Vanichkina, E. M. Poth, N. J. Beveridge, V. S. Ratnu, S. P. Nayler, K. Nones, J. Hu, T. W. Bredy, S. Nakagawa, F. Rigo, R. J. Taft, M. J. Cairns, S. Blackshaw, E. J. Wolvetang, J. S. Mattick, The long non-coding RNA Gomafu is acutely regulated in response to neuronal activation and involved in schizophrenia-associated alternative splicing. *Mol. Psychiatry* **19**, 486–494 (2014). [doi:10.1038/mp.2013.45](https://doi.org/10.1038/mp.2013.45) [Medline](#)
79. M. Koga, H. Ishiguro, S. Yazaki, Y. Horiuchi, M. Arai, K. Niizato, S. Iritani, M. Itokawa, T. Inada, N. Iwata, N. Ozaki, H. Ujike, H. Kunugi, T. Sasaki, M. Takahashi, Y. Watanabe, T. Someya, A. Kakita, H. Takahashi, H. Nawa, C. Muchardt, M. Yaniv, T. Arinami, Involvement of SMARCA2/BRM in the SWI/SNF chromatin-remodeling complex in schizophrenia. *Hum. Mol. Genet.* **18**, 2483–2494 (2009). [doi:10.1093/hmg/ddp166](https://doi.org/10.1093/hmg/ddp166) [Medline](#)
80. I. D. Krantz, J. McCallum, C. DeScipio, M. Kaur, L. A. Gillis, D. Yaeger, L. Jukofsky, N. Wasserman, A. Bottani, C. A. Morris, M. J. M. Nowaczyk, H. Toriello, M. J. Bamshad, J.

- C. Carey, E. Rappaport, S. Kawauchi, A. D. Lander, A. L. Calof, H. H. Li, M. Devoto, L. G. Jackson, Cornelia de Lange syndrome is caused by mutations in NIPBL, the human homolog of *Drosophila melanogaster* Nipped-B. *Nat. Genet.* **36**, 631–635 (2004). [doi:10.1038/ng1364](https://doi.org/10.1038/ng1364) [Medline](#)
81. S. J. Sanders, X. He, A. J. Willsey, A. G. Ercan-Sençicek, K. E. Samocha, A. E. Cicek, M. T. Murtha, V. H. Bal, S. L. Bishop, S. Dong, A. P. Goldberg, C. Jinlu, J. F. Keaney 3rd, L. Klei, J. D. Mandell, D. Moreno-De-Luca, C. S. Poultney, E. B. Robinson, L. Smith, T. Solli-Nowlan, M. Y. Su, N. A. Teran, M. F. Walker, D. M. Werling, A. L. Beaudet, R. M. Cantor, E. Fombonne, D. H. Geschwind, D. E. Grice, C. Lord, J. K. Lowe, S. M. Mane, D. M. Martin, E. M. Morrow, M. E. Talkowski, J. S. Sutcliffe, C. A. Walsh, T. W. Yu, D. H. Ledbetter, C. L. Martin, E. H. Cook, J. D. Buxbaum, M. J. Daly, B. Devlin, K. Roeder, M. W. State; Autism Sequencing Consortium, Insights into Autism Spectrum Disorder Genomic Architecture and Biology from 71 Risk Loci. *Neuron* **87**, 1215–1233 (2015). [doi:10.1016/j.neuron.2015.09.016](https://doi.org/10.1016/j.neuron.2015.09.016) [Medline](#)
82. M. Melé, P. G. Ferreira, F. Reverter, D. S. DeLuca, J. Monlong, M. Sammeth, T. R. Young, J. M. Goldmann, D. D. Pervouchine, T. J. Sullivan, R. Johnson, A. V. Segrè, S. Djebali, A. Niarchou, F. A. Wright, T. Lappalainen, M. Calvo, G. Getz, E. T. Dermitzakis, K. G. Ardlie, R. Guigó, R. Guigo; GTEx Consortium, The human transcriptome across tissues and individuals. *Science* **348**, 660–665 (2015). [doi:10.1126/science.aaa0355](https://doi.org/10.1126/science.aaa0355) [Medline](#)
83. M. Quesnel-Vallières, Z. Dargaei, M. Irimia, T. Gonatopoulos-Pournatzis, J. Y. Ip, M. Wu, T. Sterne-Weiler, S. Nakagawa, M. A. Woodin, B. J. Blencowe, S. P. Cordes, Misregulation of an Activity-Dependent Splicing Network as a Common Mechanism Underlying Autism Spectrum Disorders. *Mol. Cell* **64**, 1023–1034 (2016). [doi:10.1016/j.molcel.2016.11.033](https://doi.org/10.1016/j.molcel.2016.11.033) [Medline](#)
84. T. Steijger, J. F. Abril, P. G. Engström, F. Kokocinski, T. J. Hubbard, R. Guigó, J. Harrow, P. Bertone; RGASP Consortium, Assessment of transcript reconstruction methods for RNA-seq. *Nat. Methods* **10**, 1177–1184 (2013). [doi:10.1038/nmeth.2714](https://doi.org/10.1038/nmeth.2714) [Medline](#)
85. M. I. Love, J. B. Hogenesch, R. A. Irizarry, Modeling of RNA-seq fragment sequence bias reduces systematic errors in transcript abundance estimation. *Nat. Biotechnol.* **34**, 1287–1291 (2016). [doi:10.1038/nbt.3682](https://doi.org/10.1038/nbt.3682) [Medline](#)
86. M. L. Estes, A. K. McAllister, Immune mediators in the brain and peripheral tissues in autism spectrum disorder. *Nat. Rev. Neurosci.* **16**, 469–486 (2015). [doi:10.1038/nrn3978](https://doi.org/10.1038/nrn3978) [Medline](#)
87. U. Meyer, J. Feldon, O. Dammann, Schizophrenia and autism: Both shared and disorder-specific pathogenesis via perinatal inflammation? *Pediatr. Res.* **69**, 26R–33R (2011). [doi:10.1203/PDR.0b013e318212c196](https://doi.org/10.1203/PDR.0b013e318212c196) [Medline](#)
88. J. D. Rosenblat, E. Brietzke, R. B. Mansur, N. A. Maruschak, Y. Lee, R. S. McIntyre, Inflammation as a neurobiological substrate of cognitive impairment in bipolar disorder: Evidence, pathophysiology and treatment implications. *J. Affect. Disord.* **188**, 149–159 (2015). [doi:10.1016/j.jad.2015.08.058](https://doi.org/10.1016/j.jad.2015.08.058) [Medline](#)
89. T. Lappalainen, Functional genomics bridges the gap between quantitative genetics and molecular biology. *Genome Res.* **25**, 1427–1431 (2015). [doi:10.1101/gr.190983.115](https://doi.org/10.1101/gr.190983.115) [Medline](#)

90. PsychENCODE Capstone Data Collection, doi: [doi.org/10.7303/syn12080241](https://doi.org/10.7303/syn12080241).
91. M. C. Oldham, P. Langfelder, S. Horvath, Network methods for describing sample relationships in genomic datasets: Application to Huntington's disease. *BMC Syst. Biol.* **6**, 63 (2012). [doi:10.1186/1752-0509-6-63](https://doi.org/10.1186/1752-0509-6-63) [Medline](#)
92. K. S. Pollard, M. J. Hubisz, K. R. Rosenbloom, A. Siepel, Detection of nonneutral substitution rates on mammalian phylogenies. *Genome Res.* **20**, 110–121 (2010). [doi:10.1101/gr.097857.109](https://doi.org/10.1101/gr.097857.109) [Medline](#)
93. A. Siepel, G. Bejerano, J. S. Pedersen, A. S. Hinrichs, M. Hou, K. Rosenbloom, H. Clawson, J. Spieth, L. W. Hillier, S. Richards, G. M. Weinstock, R. K. Wilson, R. A. Gibbs, W. J. Kent, W. Miller, D. Haussler, Evolutionarily conserved elements in vertebrate, insect, worm, and yeast genomes. *Genome Res.* **15**, 1034–1050 (2005). [doi:10.1101/gr.3715005](https://doi.org/10.1101/gr.3715005) [Medline](#)
94. N. N. Parikshak, R. Luo, A. Zhang, H. Won, J. K. Lowe, V. Chandran, S. Horvath, D. H. Geschwind, Integrative functional genomic analyses implicate specific molecular pathways and circuits in autism. *Cell* **155**, 1008–1021 (2013). [doi:10.1016/j.cell.2013.10.031](https://doi.org/10.1016/j.cell.2013.10.031) [Medline](#)
95. B. J. Vilhjálmsson, J. Yang, H. K. Finucane, A. Gusev, S. Lindström, S. Ripke, G. Genovese, P. R. Loh, G. Bhatia, R. Do, T. Hayeck, H. H. Won, S. Kathiresan, M. Pato, C. Pato, R. Tamimi, E. Stahl, N. Zaitlen, B. Pasaniuc, G. Belbin, E. E. Kenny, M. H. Schierup, P. De Jager, N. A. Patsopoulos, S. McCarroll, M. Daly, S. Purcell, D. Chasman, B. Neale, M. Goddard, P. M. Visscher, P. Kraft, N. Patterson, A. L. Price; Schizophrenia Working Group of the Psychiatric Genomics Consortium, Discovery, Biology, and Risk of Inherited Variants in Breast Cancer (DRIVE) study, Modeling Linkage Disequilibrium Increases Accuracy of Polygenic Risk Scores. *Am. J. Hum. Genet.* **97**, 576–592 (2015). [doi:10.1016/j.ajhg.2015.09.001](https://doi.org/10.1016/j.ajhg.2015.09.001) [Medline](#)
96. J. Yang, S. H. Lee, M. E. Goddard, P. M. Visscher, GCTA: A tool for genome-wide complex trait analysis. *Am. J. Hum. Genet.* **88**, 76–82 (2011). [doi:10.1016/j.ajhg.2010.11.011](https://doi.org/10.1016/j.ajhg.2010.11.011) [Medline](#)
97. D. M. Ruderfer, S. Ripke, A. McQuillin, J. Boocock, E. A. Stahl, J. M. W. Pavlides, N. Mullins, A. W. Charney, A. P. S. Ori, L. M. O. Loohuis, E. Domenici, A. Di Florio, S. Papiol, J. L. Kalman, V. Trubetskoy, R. Adolfsson, I. Agartz, E. Agerbo, H. Akil, D. Albani, M. Albus, M. Alda, M. Alexander, N. Alliey-Rodriguez, T. D. Als, F. Amin, A. Anjorin, M. J. Arranz, S. Awasthi, S. A. Bacanu, J. A. Badner, M. Baekvad-Hansen, S. Bakker, G. Band, J. D. Barchas, I. Barroso, N. Bass, M. Bauer, B. T. Baune, M. Begemann, C. Bellenguez, R. A. Belliveau Jr., F. Bellivier, S. Bender, J. Bene, S. E. Bergen, W. H. Berrettini, E. Bevilacqua, J. M. Biernacka, T. B. Bigdeli, D. W. Black, H. Blackburn, J. M. Blackwell, D. H. R. Blackwood, C. B. Pedersen, M. Boehnke, M. Boks, A. D. Borglum, E. Bramon, G. Breen, M. A. Brown, R. Bruggeman, N. G. Buccola, R. L. Buckner, M. Budde, B. Bulik-Sullivan, S. J. Bumpstead, W. Bunney, M. Burmeister, J. D. Buxbaum, J. Bybjerg-Grauholt, W. Byerley, W. Cahn, G. Cai, M. J. Cairns, D. Campion, R. M. Cantor, V. J. Carr, N. Carrera, J. P. Casas, M. Casas, S. V. Catts, P. Cervantes, K. D. Chambert, R. C. K. Chan, E. Y. H. Chen, R. Y. L. Chen, W. Cheng, E. F. C. Cheung, S. A. Chong, T.-K. Clarke, C. R. Cloninger, D. Cohen, N. Cohen, J. R. I.

Coleman, D. A. Collier, P. Cormican, W. Coryell, N. Craddock, D. W. Craig, B. Crespo-Facorro, J. J. Crowley, C. Cruceanu, D. Curtis, P. M. Czerski, A. M. Dale, M. J. Daly, U. Dannlowski, A. Darvasi, M. Davidson, K. L. Davis, C. A. de Leeuw, F. Degenhardt, J. Del Favero, L. E. DeLisi, P. Deloukas, D. Demontis, J. R. DePaulo, M. di Forti, D. Dikeos, T. Dinan, S. Djurovic, A. L. Dobbyn, P. Donnelly, G. Donohoe, E. Drapeau, S. Dronov, J. Duan, F. Dudbridge, A. Duncanson, H. Edenberg, S. Edkins, H. Ehrenreich, P. Eichhammer, T. Elvsashagen, J. Eriksson, V. Escott-Price, T. Esko, L. Essioux, B. Etain, C. C. Fan, K.-H. Farh, M. S. Farrell, M. Flickinger, T. M. Foroud, L. Forty, J. Frank, L. Franke, C. Fraser, R. Freedman, C. Freeman, N. B. Freimer, J. I. Friedman, M. Fromer, M. A. Frye, J. M. Fullerton, K. Gade, J. Garnham, H. A. Gaspar, P. V. Gejman, G. Genovese, L. Georgieva, C. Giambartolomei, E. Giannoulatou, I. Giegling, M. Gill, M. Gillman, M. G. Pedersen, P. Giusti-Rodriguez, S. Godard, F. Goes, J. I. Goldstein, S. Gopal, S. D. Gordon, K. Gordon-Smith, J. Gratten, E. Gray, E. K. Green, M. J. Green, T. A. Greenwood, M. Grigoriou-Serbanescu, J. Grove, W. Guan, H. Gurling, J. G. Parra, R. Gwilliam, L. de Haan, J. Hall, M.-H. Hall, C. Hammer, N. Hammond, M. L. Hamshire, M. Hansen, T. Hansen, V. Haroutunian, A. M. Hartmann, J. Hauser, M. Hautzinger, U. Heilbronner, G. Hellenthal, F. A. Henskens, S. Herms, M. Hipolito, J. N. Hirschhorn, P. Hoffmann, M. V. Hollegaard, D. M. Hougaard, H. Huang, L. Huckins, C. M. Hultman, S. E. Hunt, M. Ikeda, N. Iwata, C. Iyegbe, A. V. Jablensky, S. Jamain, J. Jankowski, A. Jayakumar, I. Joa, I. Jones, L. A. Jones, E. G. Jonsson, A. Julia, A. Jureus, A. K. Kahler, R. S. Kahn, L. Kalaydjieva, R. Kandaswamy, S. Karachanak-Yankova, J. Karjalainen, R. Karlsson, D. Kavanagh, M. C. Keller, B. J. Kelly, J. Kelsoe, J. L. Kennedy, A. Khrunin, Y. Kim, G. Kirov, S. Kittel-Schneider, J. Klovins, J. Knight, S. V. Knott, J. A. Knowles, M. Kogevinas, B. Konte, E. Kravariti, V. Kucinskas, Z. A. Kucinskiene, R. Kupka, H. Kuzelova-Ptackova, M. Landen, C. Langford, C. Laurent, J. Lawrence, S. Lawrie, W. B. Lawson, M. Leber, M. Leboyer, P. H. Lee, J. L. C. Keong, S. E. Legge, T. Lencz, B. Lerer, D. F. Levinson, S. E. Levy, C. M. Lewis, J. Z. Li, M. Li, Q. S. Li, T. Li, K.-Y. Liang, J. Liddle, J. Lieberman, S. Limborska, K. Lin, D. H. Linszen, J. Lissowska, C. Liu, J. Liu, J. Lonnqvist, C. M. Loughland, J. Lubinski, S. Lucae, M. Macek Jr., D. J. MacIntyre, P. K. E. Magnusson, B. S. Maher, P. B. Mahon, W. Maier, A. K. Malhotra, J. Mallet, U. F. Malt, H. S. Markus, S. Marsal, N. G. Martin, I. Mata, C. G. Mathew, M. Mattheisen, M. Mattingsdal, F. Mayoral, O. T. McCann, R. W. McCarley, S. A. McCarroll, M. I. McCarthy, C. McDonald, S. L. McElroy, P. McGuffin, M. G. McInnis, A. M. McIntosh, J. D. McKay, F. J. McMahon, H. Medeiros, S. E. Medland, S. Meier, C. J. Meijer, B. Melegh, I. Melle, F. Meng, R. I. Mesholam-Gately, A. Metspalu, P. T. Michie, L. Milani, V. Milanova, P. B. Mitchell, Y. Mokrab, G. W. Montgomery, J. L. Moran, G. Morken, D. W. Morris, O. Mors, P. B. Mortensen, B. J. Mowry, T. W. Mühliesen, B. Müller-Myhsok, K. C. Murphy, R. M. Murray, R. M. Myers, I. Myint-Germeys, B. M. Neale, M. Nelis, I. Nenadic, D. A. Nertney, G. Nestadt, K. K. Nicodemus, C. M. Nievergelt, L. Nikitina-Zake, V. Nimgaonkar, L. Nisenbaum, M. Nordentoft, A. Nordin, M. M. Nöthen, E. A. Nwulia, E. O'Callaghan, C. O'Donovan, C. O'Dushlaine, F. A. O'Neill, K. J. Oedegaard, S.-Y. Oh, A. Olincy, L. Olsen, L. Oruc, J. Van Os, M. J. Owen, S. A. Paciga, C. N. A. Palmer, A. Palotie, C. Pantelis, G. N. Papadimitriou, E. Parkhomenko, C. Pato, M. T. Pato, T. Paunio, R. Pearson, D. O. Perkins, R. H. Perlis, A. Perry, T. H. Pers, T. L. Petryshen, A. Pfennig, M. Picchioni, O. Pietilainen, J. Pimm, M. Pirinen, R. Plomin, A. J. Pocklington, D. Posthuma, J. B. Potash,

S. C. Potter, J. Powell, A. Price, A. E. Pulver, S. M. Purcell, D. Quested, J. A. Ramos-Quiroga, H. B. Rasmussen, A. Rautanen, R. Ravindrarajah, E. J. Regeer, A. Reichenberg, A. Reif, M. A. Reimers, M. Ribases, J. P. Rice, A. L. Richards, M. Ricketts, B. P. Riley, F. Rivas, M. Rivera, J. L. Roffman, G. A. Rouleau, P. Roussos, D. Rujescu, V. Salomaa, C. Sanchez-Mora, A. R. Sanders, S. J. Sawcer, U. Schall, A. F. Schatzberg, W. A. Scheftner, P. R. Schofield, N. J. Schork, S. G. Schwab, E. M. Scolnick, L. J. Scott, R. J. Scott, L. J. Seidman, A. Serretti, P. C. Sham, C. S. Weickert, T. Shekhtman, J. Shi, P. D. Shilling, E. Sigurdsson, J. M. Silverman, K. Sim, C. Slaney, P. Slominsky, O. B. Smeland, J. W. Smoller, H.-C. So, J. L. Sobell, E. Soderman, C. S. Hansen, C. C. A. Spencer, A. T. Spijker, D. St Clair, H. Stefansson, K. Stefansson, S. Steinberg, E. Stogmann, E. Stordal, A. Strange, R. E. Straub, J. S. Strauss, F. Streit, E. Strengman, J. Strohmaier, T. S. Stroup, Z. Su, M. Subramaniam, J. Suvisaari, D. M. Svarkic, J. P. Szatkiewicz, S. Szelinger, A. Tashakkori-Ghanbaria, S. Thirumalai, R. C. Thompson, T. E. Thorgeirsson, D. Toncheva, P. A. Tooney, S. Tosato, T. Toulopoulou, R. C. Trembath, J. Treutlein, V. Trubetskoy, G. Turecki, A. E. Vaaler, H. Vedder, E. Vieta, J. Vincent, P. M. Visscher, A. C. Viswanathan, D. Vukcevic, J. Waddington, M. Waller, D. Walsh, M. Walshe, J. T. R. Walters, D. Wang, Q. Wang, W. Wang, Y. Wang, S. J. Watson, B. T. Webb, T. W. Weickert, D. R. Weinberger, M. Weisbrod, M. Weiser, T. Werge, P. Weston, P. Whittaker, S. Widaa, D. Wiersma, D. B. Wildenauer, N. M. Williams, S. Williams, S. H. Witt, A. R. Wolen, E. H. M. Wong, N. W. Wood, B. K. Wormley, J. Q. Wu, S. Xi, W. Xu, A. H. Young, C. C. Zai, P. Zandi, P. Zhang, X. Zheng, F. Zimprich, S. Zollner, A. Corvin, A. H. Fanous, S. Cichon, M. Rietschel, E. S. Gershon, T. G. Schulze, A. B. Cuellar-Barboza, A. J. Forstner, P. A. Holmans, J. I. Nurnberger, O. A. Andreassen, S. H. Lee, M. C. O'Donovan, P. F. Sullivan, R. A. Ophoff, N. R. Wray, P. Sklar, K. S. Kendler; Bipolar Disorder and Schizophrenia Working Group of the Psychiatric Genomics Consortium. Electronic address: douglas.ruderfer@vanderbilt.edu; Bipolar Disorder and Schizophrenia Working Group of the Psychiatric Genomics Consortium, Genomic Dissection of Bipolar Disorder and Schizophrenia, Including 28 Subphenotypes. *Cell* **173**, 1705–1715.e16 (2018). [doi:10.1016/j.cell.2018.05.046](https://doi.org/10.1016/j.cell.2018.05.046) [Medline](#)

98. B. B. Lake, S. Chen, B. C. Sos, J. Fan, G. E. Kaeser, Y. C. Yung, T. E. Duong, D. Gao, J. Chun, P. V. Kharchenko, K. Zhang, Integrative single-cell analysis of transcriptional and epigenetic states in the human adult brain. *Nat. Biotechnol.* **36**, 70–80 (2018). [doi:10.1038/nbt.4038](https://doi.org/10.1038/nbt.4038) [Medline](#)
99. T. Goldmann, P. Wieghofer, M. J. C. Jordão, F. Prutek, N. Hagemeyer, K. Frenzel, L. Amann, O. Staszewski, K. Kierdorf, M. Krueger, G. Locatelli, H. Hochgerner, R. Zeiser, S. Epelman, F. Geissmann, J. Priller, F. M. V. Rossi, I. Bechmann, M. Kerschensteiner, S. Linnarsson, S. Jung, M. Prinz, Origin, fate and dynamics of macrophages at central nervous system interfaces. *Nat. Immunol.* **17**, 797–805 (2016). [doi:10.1038/ni.3423](https://doi.org/10.1038/ni.3423) [Medline](#)
100. H. Keren-Shaul, A. Spinrad, A. Weiner, O. Matcovitch-Natan, R. Dvir-Szternfeld, T. K. Ulland, E. David, K. Baruch, D. Lara-Astaiso, B. Toth, S. Itzkovitz, M. Colonna, M. Schwartz, I. Amit, A Unique Microglia Type Associated with Restricting Development of Alzheimer's Disease. *Cell* **169**, 1276–1290.e17 (2017). [doi:10.1016/j.cell.2017.05.018](https://doi.org/10.1016/j.cell.2017.05.018) [Medline](#)

101. A. Zeisel, A. B. Muñoz-Manchado, S. Codeluppi, P. Lönnerberg, G. La Manno, A. Juréus, S. Marques, H. Munguba, L. He, C. Betsholtz, C. Rolny, G. Castelo-Branco, J. Hjerling-Leffler, S. Linnarsson, Brain structure. Cell types in the mouse cortex and hippocampus revealed by single-cell RNA-seq. *Science* **347**, 1138–1142 (2015).  
[doi:10.1126/science.aaa1934](https://doi.org/10.1126/science.aaa1934) [Medline](#)
102. Y. Zhang, S. A. Sloan, L. E. Clarke, C. Caneda, C. A. Plaza, P. D. Blumenthal, H. Vogel, G. K. Steinberg, M. S. B. Edwards, G. Li, J. A. Duncan 3rd, S. H. Cheshier, L. M. Shuer, E. F. Chang, G. A. Grant, M. G. H. Gephart, B. A. Barres, Purification and Characterization of Progenitor and Mature Human Astrocytes Reveals Transcriptional and Functional Differences with Mouse. *Neuron* **89**, 37–53 (2016).  
[doi:10.1016/j.neuron.2015.11.013](https://doi.org/10.1016/j.neuron.2015.11.013) [Medline](#)
103. B. Wilkinson, N. Grepo, B. L. Thompson, J. Kim, K. Wang, O. V. Evgrafov, W. Lu, J. A. Knowles, D. B. Campbell, The autism-associated gene chromodomain helicase DNA-binding protein 8 (CHD8) regulates noncoding RNAs and autism-related genes. *Transl. Psychiatry* **5**, e568 (2015). [doi:10.1038/tp.2015.62](https://doi.org/10.1038/tp.2015.62) [Medline](#)
104. K. E. Samocha, E. B. Robinson, S. J. Sanders, C. Stevens, A. Sabo, L. M. McGrath, J. A. Kosmicki, K. Rehnström, S. Mallick, A. Kirby, D. P. Wall, D. G. MacArthur, S. B. Gabriel, M. DePristo, S. M. Purcell, A. Palotie, E. Boerwinkle, J. D. Buxbaum, E. H. Cook Jr., R. A. Gibbs, G. D. Schellenberg, J. S. Sutcliffe, B. Devlin, K. Roeder, B. M. Neale, M. J. Daly, A framework for the interpretation of de novo mutation in human disease. *Nat. Genet.* **46**, 944–950 (2014). [doi:10.1038/ng.3050](https://doi.org/10.1038/ng.3050) [Medline](#)
105. I. Iossifov, D. Levy, J. Allen, K. Ye, M. Ronemus, Y. H. Lee, B. Yamrom, M. Wigler, Low load for disruptive mutations in autism genes and their biased transmission. *Proc. Natl. Acad. Sci. U.S.A.* **112**, E5600–E5607 (2015). [doi:10.1073/pnas.1516376112](https://doi.org/10.1073/pnas.1516376112) [Medline](#)
106. K. J. Karczewski, B. Weisburd, B. Thomas, M. Solomonson, D. M. Ruderfer, D. Kavanagh, T. Hamamsy, M. Lek, K. E. Samocha, B. B. Cummings, D. Birnbaum, M. J. Daly, D. G. MacArthur; The Exome Aggregation Consortium, The ExAC browser: Displaying reference data information from over 60 000 exomes. *Nucleic Acids Res.* **45** (D1), D840–D845 (2017). [doi:10.1093/nar/gkw971](https://doi.org/10.1093/nar/gkw971) [Medline](#)
107. D. Zhang, L. Cheng, J. A. Badner, C. Chen, Q. Chen, W. Luo, D. W. Craig, M. Redman, E. S. Gershon, C. Liu, Genetic control of individual differences in gene-specific methylation in human brain. *Am. J. Hum. Genet.* **86**, 411–419 (2010). [doi:10.1016/j.ajhg.2010.02.005](https://doi.org/10.1016/j.ajhg.2010.02.005) [Medline](#)
108. A. E. Jaffe *et al.*, Developmental And Genetic Regulation Of The Human Cortex Transcriptome In Schizophrenia. bioRxiv 124321 (2017).
109. PEC\_DAC\_RNAseq.py, doi:[10.7303/syn12026837.1](https://doi.org/10.7303/syn12026837.1).
110. J. Reimand, T. Arak, J. Vilo, g:Profiler—A web server for functional interpretation of gene lists (2011 update). *Nucleic Acids Res.* **39** (suppl\_2), W307–W315 (2011).  
[doi:10.1093/nar/gkr378](https://doi.org/10.1093/nar/gkr378) [Medline](#)
111. M. Lek, K. J. Karczewski, E. V. Minikel, K. E. Samocha, E. Banks, T. Fennell, A. H. O'Donnell-Luria, J. S. Ware, A. J. Hill, B. B. Cummings, T. Tukiainen, D. P. Birnbaum, J. A. Kosmicki, L. E. Duncan, K. Estrada, F. Zhao, J. Zou, E. Pierce-Hoffman, J.

Berghout, D. N. Cooper, N. Deflaux, M. DePristo, R. Do, J. Flannick, M. Fromer, L. Gauthier, J. Goldstein, N. Gupta, D. Howrigan, A. Kiezun, M. I. Kurki, A. L. Moonshine, P. Natarajan, L. Orozco, G. M. Peloso, R. Poplin, M. A. Rivas, V. Ruano-Rubio, S. A. Rose, D. M. Ruderfer, K. Shakir, P. D. Stenson, C. Stevens, B. P. Thomas, G. Tiao, M. T. Tusie-Luna, B. Weisburd, H.-H. Won, D. Yu, D. M. Altshuler, D. Ardiissino, M. Boehnke, J. Danesh, S. Donnelly, R. Elosua, J. C. Florez, S. B. Gabriel, G. Getz, S. J. Glatt, C. M. Hultman, S. Kathiresan, M. Laakso, S. McCarroll, M. I. McCarthy, D. McGovern, R. McPherson, B. M. Neale, A. Palotie, S. M. Purcell, D. Saleheen, J. M. Scharf, P. Sklar, P. F. Sullivan, J. Tuomilehto, M. T. Tsuang, H. C. Watkins, J. G. Wilson, M. J. Daly, D. G. MacArthur; Exome Aggregation Consortium, Analysis of protein-coding genetic variation in 60,706 humans. *Nature* **536**, 285–291 (2016).  
[doi:10.1038/nature19057](https://doi.org/10.1038/nature19057) [Medline](#)

112. B. B. Lake, R. Ai, G. E. Kaeser, N. S. Salathia, Y. C. Yung, R. Liu, A. Wildberg, D. Gao, H.-L. Fung, S. Chen, R. Vijayaraghavan, J. Wong, A. Chen, X. Sheng, F. Kaper, R. Shen, M. Ronaghi, J.-B. Fan, W. Wang, J. Chun, K. Zhang, Neuronal subtypes and diversity revealed by single-nucleus RNA sequencing of the human brain. *Science* **352**, 1586–1590 (2016). [doi:10.1126/science.aaf1204](https://doi.org/10.1126/science.aaf1204) [Medline](#)
113. S. Darmanis, S. A. Sloan, Y. Zhang, M. Enge, C. Caneda, L. M. Shuer, M. G. Hayden Gephart, B. A. Barres, S. R. Quake, A survey of human brain transcriptome diversity at the single cell level. *Proc. Natl. Acad. Sci. U.S.A.* **112**, 7285–7290 (2015).  
[doi:10.1073/pnas.1507125112](https://doi.org/10.1073/pnas.1507125112) [Medline](#)
114. J. P. Doyle, J. D. Dougherty, M. Heiman, E. F. Schmidt, T. R. Stevens, G. Ma, S. Bupp, P. Shrestha, R. D. Shah, M. L. Doughty, S. Gong, P. Greengard, N. Heintz, Application of a translational profiling approach for the comparative analysis of CNS cell types. *Cell* **135**, 749–762 (2008). [doi:10.1016/j.cell.2008.10.029](https://doi.org/10.1016/j.cell.2008.10.029) [Medline](#)
115. A. Dobin, C. A. Davis, F. Schlesinger, J. Drenkow, C. Zaleski, S. Jha, P. Batut, M. Chaisson, T. R. Gingeras, STAR: Ultrafast universal RNA-seq aligner. *Bioinformatics* **29**, 15–21 (2013). [doi:10.1093/bioinformatics/bts635](https://doi.org/10.1093/bioinformatics/bts635) [Medline](#)
116. F. Hahne, R. Ivanek, Visualizing Genomic Data Using Gviz and Bioconductor. *Methods Mol. Biol.* **1418**, 335–351 (2016). [doi:10.1007/978-1-4939-3578-9\\_16](https://doi.org/10.1007/978-1-4939-3578-9_16) [Medline](#)
117. I. Letunic, P. Bork, 20 years of the SMART protein domain annotation resource. *Nucleic Acids Res.* **46** (D1), D493–D496 (2018). [doi:10.1093/nar/gkx922](https://doi.org/10.1093/nar/gkx922) [Medline](#)
118. R. D. Finn, P. Coggill, R. Y. Eberhardt, S. R. Eddy, J. Mistry, A. L. Mitchell, S. C. Potter, M. Punta, M. Qureshi, A. Sangrador-Vegas, G. A. Salazar, J. Tate, A. Bateman, The Pfam protein families database: Towards a more sustainable future. *Nucleic Acids Res.* **44** (D1), D279–D285 (2016). [doi:10.1093/nar/gkv1344](https://doi.org/10.1093/nar/gkv1344) [Medline](#)
119. A. G. Baltz, M. Munschauer, B. Schwahnhäusser, A. Vasile, Y. Murakawa, M. Schueler, N. Youngs, D. Penfold-Brown, K. Drew, M. Milek, E. Wyler, R. Bonneau, M. Selbach, C. Dieterich, M. Landthaler, The mRNA-bound proteome and its global occupancy profile on protein-coding transcripts. *Mol. Cell* **46**, 674–690 (2012).  
[doi:10.1016/j.molcel.2012.05.021](https://doi.org/10.1016/j.molcel.2012.05.021) [Medline](#)
120. A. Castello, B. Fischer, K. Eichelbaum, R. Horos, B. M. Beckmann, C. Strein, N. E. Davey, D. T. Humphreys, T. Preiss, L. M. Steinmetz, J. Krijgsveld, M. W. Hentze, Insights into

RNA biology from an atlas of mammalian mRNA-binding proteins. *Cell* **149**, 1393–1406 (2012). [doi:10.1016/j.cell.2012.04.031](https://doi.org/10.1016/j.cell.2012.04.031) [Medline](#)

121. S. C. Kwon, H. Yi, K. Eichelbaum, S. Föhr, B. Fischer, K. T. You, A. Castello, J. Krijgsveld, M. W. Hentze, V. N. Kim, The RNA-binding protein repertoire of embryonic stem cells. *Nat. Struct. Mol. Biol.* **20**, 1122–1130 (2013). [doi:10.1038/nsmb.2638](https://doi.org/10.1038/nsmb.2638) [Medline](#)
122. E. L. Huttlin, L. Ting, R. J. Bruckner, F. Gebreab, M. P. Gygi, J. Szpyt, S. Tam, G. Zarraga, G. Colby, K. Baltier, R. Dong, V. Guarani, L. P. Vaites, A. Ordureau, R. Rad, B. K. Erickson, M. Wühr, J. Chick, B. Zhai, D. Kolippakkam, J. Mintseris, R. A. Obar, T. Harris, S. Artavanis-Tsakonas, M. E. Sowa, P. De Camilli, J. A. Paulo, J. W. Harper, S. P. Gygi, The BioPlex Network: A Systematic Exploration of the Human Interactome. *Cell* **162**, 425–440 (2015). [doi:10.1016/j.cell.2015.06.043](https://doi.org/10.1016/j.cell.2015.06.043) [Medline](#)
123. T. S. Keshava Prasad, R. Goel, K. Kandasamy, S. Keerthikumar, S. Kumar, S. Mathivanan, D. Telikicherla, R. Raju, B. Shafreen, A. Venugopal, L. Balakrishnan, A. Marimuthu, S. Banerjee, D. S. Somanathan, A. Sebastian, S. Rani, S. Ray, C. J. Harrys Kishore, S. Kanth, M. Ahmed, M. K. Kashyap, R. Mohmood, Y. L. Ramachandra, V. Krishna, B. A. Rahiman, S. Mohan, P. Ranganathan, S. Ramabadran, R. Chaerkady, A. Pandey, Human Protein Reference Database—2009 update. *Nucleic Acids Res.* **37** (Database), D767–D772 (2009). [doi:10.1093/nar/gkn892](https://doi.org/10.1093/nar/gkn892) [Medline](#)
124. K. Lage, E. O. Karlberg, Z. M. Størling, P. Í. Ólason, A. G. Pedersen, O. Rigina, A. M. Hinsby, Z. Tümer, F. Pociot, N. Tommerup, Y. Moreau, S. Brunak, A human phenome-interactome network of protein complexes implicated in genetic disorders. *Nat. Biotechnol.* **25**, 309–316 (2007). [doi:10.1038/nbt1295](https://doi.org/10.1038/nbt1295) [Medline](#)
125. J. Das, H. Yu, HINT: High-quality protein interactomes and their applications in understanding human disease. *BMC Syst. Biol.* **6**, 92 (2012). [doi:10.1186/1752-0509-6-92](https://doi.org/10.1186/1752-0509-6-92) [Medline](#)
126. A. Chatr-aryamontri, R. Oughtred, L. Boucher, J. Rust, C. Chang, N. K. Kolas, L. O'Donnell, S. Oster, C. Theesfeld, A. Sellam, C. Stark, B.-J. Breitkreutz, K. Dolinski, M. Tyers, The BioGRID interaction database: 2017 update. *Nucleic Acids Res.* **45** (D1), D369–D379 (2017). [doi:10.1093/nar/gkw1102](https://doi.org/10.1093/nar/gkw1102) [Medline](#)
127. K. Zuberi, M. Franz, H. Rodriguez, J. Montojo, C. T. Lopes, G. D. Bader, Q. Morris, GeneMANIA prediction server 2013 update. *Nucleic Acids Res.* **41**, W115–W122 (2013). [doi:10.1093/nar/gkt533](https://doi.org/10.1093/nar/gkt533) [Medline](#)
128. D. Szklarczyk, J. H. Morris, H. Cook, M. Kuhn, S. Wyder, M. Simonovic, A. Santos, N. T. Doncheva, A. Roth, P. Bork, L. J. Jensen, C. von Mering, The STRING database in 2017: Quality-controlled protein-protein association networks, made broadly accessible. *Nucleic Acids Res.* **45**, D362–D368 (2017). [doi:10.1093/nar/gkw937](https://doi.org/10.1093/nar/gkw937) [Medline](#)
129. A. Ruepp, B. Waegele, M. Lechner, B. Brauner, I. Dunger-Kaltenbach, G. Fobo, G. Frishman, C. Montrone, H.-W. Mewes, CORUM: The comprehensive resource of mammalian protein complexes—2009. *Nucleic Acids Res.* **38** (suppl\_1), D497–D501 (2010). [doi:10.1093/nar/gkp914](https://doi.org/10.1093/nar/gkp914) [Medline](#)

130. A. R. Quinlan, I. M. Hall, BEDTools: A flexible suite of utilities for comparing genomic features. *Bioinformatics* **26**, 841–842 (2010). [doi:10.1093/bioinformatics/btq033](https://doi.org/10.1093/bioinformatics/btq033) [Medline](#)
131. M. J. Mason, G. Fan, K. Plath, Q. Zhou, S. Horvath, Signed weighted gene co-expression network analysis of transcriptional regulation in murine embryonic stem cells. *BMC Genomics* **10**, 327 (2009). [doi:10.1186/1471-2164-10-327](https://doi.org/10.1186/1471-2164-10-327) [Medline](#)
132. C. S. Benton, B. H. Miller, S. Skwerer, O. Suzuki, L. E. Schultz, M. D. Cameron, J. S. Marron, M. T. Pletcher, T. Wiltshire, Evaluating genetic markers and neurobiochemical analytes for fluoxetine response using a panel of mouse inbred strains. *Psychopharmacology (Berl.)* **221**, 297–315 (2012). [doi:10.1007/s00213-011-2574-z](https://doi.org/10.1007/s00213-011-2574-z) [Medline](#)
133. N. R. Wray, S. Ripke, M. Mattheisen, M. Trzaskowski, E. M. Byrne, A. Abdellaoui, M. J. Adams, E. Agerbo, T. M. Air, T. M. F. Andlauer, S.-A. Bacanu, M. Bækvad-Hansen, A. F. T. Beekman, T. B. Bigdeli, E. B. Binder, D. R. H. Blackwood, J. Bryois, H. N. Buttenschøn, J. Bybjerg-Grauholt, N. Cai, E. Castelao, J. H. Christensen, T.-K. Clarke, J. I. R. Coleman, L. Colodro-Conde, B. Couvy-Duchesne, N. Craddock, G. E. Crawford, C. A. Crowley, H. S. Dashti, G. Davies, I. J. Deary, F. Degenhardt, E. M. Derkx, N. Direk, C. V. Dolan, E. C. Dunn, T. C. Eley, N. Eriksson, V. Escott-Price, F. H. F. Kiadeh, H. K. Finucane, A. J. Forstner, J. Frank, H. A. Gaspar, M. Gill, P. Giusti-Rodríguez, F. S. Goes, S. D. Gordon, J. Grove, L. S. Hall, E. Hannon, C. S. Hansen, T. F. Hansen, S. Herms, I. B. Hickie, P. Hoffmann, G. Homuth, C. Horn, J.-J. Hottenga, D. M. Hougaard, M. Hu, C. L. Hyde, M. Ising, R. Jansen, F. Jin, E. Jorgenson, J. A. Knowles, I. S. Kohane, J. Kraft, W. W. Kretzschmar, J. Krogh, Z. Kutalik, J. M. Lane, Y. Li, Y. Li, P. A. Lind, X. Liu, L. Lu, D. J. MacIntyre, D. F. MacKinnon, R. M. Maier, W. Maier, J. Marchini, H. Mbarek, P. McGrath, P. McGuffin, S. E. Medland, D. Mehta, C. M. Middeldorp, E. Mihailov, Y. Milaneschi, L. Milani, J. Mill, F. M. Mondimore, G. W. Montgomery, S. Mostafavi, N. Mullins, M. Nauck, B. Ng, M. G. Nivard, D. R. Nyholt, P. F. O'Reilly, H. Oskarsson, M. J. Owen, J. N. Painter, C. B. Pedersen, M. G. Pedersen, R. E. Peterson, E. Pettersson, W. J. Peyrot, G. Pistis, D. Posthuma, S. M. Purcell, J. A. Quiroz, P. Qvist, J. P. Rice, B. P. Riley, M. Rivera, S. Saeed Mirza, R. Saxena, R. Schoevers, E. C. Schulte, L. Shen, J. Shi, S. I. Shyn, E. Sigurdsson, G. B. C. Sinnamon, J. H. Smit, D. J. Smith, H. Stefansson, S. Steinberg, C. A. Stockmeier, F. Streit, J. Strohmaier, K. E. Tansey, H. Teismann, A. Teumer, W. Thompson, P. A. Thomson, T. E. Thorgeirsson, C. Tian, M. Traylor, J. Treutlein, V. Trubetskoy, A. G. Uitterlinden, D. Umbricht, S. Van der Auwera, A. M. van Hemert, A. Viktorin, P. M. Visscher, Y. Wang, B. T. Webb, S. M. Weinsheimer, J. Wellmann, G. Willemse, S. H. Witt, Y. Wu, H. S. Xi, J. Yang, F. Zhang, V. Arolt, B. T. Baune, K. Berger, D. I. Boomsma, S. Cichon, U. Dannowski, E. C. J. de Geus, J. R. DePaulo, E. Domenici, K. Domschke, T. Esko, H. J. Grabe, S. P. Hamilton, C. Hayward, A. C. Heath, D. A. Hinds, K. S. Kendler, S. Kloiber, G. Lewis, Q. S. Li, S. Lucae, P. F. A. Madden, P. K. Magnusson, N. G. Martin, A. M. McIntosh, A. Metspalu, O. Mors, P. B. Mortensen, B. Müller-Myhsok, M. Nordentoft, M. M. Nöthen, M. C. O'Donovan, S. A. Paciga, N. L. Pedersen, B. W. J. H. Penninx, R. H. Perlis, D. J. Porteous, J. B. Potash, M. Preisig, M. Rietschel, C. Schaefer, T. G. Schulze, J. W. Smoller, K. Stefansson, H. Tiemeier, R. Uher, H. Völzke, M. M. Weissman, T. Werge, A. R. Winslow, C. M. Lewis, D. F. Levinson, G. Breen, A. D. Børglum, P. F. Sullivan; eQTLGen; 23andMe; Major Depressive Disorder Working

Group of the Psychiatric Genomics Consortium, Genome-wide association analyses identify 44 risk variants and refine the genetic architecture of major depression. *Nat. Genet.* **50**, 668–681 (2018). [doi:10.1038/s41588-018-0090-3](https://doi.org/10.1038/s41588-018-0090-3) [Medline](#)

134. A. Okbay, B. M. L. Baselmans, J.-E. De Neve, P. Turley, M. G. Nivard, M. A. Fontana, S. F. W. Meddents, R. K. Linnér, C. A. Rietveld, J. Derringer, J. Gratten, J. J. Lee, J. Z. Liu, R. de Vlaming, T. S. Ahluwalia, J. Buchwald, A. Cavadino, A. C. Frazier-Wood, N. A. Furlotte, V. Garfield, M. H. Geisel, J. R. Gonzalez, S. Haitjema, R. Karlsson, S. W. van der Laan, K.-H. Ladwig, J. Lahti, S. J. van der Lee, P. A. Lind, T. Liu, L. Matteson, E. Mihailov, M. B. Miller, C. C. Minica, I. M. Nolte, D. Mook-Kanamori, P. J. van der Most, C. Oldmeadow, Y. Qian, O. Raitakari, R. Rawal, A. Realo, R. Rueedi, B. Schmidt, A. V. Smith, E. Stergiakouli, T. Tanaka, K. Taylor, G. Thorleifsson, J. Wedenoja, J. Wellmann, H.-J. Westra, S. M. Willems, W. Zhao, N. Amin, A. Bakshi, S. Bergmann, G. Bjornsdottir, P. A. Boyle, S. Cherney, S. R. Cox, G. Davies, O. S. P. Davis, J. Ding, N. Direk, P. Eibich, R. T. Emeny, G. Fatemifar, J. D. Faul, L. Ferrucci, A. J. Forstner, C. Gieger, R. Gupta, T. B. Harris, J. M. Harris, E. G. Holliday, J.-J. Hottenga, P. L. De Jager, M. A. Kaakinen, E. Kajantie, V. Karhunen, I. Kolcic, M. Kumari, L. J. Launer, L. Franke, R. Li-Gao, D. C. Liewald, M. Koini, A. Loukola, P. Marques-Vidal, G. W. Montgomery, M. A. Mosing, L. Paternoster, A. Pattie, K. E. Petrovic, L. Pulkki-Råback, L. Quaye, K. Räikkönen, I. Rudan, R. J. Scott, J. A. Smith, A. R. Sutin, M. Trzaskowski, A. E. Vinkhuyzen, L. Yu, D. Zabaneh, J. R. Attia, D. A. Bennett, K. Berger, L. Bertram, D. I. Boomsma, H. Snieder, S.-C. Chang, F. Cucca, I. J. Deary, C. M. van Duijn, J. G. Eriksson, U. Bültmann, E. J. C. de Geus, P. J. F. Groenen, V. Gudnason, T. Hansen, C. A. Hartman, C. M. A. Haworth, C. Hayward, A. C. Heath, D. A. Hinds, E. Hyppönen, W. G. Iacono, M.-R. Järvelin, K.-H. Jöckel, J. Kaprio, S. L. R. Kardia, L. Keltikangas-Järvinen, P. Kraft, L. D. Kubzansky, T. Lehtimäki, P. K. E. Magnusson, N. G. Martin, M. McGue, A. Metspalu, M. Mills, R. de Mutsert, A. J. Oldehinkel, G. Pasterkamp, N. L. Pedersen, R. Plomin, O. Polasek, C. Power, S. S. Rich, F. R. Rosendaal, H. M. den Ruijter, D. Schlessinger, H. Schmidt, R. Svento, R. Schmidt, B. Z. Alizadeh, T. I. A. Sørensen, T. D. Spector, J. M. Starr, K. Stefansson, A. Steptoe, A. Terracciano, U. Thorsteinsdottir, A. R. Thurik, N. J. Timpson, H. Tiemeier, A. G. Uitterlinden, P. Vollenweider, G. G. Wagner, D. R. Weir, J. Yang, D. C. Conley, G. D. Smith, A. Hofman, M. Johannesson, D. I. Laibson, S. E. Medland, M. N. Meyer, J. K. Pickrell, T. Esko, R. F. Krueger, J. P. Beauchamp, P. D. Koellinger, D. J. Benjamin, M. Bartels, D. Cesarini; LifeLines Cohort Study, Genetic variants associated with subjective well-being, depressive symptoms, and neuroticism identified through genome-wide analyses. *Nat. Genet.* **48**, 624–633 (2016). [doi:10.1038/ng.3552](https://doi.org/10.1038/ng.3552) [Medline](#)
135. A. Okbay, J. P. Beauchamp, M. A. Fontana, J. J. Lee, T. H. Pers, C. A. Rietveld, P. Turley, G.-B. Chen, V. Emilsson, S. F. W. Meddents, S. Oskarsson, J. K. Pickrell, K. Thom, P. Timshel, R. de Vlaming, A. Abdellaoui, T. S. Ahluwalia, J. Bacelis, C. Baumbach, G. Bjornsdottir, J. H. Brandsma, M. Pina Concas, J. Derringer, N. A. Furlotte, T. E. Galesloot, G. Girotto, R. Gupta, L. M. Hall, S. E. Harris, E. Hofer, M. Horikoshi, J. E. Huffman, K. Kaasik, I. P. Kalafati, R. Karlsson, A. Kong, J. Lahti, S. J. van der Lee, C. deLeeuw, P. A. Lind, K.-O. Lindgren, T. Liu, M. Mangino, J. Marten, E. Mihailov, M. B. Miller, P. J. van der Most, C. Oldmeadow, A. Payton, N. Pervjakova, W. J. Peyrot, Y. Qian, O. Raitakari, R. Rueedi, E. Salvi, B. Schmidt, K. E. Schraut, J. Shi, A. V. Smith, R. A. Poot, B. St Pourcain, A. Teumer, G. Thorleifsson, N. Verweij, D. Vuckovic, J.

Wellmann, H.-J. Westra, J. Yang, W. Zhao, Z. Zhu, B. Z. Alizadeh, N. Amin, A. Bakshi, S. E. Baumeister, G. Biino, K. Bønnelykke, P. A. Boyle, H. Campbell, F. P. Cappuccio, G. Davies, J.-E. De Neve, P. Deloukas, I. Demuth, J. Ding, P. Eibich, L. Eisele, N. Eklund, D. M. Evans, J. D. Faul, M. F. Feitosa, A. J. Forstner, I. Gandin, B. Gunnarsson, B. V. Halldórsson, T. B. Harris, A. C. Heath, L. J. Hocking, E. G. Holliday, G. Homuth, M. A. Horan, J.-J. Hottenga, P. L. de Jager, P. K. Joshi, A. Jugessur, M. A. Kaakinen, M. Kähönen, S. Kanoni, L. Keltigangas-Järvinen, L. A. L. M. Kiemeney, I. Kolcic, S. Koskinen, A. T. Kraja, M. Kroh, Z. Kutalik, A. Latvala, L. J. Launer, M. P. Lebreton, D. F. Levinson, P. Lichtenstein, P. Lichtner, D. C. M. Liewald, A. Loukola, P. A. Madden, R. Mägi, T. Mäki-Opas, R. E. Marioni, P. Marques-Vidal, G. A. Meddens, G. McMahon, C. Meisinger, T. Meitinger, Y. Milaneschi, L. Milani, G. W. Montgomery, R. Myhre, C. P. Nelson, D. R. Nyholt, W. E. Ollier, A. Palotie, L. Paternoster, N. L. Pedersen, K. E. Petrovic, D. J. Porteous, K. Räikkönen, S. M. Ring, A. Robino, O. Rostapshova, I. Rudan, A. Rustichini, V. Salomaa, A. R. Sanders, A. P. Sarin, H. Schmidt, R. J. Scott, B. H. Smith, J. A. Smith, J. A. Staessen, E. Steinhagen-Thiessen, K. Strauch, A. Terracciano, M. D. Tobin, S. Ulivi, S. Vaccargiu, L. Quaye, F. J. van Rooij, C. Venturini, A. A. Vinkhuyzen, U. Völker, H. Völzke, J. M. Vonk, D. Vozzi, J. Waage, E. B. Ware, G. Willemse, J. R. Attia, D. A. Bennett, K. Berger, L. Bertram, H. Bisgaard, D. I. Boomsma, I. B. Borecki, U. Bültmann, C. F. Chabris, F. Cucca, D. Cusi, I. J. Deary, G. V. Dedoussis, C. M. van Duijn, J. G. Eriksson, B. Franke, L. Franke, P. Gasparini, P. V. Gejman, C. Gieger, H. J. Grabe, J. Gratten, P. J. Groenen, V. Gudnason, P. van der Harst, C. Hayward, D. A. Hinds, W. Hoffmann, E. Hyppönen, W. G. Iacono, B. Jacobsson, M. R. Järvelin, K. H. Jöckel, J. Kaprio, S. L. Kardia, T. Lehtimäki, S. F. Lehrer, P. K. Magnusson, N. G. Martin, M. McGue, A. Metspalu, N. Pendleton, B. W. Penninx, M. Perola, N. Pirastu, M. Pirastu, O. Polasek, D. Posthuma, C. Power, M. A. Province, N. J. Samani, D. Schlessinger, R. Schmidt, T. I. Sørensen, T. D. Spector, K. Stefansson, U. Thorsteinsdóttir, A. R. Thurik, N. J. Timpson, H. Tiemeier, J. Y. Tung, A. G. Uitterlinden, V. Vitart, P. Vollenweider, D. R. Weir, J. F. Wilson, A. F. Wright, D. C. Conley, R. F. Krueger, G. Davey Smith, A. Hofman, D. I. Laibson, S. E. Medland, M. N. Meyer, J. Yang, M. Johannesson, P. M. Visscher, T. Esko, P. D. Koellinger, D. Cesarini, D. J. Benjamin, D. J. Benjamin; LifeLines Cohort Study, Genome-wide association study identifies 74 loci associated with educational attainment. *Nature* **533**, 539–542 (2016).  
[doi:10.1038/nature17671](https://doi.org/10.1038/nature17671) [Medline](#)

136. A. P. Morris, B. F. Voight, T. M. Teslovich, T. Ferreira, A. V. Segrè, V. Steinthorsdóttir, R. J. Strawbridge, H. Khan, H. Grallert, A. Mahajan, I. Prokopenko, H. M. Kang, C. Dina, T. Esko, R. M. Fraser, S. Kanoni, A. Kumar, V. Lagou, C. Langenberg, J. Luan, C. M. Lindgren, M. Müller-Nurasyid, S. Pechlivanis, N. W. Rayner, L. J. Scott, S. Wiltshire, L. Yengo, L. Kinnunen, E. J. Rossin, S. Raychaudhuri, A. D. Johnson, A. S. Dimas, R. J. Loos, S. Vedantam, H. Chen, J. C. Florez, C. Fox, C. T. Liu, D. Rybin, D. J. Couper, W. H. Kao, M. Li, M. C. Cornelis, P. Kraft, Q. Sun, R. M. van Dam, H. M. Stringham, P. S. Chines, K. Fischer, P. Fontanillas, O. L. Holmen, S. E. Hunt, A. U. Jackson, A. Kong, R. Lawrence, J. Meyer, J. R. Perry, C. G. Platou, S. Potter, E. Rehnberg, N. Robertson, S. Sivapalaratnam, A. Stančáková, K. Stirrups, G. Thorleifsson, E. Tikkanen, A. R. Wood, P. Almgren, M. Atalay, R. Benediktsson, L. L. Bonnycastle, N. Burtt, J. Carey, G. Charpentier, A. T. Crenshaw, A. S. Doney, M. Dorkhan, S. Edkins, V. Emilsson, E. Eury, T. Forsen, K. Gertow, B. Gigante, G. B. Grant, C. J. Groves, C. Guiducci, C. Herder, A.

B. Hreidarsson, J. Hui, A. James, A. Jonsson, W. Rathmann, N. Klopp, J. Kravic, K. Krjutškov, C. Langford, K. Leander, E. Lindholm, S. Lobbens, S. Männistö, G. Mirza, T. W. Mühlleisen, B. Musk, M. Parkin, L. Rallidis, J. Saramies, B. Sennblad, S. Shah, G. Sigurðsson, A. Silveira, G. Steinbach, B. Thorand, J. Trakalo, F. Veglia, R. Wennauer, W. Winckler, D. Zabaneh, H. Campbell, C. van Duijn, A. G. Uitterlinden, A. Hofman, E. Sijbrands, G. R. Abecasis, K. R. Owen, E. Zeggini, M. D. Trip, N. G. Forouhi, A. C. Syvänen, J. G. Eriksson, L. Peltonen, M. M. Nöthen, B. Balkau, C. N. Palmer, V. Lyssenko, T. Tuomi, B. Isomaa, D. J. Hunter, L. Qi, A. R. Shuldiner, M. Roden, I. Barroso, T. Wilsgaard, J. Beilby, K. Hovingh, J. F. Price, J. F. Wilson, R. Rauramaa, T. A. Lakka, L. Lind, G. Dedoussis, I. Njølstad, N. L. Pedersen, K. T. Khaw, N. J. Wareham, S. M. Keinanen-Kiukaanniemi, T. E. Saaristo, E. Korpi-Hyövälti, J. Saltevo, M. Laakso, J. Kuusisto, A. Metspalu, F. S. Collins, K. L. Mohlke, R. N. Bergman, J. Tuomilehto, B. O. Boehm, C. Gieger, K. Hveem, S. Cauchi, P. Froguel, D. Baldassarre, E. Tremoli, S. E. Humphries, D. Saleheen, J. Danesh, E. Ingelsson, S. Ripatti, V. Salomaa, R. Erbel, K. H. Jöckel, S. Moebus, A. Peters, T. Illig, U. de Faire, A. Hamsten, A. D. Morris, P. J. Donnelly, T. M. Frayling, A. T. Hattersley, E. Boerwinkle, O. Melander, S. Kathiresan, P. M. Nilsson, P. Deloukas, U. Thorsteinsdottir, L. C. Groop, K. Stefansson, F. Hu, J. S. Pankow, J. Dupuis, J. B. Meigs, D. Altshuler, M. Boehnke, M. I. McCarthy; Wellcome Trust Case Control Consortium; Meta-Analyses of Glucose and Insulin-related traits Consortium (MAGIC) Investigators; Genetic Investigation of ANthropometric Traits (GIANT) Consortium; Asian Genetic Epidemiology Network—Type 2 Diabetes (AGEN-T2D) Consortium; South Asian Type 2 Diabetes (SAT2D) Consortium; DIAbetes Genetics Replication And Meta-analysis (DIAGRAM) Consortium, Large-scale association analysis provides insights into the genetic architecture and pathophysiology of type 2 diabetes. *Nat. Genet.* **44**, 981–990 (2012). [doi:10.1038/ng.2383](https://doi.org/10.1038/ng.2383) [Medline](#)

137. Schizophrenia Working Group of the Psychiatric Genomics Consortium, Biological insights from 108 schizophrenia-associated genetic loci. *Nature* **511**, 421–427 (2014). [doi:10.1038/nature13595](https://doi.org/10.1038/nature13595) [Medline](#)
138. Autism Spectrum Disorders Working Group of The Psychiatric Genomics Consortium, Meta-analysis of GWAS of over 16,000 individuals with autism spectrum disorder highlights a novel locus at 10q24.32 and a significant overlap with schizophrenia. *Mol. Autism* **8**, 21 (2017). [doi:10.1186/s13229-017-0137-9](https://doi.org/10.1186/s13229-017-0137-9) [Medline](#)
139. Psychiatric GWAS Consortium Bipolar Disorder Working Group, Large-scale genome-wide association analysis of bipolar disorder identifies a new susceptibility locus near ODZ4. *Nat. Genet.* **43**, 977–983 (2011). [doi:10.1038/ng.943](https://doi.org/10.1038/ng.943) [Medline](#)
140. D. M. Altshuler, R. A. Gibbs, L. Peltonen, D. M. Altshuler, R. A. Gibbs, L. Peltonen, E. Dermitzakis, S. F. Schaffner, F. Yu, L. Peltonen, E. Dermitzakis, P. E. Bonnen, D. M. Altshuler, R. A. Gibbs, P. I. de Bakker, P. Deloukas, S. B. Gabriel, R. Gwilliam, S. Hunt, M. Inouye, X. Jia, A. Palotie, M. Parkin, P. Whittaker, F. Yu, K. Chang, A. Hawes, L. R. Lewis, Y. Ren, D. Wheeler, R. A. Gibbs, D. M. Muzny, C. Barnes, K. Darvishi, M. Hurles, J. M. Korn, K. Kristiansson, C. Lee, S. A. McCarrol, J. Nemesh, E. Dermitzakis, A. Keinan, S. B. Montgomery, S. Pollack, A. L. Price, N. Soranzo, P. E. Bonnen, R. A. Gibbs, C. Gonzaga-Jauregui, A. Keinan, A. L. Price, F. Yu, V. Anttila, W. Brodeur, M. J. Daly, S. Leslie, G. McVean, L. Moutsianas, H. Nguyen, S. F. Schaffner, Q. Zhang, M. J.

Ghori, R. McGinnis, W. McLaren, S. Pollack, A. L. Price, S. F. Schaffner, F. Takeuchi, S. R. Grossman, I. Shlyakhter, E. B. Hostetter, P. C. Sabeti, C. A. Adebamowo, M. W. Foster, D. R. Gordon, J. Licinio, M. C. Manca, P. A. Marshall, I. Matsuda, D. Ngare, V. O. Wang, D. Reddy, C. N. Rotimi, C. D. Royal, R. R. Sharp, C. Zeng, L. D. Brooks, J. E. McEwen; International HapMap 3 Consortium, Integrating common and rare genetic variation in diverse human populations. *Nature* **467**, 52–58 (2010).

[doi:10.1038/nature09298](https://doi.org/10.1038/nature09298) [Medline](#)

141. S. Mostafavi, A. Battle, X. Zhu, A. E. Urban, D. Levinson, S. B. Montgomery, D. Koller, Normalizing RNA-sequencing data by modeling hidden covariates with prior knowledge. *PLOS ONE* **8**, e68141 (2013). [doi:10.1371/journal.pone.0068141](https://doi.org/10.1371/journal.pone.0068141) [Medline](#)
142. H. T. Nguyen, J. Bryois, A. Kim, A. Dobbyn, L. M. Huckins, A. B. Munoz-Manchado, D. M. Ruderfer, G. Genovese, M. Fromer, X. Xu, D. Pinto, S. Linnarsson, M. Verhage, A. B. Smit, J. Hjerling-Leffler, J. D. Buxbaum, C. Hultman, P. Sklar, S. M. Purcell, K. Lage, X. He, P. F. Sullivan, E. A. Stahl, Integrated Bayesian analysis of rare exonic variants to identify risk genes for schizophrenia and neurodevelopmental disorders. *Genome Med.* **9**, 114 (2017). [doi:10.1186/s13073-017-0497-y](https://doi.org/10.1186/s13073-017-0497-y) [Medline](#)
143. D. Polioudakis *et al.*, A single cell transcriptomic analysis of human neocortical development. *bioRxiv* 401885 (2018).
144. A. Untergasser, I. Cutcutache, T. Koressaar, J. Ye, B. C. Faircloth, M. Remm, S. G. Rozen, Primer3—New capabilities and interfaces. *Nucleic Acids Res.* **40**, e115 (2012). [doi:10.1093/nar/gks596](https://doi.org/10.1093/nar/gks596) [Medline](#)
145. S. F. Altschul, W. Gish, W. Miller, E. W. Myers, D. J. Lipman, Basic local alignment search tool. *J. Mol. Biol.* **215**, 403–410 (1990). [doi:10.1016/S0022-2836\(05\)80360-2](https://doi.org/10.1016/S0022-2836(05)80360-2) [Medline](#)
146. M. Li, Gabriel Santpere, Yuka Imamura Kawasawa, Oleg V. Evgrafov, Forrest O. Gulden, Sirisha Pochareddy, Susan M. Sunkin, Zhen Li, Yurae Shin, Robert R. Kitchen, Ying Zhu, Donna M. Werling, Andre M. M. Sousa, Hyojung Kang, Mihovil Pletikos, Jinmyung Choi, Sydney Muchnik, Xuming Xu, Daifeng Wang, Shuang Liu, Paola Giusti-Rodríguez, Christiaan A. de Leeuw, Antonio Pardinas, BrainSpan Consortium, PsychENCODE Consortium, PsychENCODE Consortium Developmental Subgroup, Ming Hu, Fulai Jin, Yun Li, Michael Owen, Michael O'Donovan, James Walters, Danielle Postuma, Patrick Sullivan, Patt Levitt, Daniel R. Weinberger, Joel E. Kleinman, Daniel H. Geschwind, Stephan Sanders, Michael J. Hawrylycz, Matthew State, Mark B. Gerstein, Ed S. Lein, James A. Knowles, Nenad Sestan, Integrative functional genomic analysis of human brain development and neuropsychiatric risks. *Science* **362**, eaat7615 (2018).